The Hong Kong Polytechnic University

Department of Civil and Structural Engineering

Second-order Analysis and Design of Angle Trusses and Frames

Cho Suk Han

A thesis submitted in partial fulfilment of the requirements for the Degree of Doctor of Philosophy

November 2006

CERTIFICATE OF ORIGINALITY

I hereby declare that this thesis is my own work and that, to the best of my knowledge and belief, it reproduces no material previously published or written, nor material that has been accepted for the award of any other degree or diploma, except where due acknowledgement has been made in the text.

_____

CHO Suk Han

Abstract

Single angle members have a broad range of applications. Very often angle members are connected eccentrically. As a result, not only is an angle member subject to axial force, but it is also subject to a pair of end moments. In addition, the connection at each end provides some fixity so neither pinned nor the fixed end represents the reality. Many national design codes allow for the effects due to load eccentricity and end restraint by modifying the slenderness ratio and reducing the compressive strength of the member. The concept behind this method is inconsistent with strength design of members of other cross-sectional types such as I or box sections of which the buckling strength is controlled by the Perry constant or the initial imperfection parameters. Moreover, in practice, it is difficult to determine accurately the effective length. Sometimes, it is assumed the two ends of the member are immovable. The thesis proposes a few methods for design of angle frames and trusses by the second-order analysis. Laboratory tests of angles as web members of a truss were carried out. The test results are compared with the proposed theoretical and code design loads. In the computational method proposed in this thesis, there is no need to consider any effective length because the second-order $P-\Delta$ and $P-\delta$ effects are considered automatically by geometry update. The proposed method is readily applicable to design of practical steel trusses made of angle sections and demonstrated by a few worked examples. It is further expected the developed design method will improve the safety and economy of structures made of angle sections while he concept can be extended to second-order

analysis and design of structures made of other asymmetric sections like channels and T-sections commonly connected eccentrically.

List of Publications

Refereed journal articles:

CHO S.H. and CHAN S.L. Practical second-order analysis and design of single angle trusses by an equivalent imperfection approach. Steel and Composite Structures. Vol. 5, no. 6, pp. 443-57 (2005)

CHAN S.L. and CHO S.H. Second-order P-Δ-δ analysis and design of angle trusses allowing for imperfections and semi-rigid connections. Advanced Steel Construction. Vol. 1, no. 1, pp. 169-83 (2005)

CHO S.H. and CHAN S.L. Second-order analysis and design of angle trusses Part 1: Elastic analysis and design. Engineering Structures. (Accepted)

CHO S.H. and CHAN S.L. Second-order analysis and design of angle trusses Part 2: Plastic analysis and design. Engineering Structures. (Accepted)

Conference presentations:

CHAN S.L. and CHO S.H. Design of steel frames using calibrated design curves for buckling strength of hot-rolled members. Proceedings, 3rd International Conference on Advances in Steel Structures (ICASS'02), Hong Kong, China, pp.1193-1200, 9-11 Dec 2002

CHO S.H. and CHAN S.L. Experimental evaluation of simulation design for light-angle trusses. Proceedings, 1st International Conference on Advances in Experimental Structural Engineering (AESE 2005), Nagoya, Japan, pp. 951-58, 19-21 Jul 2005

Acknowledgements

I would like to firstly acknowledge the financial support of “Second-order Analysis and Design of Angle Trusses and Frames” by the Research Grant Council grant from the Hong Kong SAR Government. I am grateful for the Tuition Scholarship offered by the Hong Kong Polytechnic University from 2002 to 2006.

Secondly, I am sincerely thankful to my supervisor, Prof Siu-lai Chan of the Department of Civil and Structural Engineering of the Hong Kong Polytechnic University, who has offered me a valuable opportunity to carry out this research project and provided me guidance, comments and suggestions throughout the study.

I would also like to show gratitude to Mr Man-chuen Ng, our Senior Technician, for his kindheartedness and technical support for the laboratory works.

Table of Contents

Chapter 1 Introduction

1.1 Background

Single angle members have a broad range of applications, such as web members of trusses, members of latticed towers and bracing members. Figure 1.1 shows a picture of a lattice tower for cable cars. Typical equal and unequal angle sections are shown in Figure1.2. Angle sections are relatively weak in resisting compression compared with other steel sections but are widely used because of its light weight and the L-shaped section making the angles very suitable for light gauge construction for the ease of storage, transportation and fabrication. Angles are poor in compression because of its complicated structural behaviour for the following reasons. Firstly, it is not uncommon to bolt or weld an angle member to another member directly or to a gusset plate at its end through their leg. Therefore, the load is usually transmitted through one leg. Since the centroid of an angle section is not located on the leg, in most of the practical loading conditions, the angle is subject to axial force as well as a pair of end moments due to the load eccentricity. Twisting due to lateral load may also appear simultaneously as the shear centre is located at the point of intersection of the two legs which is away from the centroid. Secondly, the connection at each end provides a restraining effect which is beneficial to the compression capacity of the angle members. Finally, since angles are not doubly-symmetric, their principal axes are always inclined to the horizontal and vertical axes. Therefore, it is necessary to transform the rectangular axes to the principal axes for calculation and thus further complicates the analysis of angle members. The above-mentioned features are almost unique to angle sections

making the design of single angle members controversial for some time. In a rational design procedure, the adverse effect of the end eccentricity and the beneficial effect due to the end restraint on the compression capacity should be considered.

Conventionally, when designing steel structures, engineers usually adopted linear analysis to determine the internal forces and moments of all members under external loads. After that, the resistance of each individual member is determined according to the design rules given in the codes. A sufficiently safe structure is having its resistance larger than the factored forces and moments. However, in most of the conventional design methods widely used today, the design procedure for structures using angle sections appears to be overly simplified. Many assumptions, which are not very accurate, are made so as to simplify the analysis procedure. For example, the load eccentricity and the end restraint are neglected during the analysis. This can be explained that rational computer analyses modelling the realistic behaviour of steel angle structures considering the existence of initial curvature, residual stresses, end restraints and material nonlinearity were time consuming, expensive and thus inappropriate for routine design in the past days when computer was a luxury item. Today, in the era of widespread use of personal computers, it is a good opportunity to develop a more rational design method for angle structures and acquire better understanding of the true behaviour of angle structures.

In the past decade, advanced analysis has been widely developed to achieve a more accurate and efficient analysis method. Advanced analysis combines the second-order effects of geometrical change and material yielding with sufficient accuracy for practical purposes so that isolated member capacity checks can be avoided. The effect of initial imperfections, residual stress etc. are taken into account in the analysis and a practical design can be carried out directly on the basis of the section capacity computed by this type of rigorous analysis. In other words, the overall member buckling resistance check is not required to carry out individually. This type of design method is of growing importance for structures with doubly-symmetric sections. However, this method may not be suitable of structures with angle sections due to their complicated structural behaviour under compression.

In this chapter, as an introductory part, the fundamental structural behaviour of axially loaded angle members is delivered; the $P-\delta$ and $P-\Delta$ effects and the well-known term “effective length” of compression members are explained in details and some currently used analysis methods will be briefly described.

1.2 Structural behaviour of angles as axially loaded members

As compression members are usually far more critical than tension members, the section will mainly focus on the structural behaviour of angles in compression. The information below can be found in many standard reference books [1,2].

1.2.1 Tension members

A member subject to longitudinal tensile load is usually called a tie. Single angle used as a web member or a bracing member can be a tie. When a tension force is applied on the axis of centre of gravity of the section, the tensile stress is assumed to be uniform over the cross-section. Assuming there is no loss of area of the member at the connections, the member will start yielding at:

$$P_t = p_y A_g \tag{1.1}$$

where P_t is the tensile strength of the member

p_y is the yield stress of the material

A_g is the gross area of the section

After undergoing the large strains that occur during yielding, the member begins to strain harden. During strain hardening, the material undergoes changes in its crystalline structure, resulting in an increase of resistance of the material to further deformation.

1.2.2 Euler's theory of compression members

A member subject to longitudinal compressive load is usually called a strut. A formula for the strength of a pin-ended strut was derived with mathematical considerations. The formula was derived based on the following assumptions:

- The struts are perfectly straight and homogeneous.
- The compressive loads are perfectly axially applied.

- The struts are uniform throughout and the limit of proportionality of the material is not exceeded.

The strut will buckle when the applied load reaches the Euler buckling load, P_E, is reached which is given by:

$$P_E = \frac{\pi^2 EI}{L^2} \tag{1.2}$$

where I is the second moment of inertia of the section

L is the member length

We can also find the corresponding Euler stress, which is the average compressive stress on the cross section at the moment the load reaches Euler buckling load, from Equation (1.2):

$$p_E = \frac{P_E}{A} = \frac{\pi^2 EI}{AL^2} \tag{1.3}$$

where p_E is the Euler stress

Equation (1.3) can be written in a more comprehensive form by notating:

$$r = \sqrt{\frac{I}{A}} \tag{1.4}$$

in which r is the radius of gyration of the cross section in the plane of bending. Although r does not have an actual physical meaning, it can be considered as the distance at which the entire area could be concentrated and have the same moment of inertia as the original area.

Then Equation (1.3) becomes:

$$p_E = \frac{\pi^2 E}{(L/r)^2} \tag{1.5}$$

L/r is termed as slenderness ratio which becomes an important parameter that affects highly the Euler load of buckling of the member. It is interesting to note that from a mathematical analysis, for a given cross-sectional area, an angle section is relatively weak in resisting Euler buckling. The Euler load is inversely proportionally to the square of the slenderness ratio. Theoretically, however, members with slenderness less than $\pi^2\sqrt{E/p_y}$ are insensitive to Euler buckling and is likely to fail at squash load P_c which is given by:

$$P_c = p_y A \tag{1.6}$$

In this case, the failure mode will be similar to that of a tension member except the direction of the stress.

1.2.3 Bending of members with load eccentricity

Angles are seldom loaded concentrically. Angles provide a fast track of fabrication and erection by making connections through one leg only to one another, or to a gusset, or to a tee through the flange. These eccentric connections introduce bending moments at each end thus bending stresses in the member which further reduce the compression capacity of a member. If the member is treated as an ideal pin-ended column, the maximum compressive stress $p_{\max}$ of the member can be calculated by the secant formula:

$$p_{\max} = \frac{P}{A}\left[1 + \frac{e \cdot y}{r^2}\sec\left(\frac{L}{2r}\sqrt{\frac{P}{EA}}\right)\right] \tag{1.7}$$

in which e is the load eccentricity, y is the distance from the centroidal axis to the extreme point on the cave side of the column and $e \cdot y/r^2$ can be termed as the eccentricity ratio.

The secant formula can be used in a reverse manner, i.e. if p_y is put into $p_{\max}$, the corresponding first yield failure load can be calculated. However, numerical method must be adopted to solve the formula. Figure 1.3 shows the curves of the secant formula with various values of eccentricity ratios. This formula is seldom used in practical designs only gives a general idea of the behaviour of a pinned end strut under eccentric load and seldom used in practical design. This formula can also be used for a strut that is fixed at one end and free at the other end if the length L in the formula is replaced by $2L$. However, for the other end conditions, this formula is not valid.

1.2.4 Bending of members with initial curvature

In fact, practical members are hardly constructed perfectly and may possess some imperfections such as material imperfection due to residual stress and geometrical initial curvature which cause members bending at the beginning when the load is applied instead of buckling when the buckling load is reached. Considering a hypothetic member with initial curvature of

$$y_0 = \delta_0 \sin\frac{\pi x}{L} \tag{1.8}$$

in which y_0 is the initial curvature at distance x and δ_0 is the initial curvature at mid-span.

If a compressive load is applied axially at the ends of a member, it will bend instantly. In addition to the axial stress caused by the compressive load, the deflection induces a bending stress and the member is failed when the combined axial and bending stresses reaches the yield stress of the material. The theoretical critical compressive stress can be calculated by the Perry-Robertson formula as:

$$p_c{}^2 - p_c\left[p_y + \left(1 + \frac{\delta_0 \cdot y}{r^2}\right)p_E\right] + p_y p_E = 0 \tag{1.9}$$

where p_c is the critical stress

y is the distance from the extreme fibre in compression to the neutral axis of the cross section

Equation (1.9) can be rewritten as:

$$p_c = \frac{1}{2}\left[p_y + (\eta + 1)p_E\right] - \frac{1}{2}\sqrt{\left[p_y + (\eta + 1)p_E\right]^2 - 4p_y p_E} \tag{1.10}$$

where $\eta = \frac{\delta_0 \cdot y}{r^2} = \frac{\delta_0}{L} \cdot \frac{y}{r} \cdot \frac{L}{r} = a_0 \lambda$

in which $a_0 = \frac{\delta_0}{L} \cdot \frac{y}{r}$

Similar to Euler buckling, the failure load of this hypothetic strut largely depends on the length of it. Figure 1.4 shows the curves of Perry-Robertson formula with

various value of a_0 . However, this formula is still questionable when the slenderness ratio of a member is low because practical stocky members are insensitive to initial imperfections and more likely fail at squash load.

1.2.5 Real compression members

Real members not only possess initial crookedness, they also have residual stresses, load eccentricity and material nonlinearity which affect the ultimate compressive strength of the members. The collective effect due to these imperfections is qualitatively similar to the effect due to initial curvature alone and thus can be simulated by an equivalent value of initial curvature making use of the Perry-Robertson formula. The structural behaviour of practical struts of different slenderness ratios can be illustrated by the compressive strength curve from BS 5950 [3] in Figure 1.5. As can be seen from the graph, basically these curves can be divided into three slenderness ratio ranges as follows:

- Stocky range ($\lambda \leq 20$)
- Intermediate range ($20 < \lambda \leq 100$)
- Slender range ($\lambda > 100$)

In stocky range ($\lambda \leq 20$), the failure is mainly caused by squashing of the material and therefore the failure load does not depend on the slenderness ratio or the young modulus of the material. However, in intermediate range ($20 < \lambda \leq 100$), the failure load is far less than the Euler buckling load and the buckling is considered inelastic. It is found that the Euler formula agrees well with the actual failure load of slender

struts ($\lambda > 100$). We can conclude that the aforementioned initial imperfections have the most significant effects on members with intermediate slenderness.

1.2.6 Flexural-torsional buckling

Apart from flexural buckling or bending, stocky single angle struts in concentric compression load may also fail in a flexural-torsional buckling mode which is commonly ignored in routine design. Considering a perfect strut in concentric load, the critical load P_{cr} is the lowest root of the following equation.

$$f(P) = (P - P_x)(P - P_y)(P - P_z)(r_p^2 + y_0^2 + z_0^2) - P^2 y_0^2 (P_z - P) - P^2 z_0^2 (P_y - P) = 0 \tag{1.11}$$

in which P_y and P_z are the Euler flexural buckling loads of the strut about the $y-$and $z-$axes, P_x is the torsional buckling load about the shear centre axis, y_0 and z_0 are the coordinates of the centroid about the axes parallel to the principal axes and passing through the shear centre and r_p is the polar radius of gyration.

As the shear centre is at the intersection point of the two angle legs, there is virtually no warping rigidity and the warping constant can be assumed zero, the torsional buckling load P_x will be given by:

$$P_x = \frac{GJ}{r_0^2} \tag{1.12}$$

in which $r_0^2 = r_p^2 + y_0^2 + z_0^2$

For equal angles, since they are monosymmetric sections, by putting $y_0 = 0$, Equation (1.11) can be simplified and rearranged to:

$$P = \frac{\left(P_x + P_y\right) - \sqrt{\left(P_x + P_y\right)^2 - 4P_x P_y\left[1 - \left(z_0 / r_0\right)^2\right]}}{2\left[1 - \left(z_0 / r_0\right)^2\right]} \tag{1.13}$$

The buckling load will be the lower of P_y and P. If P_y is lower than P, flexural buckling will occur; if P is lower than P_y, flexural torsional buckling will occur. For unequal angles, as they are asymmetric, Equation (1.11) cannot be simplified; so the critical load must be obtained numerically. Trahair [2] suggested that the equation can be solved approximately by interpolating linearly using the values of $f(0)$ and for the lowest value P_1 of P_x, P_y and P_z as:

$$P \approx \frac{P_1 \cdot f(0)}{f(0) - f(P_1)} \tag{1.14}$$

This P is always less than P_1 corresponding to a flexural-torsional buckling mode. Therefore, flexural-torsional buckling should be taken into account in the design of angle structures especially for unequal angles as it is possibly the critical failure mode and may reduce compression resistance of the member unless sufficient bracing is provided to prevent the member from flexural-torsional buckling.

1.2.7 Local buckling

Angle sections are classified as thin-walled open sections. In the conventional theory of thin-walled beams, the cross section is assumed to remain undeformed

even when loaded to its ultimate strength. This assumption is true for most of the hot-rolled steel sections. However, for a relatively thin-walled cross section, the thin plate of the cross section may deform and exhibit local buckling before the member yields or buckles in any other modes mentioned previously.

1.3 The $P-\delta$ and $P-\Delta$ effects

1.3.1 The $P-\delta$ effect

The $P-\delta$ effect is referred to as the second-order effect due to the deflection along a member and the axial force applied to it. The inclusion of the $P-\delta$ effect in the formulation of the member stiffness is important for a second-order analysis. For a beam-column element, the bending coefficients vary under high tensile and compressive axial force. It can be imagined that a member under tension is always stiffer than under compression. For an element of only compression, its strength decreases as its lateral deflection increases and the lateral deflection depends on the length of the member, the initial curvature and the load applied. Without the presence of initial curvature, the element does not bend and the actual stress the section is taking cannot be calculated. Therefore, the consideration of initial curvature is important for a compression element

1.3.2 The $P-\Delta$ effect

The $P-\Delta$ effect is referred to as the second-order effect due to the change in geometry which leads to the invalidity of the global stiffness matrix soon after the application of load. Considering a simply supported beam subject to a point load

acting on its mid-span, the beam will deflect in both vertical and horizontal directions. The horizontal displacement is relatively small compared with the vertical displacement and is usually ignored in analysis. It is sufficiently safe to ignore the horizontal displacement in a structural design if the horizontal displacement is small. However, it will be dangerous to exclude this effect to large deflection structures. From a global point of view, the local deflection and the global displacements in fact mutually affect each other and the structural response of the other members as well. The $P-\Delta$ effect can be included in an analysis by simply geometry update. The $P-\delta$ effect can also be transformed to the $P-\Delta$ effect by using several elements per member.

1.4 The effective length of compression members

The structural behaviour mentioned under Section 1.2 are based on pin-ended condition which hardly exists in reality. In fact, the formulas can be used to deal with struts with other end conditions. This can be achieved by replacing the member length by the equivalent length, or the effective length, which is equal to the distance between the two points of inflexion of its deflected shape. The physical meaning of an effective length is that the equivalent length of the member with pin-ended condition will give the same failure load. For example, in Euler's theory, a member of length L with fixed-end condition should have an effective length of $0.5L$. The use of the effective length is not restricted to Euler formula. In a typical linear analysis, normally a longer effective length is used to compensate the negligence of the $P-\delta$ and $P-\Delta$ effects unless the structure is sufficiently

braced. Empirically, the effective length of the member can also be used to account for the disregard of flexural-torsional buckling in design. However, sometimes the effective length is only a rough estimation which may cause underestimate or overestimate the actual failure mode.

1.5 Types of analysis

There are different levels of analysis with various degrees of refinement which can be used for structural design including linear analysis, elastic bifurcation analysis, second-order elastic analysis, second-order inelastic analysis and advanced analysis. This section focuses on linear analysis, bifurcation analysis, second-order elastic analysis and advanced analysis.

1.5.1 Linear analysis

The linear theory, which assumes the deformations of a structure is proportional to the magnitude of the loads applied to it as shown in Figure 1.6, is widely used is in structural analysis today. For the assumption to be valid, the material must have a linear relationship between stress and strain while the structure must have a linear relationship between load and deformation. However, practically no structure behaves linearly. The theory is only approximately true provided that the deformations are small. The merits of using this type of analysis are its simplicity and the validity of the principle of superposition of different load cases. However, the linear function of the load-deflection relationship does not allow the failure load of the structure to be assessed. To check the safety of the structure, the internal

load of the structure must be checked against the resistance of the structure of which the resistance is reduced to account for the $P-\delta$ and the $P-\Delta$ effects.

1.5.2 Bifurcation analysis

The buckling load factor, λ_{cr}, which causes the structural system to buckle elastically with the structural geometry assumed remaining unchanged until buckling occurs, is known as the elastic buckling factor. In the bifurcation type of analysis, an eigenvalue problem is formuated by a standard procedure as

$$\left|K_L + \lambda_{cr} K_G\right| = 0 \tag{1.15}$$

in which K_L and K_G are the linear and the geometric stiffness matrices respectively.

For a general stiffness matrix of a structural system with *n* degrees of freedom, there exists *n* roots for the bifurcation analysis which represent *n* possible buckling modes and usually only the lowest root is of practical interest. It should be noted that the method can only provide an upper bound solution to the stability of a frame. Alternatively, this can be used to determine the exact effective length factor K for a member in a structural system for design based on linear analysis.

1.5.3 Second-order elastic analysis and advanced analysis

Unlike bifurcation analysis, second-order elastic analysis involves tracing the equilibrium or the load-deflection path as shown in Figure 1.6. As its name implies, the second-order effects such as the initial curvature of the members, the $P-\delta$ and

$P-\Delta$ effects are all included in the second-order analysis. However, material yielding is not considered in the elastic analysis. Therefore, the load-deflection path is untrue after the material is yielded. Therefore, the checking against resistance is necessary. But, there is no need to reduce the resistance of the member as the $P-\delta$ and $P-\Delta$ effects are already included in the analysis.

Advanced analysis combines the effects of material yielding and geometrical change with sufficient accuracy for practical purposes so that isolated member capacity checks can be avoided. The advantage of using advanced analysis over linear analysis and second-order analysis is that the design is completed readily with analysis.

1.6 Objectives

The objectives of the research project undertaken in this thesis are as follows.

- To develop code-free design methods for steel trusses and frames using single-angle with the aid of a second-order analysis and design programme so that the discrepancy between the analysis and design in the currently used method can be eliminated.

- To illustrate the structural response of angle members in practical truss and frame systems through a non-linear numerical approach. A number of practical examples will be carried out the study the structural behaviour of angle trusses and frames.

- To examine the compressive strength of angle members through laboratory tests. Four single angle struts were tested as web members of a two-dimensional truss to study the behaviour of single angle compression members in practical conditions.

- To assess the accuracy of the proposed design method and the design rules given in BS 5950 [3] for steel trusses and frames with single angles. The test results will be compared with the numerical results and the design values calculated according to the design code.

1.7 Outline of the thesis

Chapter 2 delivers the literature review which involves the classical investigation of angle compression members, the development of second-order analysis and the current structural analysis of steel frames structures. Chapter 3 presents a review of various national design codes regarding angle compression members and describes the procedure of conventional design using linear analysis. Chapter 4 explains the numerical procedure of second-order analysis using the Newton-Raphson incremental-iterative scheme and also other incremental-iterative numerical methods. Chapter 5 proposes two second-order elastic analysis and design methods for single-angle sections via the use of equivalent initial member imperfection. Chapter 6 proposed the second-order plastic analysis and design method for single-angle sections using the "plastic-element". Chapter 7 presents the experimental

investigation of angle compression members tested as part of a two-dimensional truss. Finally, Chapter 8 is the conclusions and recommendations.

Figure 1.1 Latticed tower structure (Ocean Park, Hong Kong)

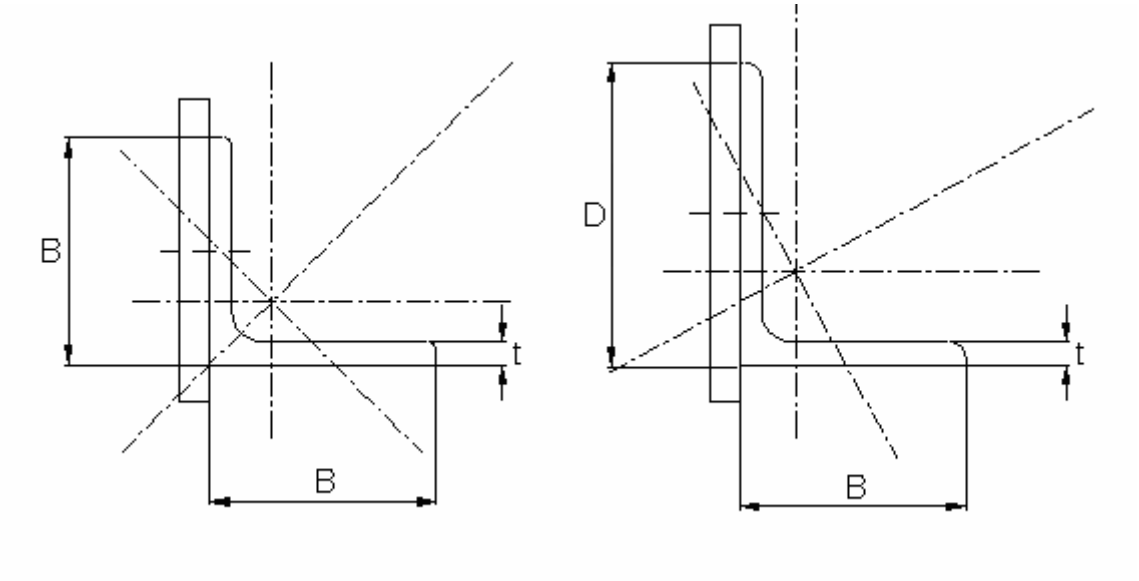

Figure 1.2 Typical equal and unequal angle sections

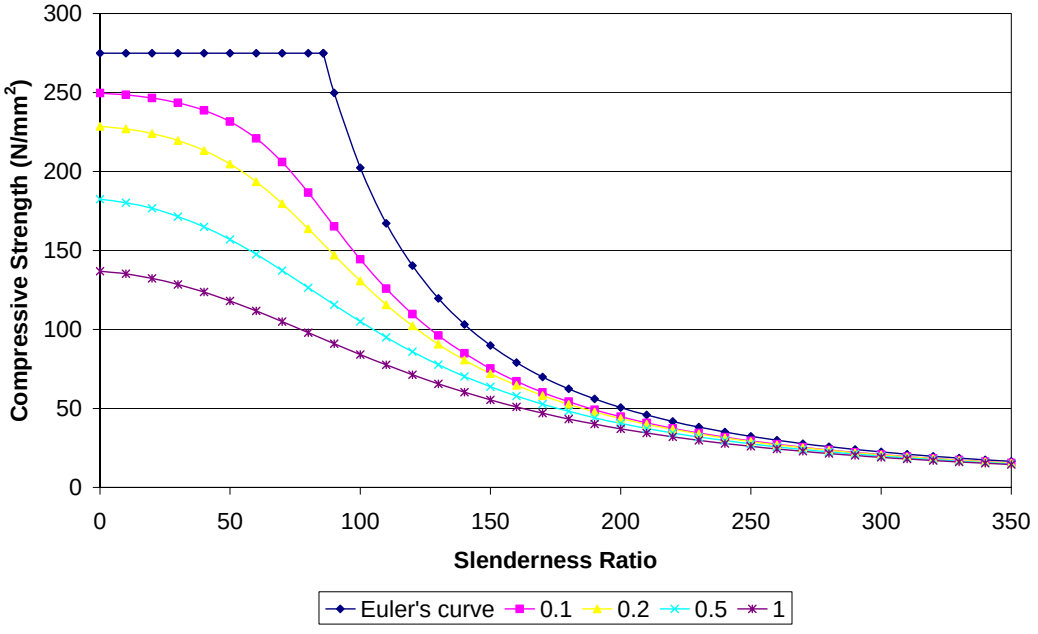

Figure 1.3 Graph of the secant formula ($E = 205000\, N/mm^2$, $p_y = 275\, N/mm^2$)

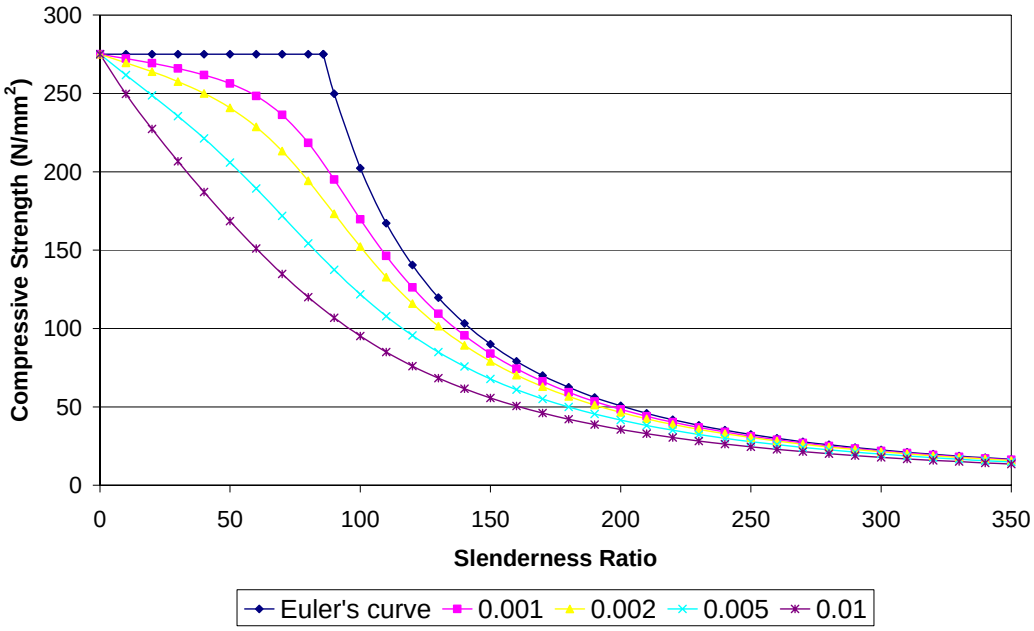

Figure 1.4 Graph of the Perry-Robertson formula

$(E = 205000\,N/mm^2\,,\, p_y = 275\,N/mm^2\,)$

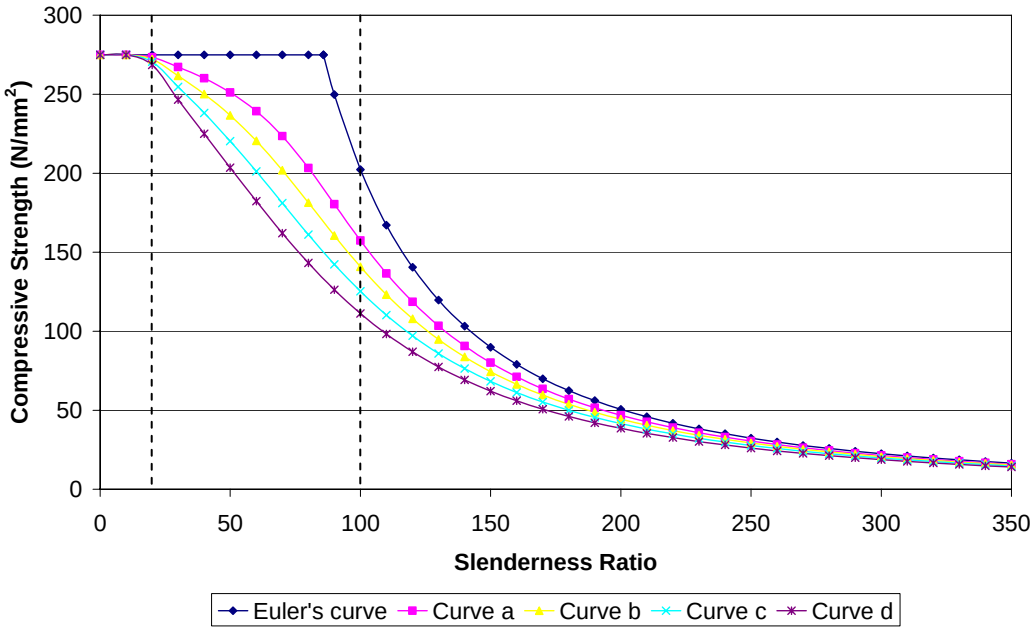

Figure 1.5 Graph of the BS 5950 compressive strength curves

$(E = 205000\,N/mm^2\,,\, p_y = 275\,N/mm^2\,)$

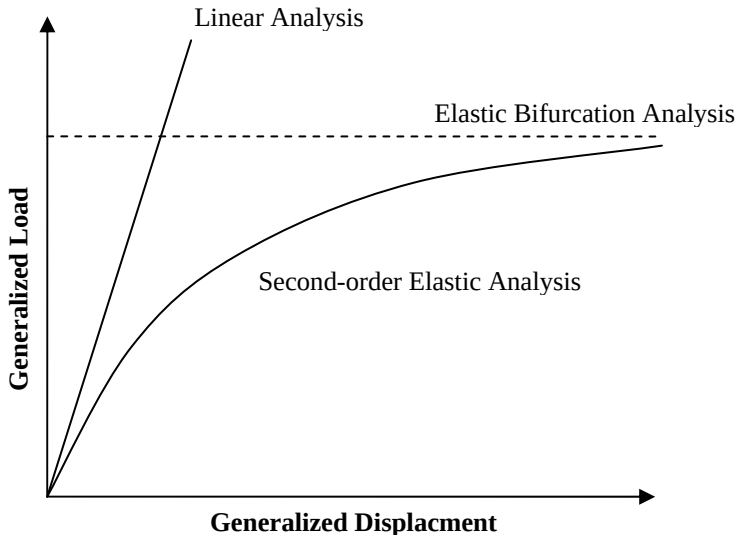

Figure 1.6 General analysis types for steel framed structures

Chapter 2 Literature Review

2.1 Introduction

This chapter presents a literature review of mainly three research areas, which involves the classical investigation of structural behaviour of angle compression members from theoretical, analytical and experimental approaches, the development of nonlinear analysis of steel structures, and the analyses of steel latticed structures.

2.2 Classical investigation of angle compression members

The structural behaviour of angle compression members introduced in Chapter 1 demonstrates that the strength of an angle strut does not only depend on the yield stress of the steel, but also its stability. An angle member rarely fails at squash load but may fail by a flexural buckling or a flexural-torsional buckling mode. Kitipornchai [4] carried out a parametric study against flexural buckling and flexural-torsional buckling of single angle compression members with the elastic buckling loads calculated and expressed in terms of dimensionless parameters such as ratio of the two leg lengths (i.e. the leg length ratio) and leg length to thickness ratio of standard rolled angle section range. It was shown that the flexural-torsional buckling mode was most significant for stocky columns especially for unequal angles while slender columns were susceptible to flexural buckling. Since most of the design rules are derived based on flexural buckling with the flexural-torsional buckling usually ignored, Kitipornchai [4] introduced an equivalent slenderness

ratio. This ratio is defined as the slenderness ratio of a member having the same cross section as the actual member, which when buckling in a pure flexural mode about the principal minor axis, has the same buckling load as the actual member buckling in a flexural-torsional mode. The equivalent slenderness ratio $(L/r)_{eq}$ can be expressed in terms of the actual slenderness ratio $(L/r)_y$ and the ratio of the elastic buckling load P_c/P_y .

$$\left(\frac{L}{r}\right)_{eq} = \left(\frac{L}{r}\right)_y \sqrt{\frac{P_y}{P_c}} \tag{2.1}$$

where P_c is the flexural-torsional buckling load

P_y is the flexural buckling load about weak axis

From the parametric solutions, the equivalent slenderness ratio can be obtained as

$$\left(\frac{L}{r}\right)_{eq} = \left(\left(\frac{L}{r}\right)_y^3 - 8(\alpha - 0.5)\beta^2\left(\frac{L}{r}\right)_y + 76\beta^3\right)^{1/3} \tag{2.2}$$

in which α is the leg length ratio and β is the leg length to thickness ratio. The proposed expressions for equivalent slenderness ratio were easy to understand and simple to use. With this slight modification on slenderness ratio, the existing design rules can still be employed.

The modification is based on a concentrically loaded pin-ended compression member in perfect conditions including the material which was linearly elastic. As the material is in fact not linearly elastic and the presence of residual compression stresses cause premature yielding especially for intermediate length compression

members, Kitipornchai and Lee [5] expanded the research to inelastic analysis of single angles as well as other sections by the finite element method using the tangent modulus concept with the Young's modulus of the material assumed to be zero in the yield region. As the torsional rigidity *GJ* was tested to be not much affected by tension or compression yielding, the shear modulus of elasticity remained unchanged. In addition, idealized residual stress distribution was assumed in the analysis. The distribution of elastic and yielded regions across the section was determined from the idealized elastic-plastic stress-strain curve. Results revealed that for equal angles (L102×102×6.5) the elastic flexural buckling curve was lower than the elastic flexural-torsional buckling curve with slenderness ratio not less than 80 for which the inelastic flexural buckling curve was always lower than the inelastic flexural-torsional curve. On the other hand, for unequal angles (L76×51×5) both the elastic and inelastic flexural-torsional buckling curves were always lower than the respective flexural buckling curve. This demonstrated that the predominant failure modes for equal angles and unequal angles are flexural buckling and flexural-torsional buckling respectively in the inelastic range regardless of the slenderness ratio. Results also revealed that angles were susceptible to local buckling which further reduces the compressive strength. Theoretical treatment of the inelastic interaction between local and global buckling is complicated. Empirically, local buckling of a slender compression member is accounted for by using the reduced effective area A_{eff} instead of gross area A and by reducing the slenderness ratio to

$$\lambda = \frac{L}{r}\sqrt{\frac{A_{eff}}{A}} \tag{2.3}$$

However, most practical angle sections used today are compact, making the local buckling less important.

In reality, concentrically loaded simply supported angle columns rarely exist; the end restraints and the load eccentricity usually co-exist since the angles are usually connected to a gusset plate through one leg. The thickness of the gusset plate not only contributes to the load eccentricity, but, it also provides some degree of end fixity. These imperfections are normally ignored in routine design for simplicity. Such approximations do not provide an accurate description of the real structure behaviour of angle struts. In fact, typical angle columns are subject to axial forces, a pair of eccentric end moments and sometimes torques introduced by the connections. As angle members normally have lower flexural rigidity and torsional rigidity, they may react drastically by deflecting laterally and twisting. It is important to note that the problem is no longer a bifurcation problem because deformation will occur with any axial load. Therefore, it becomes necessary to determine the resultant stress instead of the buckling stress. Early treatments of the elastic behaviour of an isolated beam-column were developed by Goodier [6,7], Vlasov [8] and Timoshenko [9]. Goodier [6,7] derived the following set of differential equilibrium equations.

$$EI_x\left(v''-v_0''\right)+Pv+P\left(e_x-x_0\right)\phi=0 \tag{2.4}$$

$$EI_y\left(u''-v_0''\right)+Pu+P\left(e_y-y_0\right)\phi=0 \tag{2.5}$$

$$EI_w\phi'''-\left(GJ-P\cdot r_2\right)\phi'+Pv+P\left[\left(e_x-x_0\right)v'-\left(e_y-y_0\right)\right]=0 \tag{2.6}$$

in which $r_2^{\,2} = r_1^{\,2} + \frac{\beta_x}{P} EI_x v_0'' + \frac{\beta_y}{P} EI_y u_0''$ (2.7)

and $r_1^{\,2} = \frac{I_x + I_y}{A} + x_0^{\,2} + y_0^{\,2}$ (2.8)

The closed form solutions for biaxially loaded columns with equal end eccentricities were obtained by Culver [10]. If such columns are pin-ended, a simpler solution can be obtained by assuming the deflected shape to be a half sine wave [11]. Trahair [12] carried out a theoretical investigation on elastic biaxial bending and torsion of beam-columns with symmetrical end loading and restraints. The end restraining moments were considered by relating the end restraining moments M_X and M_Y to their corresponding end rotation θ_X and θ_Y as:

$$M_X = -\frac{2R_1}{1-R_1}\frac{EI_x}{L}\theta_X \quad (2.9)$$

$$M_Y = -\frac{2R_2}{1-R_2}\frac{EI_y}{L}\theta_Y \quad (2.10)$$

The restraint coefficients R_1 and R_2 were defined as the ratios of the actual end restraining moments to those required to develop full end fixity i.e. 0 for no restraint and 1 for full restraint. Finite integral method was employed to solve the differential equations. The structural behaviour of eccentrically loaded end restrained single angle struts was studied and compared with experimental data reported by Foehl [13]. It was shown that the first yield loads were quite close to the failure load and may be used as conservative estimates of the ultimate strengths of the single angle struts.

In order to further study the structural behaviour of eccentrically loaded single angle struts, Trahair et al. [14] carried out a series of tests of eccentrically loaded single angle struts. The tested sections included L51×51×6 equal angle and L76×51×6 unequal angle. The slenderness ratio ranged from 60 to 200 which covered the range encountered in practice. At each end, one leg was welded to the web of a structure tee. This simulated the chord of a truss. Load was applied through the centre of the web of the structural tee which contributed to the load eccentricity through the connection. The load was applied to the structural tee in three ways:

(a) Both ends are fixed in both directions. However, the flexibility of the Tee stem allows out-of-plane rotation so it behaves as if partially restrained in the out-of-plane direction.

(b) The strut ends in the direction of the outstanding leg of the angle can rotate freely, but the strut ends can not rotate in the plane of the Tee stem.

(c) Opposite to End Condition (b), the strut ends can not rotate in the direction of the outstand leg of the angle, but the strut ends can rotate in the plane of the Tee stem. Similar to condition (a), the flexibility of the Tee stem allows out-of-plane rotation.

These three end conditions symbolized the extreme cases of the real situation. The value of the restraint coefficient R in Eqns. (2.9) and (2.10) for the partially restrained conditions can be calculated from the sectional and material properties of the Tee stem and the struts. Results showed that End Condition (b) gave the lowest failure loads corresponding to the situation when the chord buckles by twist-

buckling and consequently cannot restrain the single angle strut from deforming out of the plane of the truss. Although it unlikely occurs, this end condition represents the most severe case.

Adluri and Madugula [15] compared results of experimental data on eccentrically loaded single angle members free to rotate in any directions at the ends in the available literature with AISC LRFD [16] and AISC ASD [17] specifications which were based on axial force-moment interaction of doubly symmetric cross section. The experimental investigations, which covered a wide spectrum of single angle struts, were carried out by Wakabayashi and Nonaka [18], Mueller and Erzurumlu [19], and Ishida [20]. Adluri and Madugula [15] summarized these results and concluded that the interaction formulas given in AISC LRFD [16] and AISC ASD [17] are highly conservative when applied to eccentrically loaded single angle members. It is because these interaction formulas were derived primarily for doubly symmetric sections and the moment ratios in these formulas are evaluated for the case of maximum stresses about each principal axis. This practice does not pose a problem on doubly symmetric sections such as I sections because the four corners are critical for moments about both principal axes simultaneously. However, for angle sections, as they are monosymmetric or asymmetric, the points having maximum bending stress about both principal axes usually do not coincide. As a consequence, the loading capacities of the sections calculated from these interaction equations are underestimated.

Adluri and Madugula [21] carried out a theoretical study on the compressive strength of steel angles failing by failure modes other than flexural buckling. The study was based on non-linear analysis based on non-linear analysis with the residual stresses, elastic-perfectly plastic material behaviour and the initial geometric imperfection taken into account. Nine different column buckling curves were generated. Laboratory tests were also carried out and reported in a companion paper [22] to prove those curves are on the safe side. Bathon et al. [23] carried out 75 full-scale tests which cover a slenderness ratio ranging from 60 to 210. The test specimens were unrestrained against rotation and twisting at the end supports. It is possibly for the reason that the ASCE Manual 52 [24], which is based on these results, also under-predicted the capacities of single angle struts.

The aforementioned research focused on isolated members and appears to ignore the effect due to end connection details, which may also affect the compressive resistances of the angle struts. Elgaaly et al. [25] conducted an experimental program to investigate the structural behaviour of non-slender single angle struts as part of three-dimensional trusses attempting to model the actual end conditions as closely as possible. Fifty single angle specimens cover a range of slenderness ratio from 60 to 120 which may be regards as of intermediate lengths. The truss was designed so that the target failure member would fail first without introducing significant deformations in the remainder of the truss. After each test, only the failed member was replaced allowing multiple tests to be conducted under the same setting. The failure modes of the specimens involved flexural buckling about the principal minor axis, flexural buckling about the geometric axis, local buckling of

the connected leg coupled by flexural buckling about either the geometric or the principal minor axis, and flexural-torsional buckling. With the failure loads, the design rules given by the ASCE Manual 52 for the Design of Steel Transmission Tower [24] and AISC LRFD Specification for Structural Steel Buildings were evaluated [16]. In ASCE Manual 52 [24], the angles are always considered to be an axially load member; the end restraint effect and the load eccentricity are accounted for by the use of an effective slenderness ratio KL/r . AISC LRFD specification [16] considers the effect of biaxial bending induced by the load eccentricity by using appropriate interaction equation. Results showed that the nominal loads calculated from Manual 52 [24] were very close to or exceed the actual failure loads. A similar conclusion for the AISC LRFD [16] specification was drawn when the angles were considered as concentrically loaded. When the load eccentricity was taken into consideration, the AISC LRFD [16] specification nominal loads were unnecessarily conservative. The test results indicated that both design methods were inadequate for non-slender single angle members. The authors made a few suggestions to resolve the over-design in the AISC specifications. One possible way is to consider the end restraining effect by using an effective length factor less than one. Another possible way is not to add the worst case bending stresses due to load eccentricities that actually do not occur at the same point of the angle cross section. It is more precise to calculate the resultant stress at each extreme point to find out the most critical point.

In roof trusses, the single angle web members are often connected by one leg on one side of the chords and sometimes alternately on opposite side of the chords.

Theoretically, single angle struts whose web members are connected alternately on opposite sides should have less compression capacity than the same struts connected on the same side. However, most of the design codes seem to ignore this circumstance. Woolcock and Kitipornchai [26] proposed a design method based on experimental observation [14]. In the proposed method, not only is the effect of load eccentricity taken into account, but cases where web members are all on one side or on opposite side are also considered. This method was considered simpler and less conservative than the conventional axial force-biaxial bending interaction approach. The current Australian standard AS 4100-1998 [27] also follows this approach.

From the available literature, it can be seen that in most of the cases, the experimental results on eccentrically loaded steel single-angle struts can disagree to a great extent from the compressive resistances calculated using existing conventional design method. In view of this, Sakla [28] delivered an innovative approach to predict the load-carrying capacity of pin-ended single-angle struts using artificial neural networks (ANNs). The proposed ANN model was trained and validated by the reported experimental results [18-20,22]. It was shown that the model predicted better than the current AISC specifications. The model also offered an efficient alternative in predicting the load-carrying capacity of eccentrically loaded single-angle struts. The advantage of using neural network modeling is that the model can always be fine-tuned to obtain better results by inputting new training patterns as long as new data are available. However, the proposed ANN model so far is only limited to single angle struts with pin-ended.

2.3 Development of second-order analysis of steel framed structures

2.3.1 General

Finite element methods for steel framed structures allowing for second-order and nonlinear effect has been studied extensively over the past few decades. Basically, there are two main approaches in element formulations. The first approach involves solving the differential equilibrium equation for the relationship between the force, the moments and the rotations [29,30] while the second approach is to assume a cubic displacement function and apply the principle of minimum potential energy [31,32]. Oran [29,30] presented a tangent stiffness matrix for the geometrically nonlinear analysis of elastic space frames using the stability function concept. In the formulation, the rotations and translational displacements of the joints were considered to be arbitrarily large. The basic member force-deformation relationships were derived from the conventional beam-column theory, which assumes that the relative deformations of the members are small, so that the coupling between the axial force and the moment was accurately included in the matrix formulation. Meek and Tan [32] derived the element stiffness matrix by assuming a cubic deflection curve and applying the minimum potential energy principle. The stiffness matrix can be solved by the Newton-Raphson method which is a linearized incremental-iterative procedure. During the incremental-iterative process, the change in geometry and the change in bending stiffness coefficients are considered so that the second-order $P-\Delta$ and $P-\delta$ effects are included in the analysis. However, Meek and Tan [32] pointed out the linearized incremental iterative techniques appeared to be insufficient to study pre- and post buckling behaviour because of the divergence problem after the limit point and

thus introduced a modified arc-length method. The solution method facilitated the studies of snap-through buckling of thin shell structures. The results agreed well with the previously published analytical solutions. Chan and Chui [33] also suggested a number of nonlinear solution techniques, which will be discussed in details in Chapter 4, to relieve the difficulties associated with tracing the equilibrium path beyond the limit point.

2.3.2 Second-order analysis of angle struts

Hu et al. [34] and Lu et al. [35] developed a finite element method for stability analysis using the total energy approach with the effect of initial curvature, initial twist and residual stresses included in the formulation. The equilibrium path was traced using the Newton-Raphson method. The method was applied to determine the theoretical load-deformation relationships of some test struts reported in the literature. Very close agreement between the theoretical and the experimental results was achieved. The method was employed to study the ultimate strength of single-angle struts loaded concentrically and eccentrically through gusset plates. The initial curvature was imposed in the direction so that the situation is most severe. The effect of residual stresses was also taken into account in the calculations. For concentrically loaded struts, the results showed that the initial curvature posed a significant influence on the ultimate strength of the angle struts of stocky and intermediate slenderness range. For single-angle struts loaded through gusset plates, it was generally believed that the member has a higher resistance if the connection was made through the short leg (i.e. long leg outstanding) as this will provide more lateral stiffness to the truss. However,

having long legs connected to gussets is easier for connection. Interestingly, the numerical results showed that angles with short leg outstanding were more favourable for stocky members. The results also indicated that end restraint can significantly increase the strength of an eccentrically loaded single-angle strut.

Kitipornchai and Chan [36] employed a similar approach to solve the problem of elastic behaviour of restrained beam-columns. However, the element geometric stiffness matrix was derived with the effect of the shear centre not coincident with the centroid taken into account. To cope with this effect, a transformation matrix is required to relate the member forces and displacement to those at the node. Mathematically, this matrix transforms vector in a coordinate system to another parallel system with a different position of origin as shown in Figure 2.1. The equilibrium paths were then determined from the incremental and the total-force-deformation equilibrium equations using the arc-length method. The results were compared with those reported by Trahair [12]. It was shown that when the geometry was not updated, the results agreed well with the finite integral solutions. However, when the geometry was updated, the influence of the pre-buckling deformations was apparent. In other words, the conventional numerical procedure can grossly overestimate the actual member load-carrying capacity.

Sun and Butterworth [37] developed a nonlinear finite element model applicable to steel single angle compression members loaded eccentrically through one leg using an existing finite element package. Realistic initial geometric imperfections similar to a multi-wave local buckling mode were incorporated into the model, which

allows large inelastic deformations and predicts local and overall buckling behaviour. Although a relatively coarse mesh was used, the results showed that the model was able to predict behaviour up to ultimate load. However, the post-buckling behaviour was much more difficult to predict. Laboratory tests were also conducted for the purpose of calibrating the model. A parameter study was carried out to determine the ultimate axial load capacity of 121 equal angle struts and 88 unequal angle struts covering slenderness ratios from 30 to 300. Comparison of the results with nominal axial strength prescribed by the design rules given in the New Zealand Steel Structures Design Standard, NZS 3404 [38], revealed significant conservatism.

The aforementioned research work on second-order analysis were solved by numerical solution techniques. A closed-formed solution of the lateral deflection of an eccentrically loaded planar beam-column was developed by Kalaga and Adluri [39] using a potential energy approach based on the nonlinear Green strain tensor. The initial curvature of the beam-column was considered and a sine curve displacement function was assumed. By applying the formulation to a steel beam-column with a slenderness ratio of 200, it was shown that it was possible to develop reasonably accurate closed-form solutions for nonlinear beam-column for large-deflection. However, the method so far is only suitable of analysis of single member bending about one axis. The authors suggested the concept can be extended to biaxial bending and inelastic behaviour.

2.3.3 Second-order analysis for design purpose

The advantage of the second-order analysis over the traditional linear analysis is that the former is capable of accurately predicting the structural response of a steel structure under loading, thus enabling the engineers to design more economically and safely. However, the second-order analysis methods mentioned above were mostly used for research purpose, for example, to study the structural behaviour of an isolated loaded member, and rarely used in routine design in the past decades because of the enormous amount of computer time and effort required for the analysis. Although satisfactorily accurate results can be obtained by using more elements per member, it will not only cause inconvenience, but also require heavy computational time especially when a large structure under many load cases is analysed. To date, the widespread use of personal computer not only facilitates researchers to carry out studies on second-order and advanced analysis, but also provides an excellent opportunity for engineers to design structure by the second-order analysis. In order to popularize the use of advanced design method among engineers, the method must be user-friendly with only a few elements per member required to achieve satisfactory accuracy. However, in the presence of axial force, the bending stiffness coefficients are no longer constant but dependent on the magnitude and sign of the axial force, which is a function of displacements and rotations of the element, making using a single element using a cubic deflection curve not possible.

Al-Bermani and Kitipornchai [40] proposed an approach allowing the use of least elements in a nonlinear analysis accounting for both the geometric and material

nonlinearity, based on an updated Lagrangian formulation. The procedure is suitable for analyzing large-scaled space frames since the structures may be modelled using only a few elements per member. It is achieved by incorporating a displacement stiffness matrix which provides the necessary coupling between the axial, flexural and torsional deformations. However, this element does not allow for member initial imperfection, which is mandatory in some national design codes such as Eurocode 3 [41]. For simulation of member initial imperfection, two or more elements per member will be required.

Chan and Zhou [42] and Zhou and Chan [43] developed a self equilibrium pointwise equilibrating polynomial (PEP) element for slender frames. Their element, derived from a fifth-order displacement function, is capable of dealing with second-order analysis using a single element for each member. The reliability and accuracy of the PEP element can be checked by predicting the elastic buckling load of a strut using a single element strut. Interestingly, their PEP element gives a negligible error while the cubic element considerably overestimates the buckling load. However, this PEP element is still inappropriate for practical design purpose, because the mandatory requirement for member imperfection in various design codes cannot be incorporated into the analysis which can only be achievable when using more than one element per member. After all, the negligence of member initial imperfection is dangerous in actual design. Chan and Zhou [44,45] improved the PEP element so that the member initial imperfection is included. The distributed member load can also be allowed for. It was illustrated with some worked examples that the member initial imperfection undoubtedly had an adverse

effect over the behaviour of a structure. Although it was shown that the initial imperfection is less important when the stability of a structure is controlled by the global $P-\Delta$ effect and more significant when the local $P-\delta$ effect dominates the structural behaviour, it is recommended to include member imperfection in a general second-order analysis because it may not be obvious to judge the importance of the $P-\Delta$ and the $P-\delta$ effects.

Chan and Gu [46] proposed another exact element derived from the differential equilibrium equation, which requires a slightly more complicated expression for the tangent stiffness matrix than the PEP element by Chan and Zhou [44]. The difference between these two approaches lies in their completely different formulations. For the PEP element, a fifth order displacement function is assumed that adopts the energy principle and follows a standard finite element procedure to derive the element stiffness matrix. For the present curved stability function approach, the equilibrium equation is used to formulate the element, and no previous assumption of displacement function is required. In addition to structural instability, material yielding of structural members is also a major factor controlling the ultimate load of a structure. In the inelastic range, material yielding limits the moment capacity of a cross-section. The cross-section cannot further resist any moment when the section capacity is reached. For framed structures, plastic analysis can be broadly classified into two main types, namely the plastic zone method and the plastic hinge method. In the plastic zone approach, all the beam and column members of a structure are discretized into a number of elements and each cross-section is also further divided into a number of small fibers with the

fundamental stress-strain relationship is explicitly and directly used for moments and forces computation. In contrast, in the plastic hinge approach material yielding is accounted for by zero-length plastic hinges at the end(s) of each element. Plasticity is assumed to be lumped only at the two ends of an element, while the portion within the element is assumed to remain elastic throughout the analysis. The plastic zone method is more accurate than the plastic hinge method. However, owing to the huge amount of calculation work required, the plastic zone approach is more suitable for simple structures. The plastic hinge method is considered more efficient and thus preferred in practical engineering design.

In order to incorporate inelastic design into second-order analysis, Chen and Chan [47] derived an element allowing for the formulation of plastic hinges at the mid-span and two ends. The transfer of fix-ended moments from the member loads is allowed for in the analysis by inserting spring elements at the mid-span and two ends. This transferred moment will not be constant but dependent on the spring stiffness for modelling plastic hinges which will be automatically computed in the analysis. The process of gradual formation of a plastic hinge can be simulated by reducing gradually the connection stiffness. At the extreme cases of fully plastic and perfectly elastic section, the tangential connection stiffness is respectively equal to zero and infinity, which in actual computer implementation is taken as 0 and 10^9 of the element stiffness. The use of the present element will reduce not only the computer time, but also the data manipulation effort for a second-order plastic-hinge analysis.

Zhou and Chan [48] and Chan and Zhou [49] modified the PEP element to plastic point-wise equilibrium polynomial (PPEP) element by adopting a simple concept of superimposition of triangular deflected shapes due to the formation of plastic hinge to the fifth order deflection shape for elastic deflection to yield the final deflection of the element. The plastic hinge due to the combined effects of the moments and the axial force is located and the effect of plastic hinge in the stability is incorporated into the second-order analysis. The investigation began with one plastic hinge along member and was widened to three hinges along member; two at the two ends and one at the location of maximum combined stress due to axial force and moment. The proposed method takes advantage of residual strength after the first yield of first plastic hinge occurs and thus leads to a more economical design.

2.3.4 Flexural-torsional buckling analysis

Most framed structures are three-dimensional in terms of geometry, loading and structural behaviour. To simplify the analysis, usually a three-dimensional framed structure is considered as a number of two-dimensional frames. However, such simplification may not provide an adequate description of the actual behaviour of the structure. For example, a short angle strut may fail in a flexural-torsional buckling mode which is usually ignored in a two-dimensional analysis. In spite of the actual behaviour is three-dimensional, it is sensible to say that flexural-torsional buckling may not be critical in practical structures provided that sufficient lateral restraints are provided. However, in order to accomplish the complete buckling check by advanced analysis allowing for second-order effects due to axial force

and moment coupled with displacement and twist in a moderately large rotation range, Gu and Chan [50] formulated the tangent stiffness matrix for geometrically nonlinear analysis allowing for Euler, lateral and torsional buckling. In the proposed formulation, three deformation matrices due to axial force and moments, which represent the higher order-effects due to axial force and moments in the element, are derived. These matrices are then used together with linear and geometric stiffness for beam elements to analyze the structural behaviour of space frames which comprise members with negligible warping effects. Numerical examples demonstrate that the proposed element is accurate and efficient in predicting the higher-order behaviour.

2.4 Analyses of steel framed structures

White and Hajjar [51] studied two stability design approaches that are alternatives to the traditional buckling-solution based procedure, which uses the effective length factor to take into account differing end restraints in columns. The first approach is an elastic design approach based on the modification of the first-plastic hinge concept, which uses the actual column length in conjunction with notional lateral loads acting at each storey level. This procedure is also termed as the notional load approach and is permitted in various national codes such as, Australian Standard AS 4100 [27], Eurocode 3 [41], AISC LRFD [52] and the British Standard BS 5950: Part 1 [3]. The notional lateral load acting on each storey is to take into account the storey out-of-plumbness imperfection under gravity loads. An overview of the approach is given in Ref. [53]. The second

approach is based on rigorous advanced analysis, which is described previously in Section 2.3. The approach is capable of capturing member three-dimensional inelastic stability behaviour accurately. Although the former approach can give reasonable estimates of buckling loads about strong axis and weak axis, it tends to be conservative for lateral-torsional beam-column failure. On the other hand, the latter approach captures the interaction between framing members due to progressive inelastic redistribution of stiffness and strength. In addition, advanced analysis provides an efficient and flexible analysis and design method by eliminating the need to check the section capacity factor of members separately, and in the meantime providing significantly more information about the idealized structural response.

The second-order analysis and design method is widely used in designing large latticed structures, such as transmission towers, which are widely regarded as one of the most difficult forms of lattice structure to analyze. One of the reasons is it is difficult to estimate the correct wind speed. Another reason is it is difficult to assume a correct effective length. Traditionally, full-scale testing of towers has formed an integral part of the tower design. Stress calculations in the tower are normally obtained from a linear elastic analysis in which the bracing members are assumed to have pinned connection. However, such conditions rarely exist; results from full-scale tests often show that bending stresses in members could be as high as axial stress [54]. Therefore, the present technique of designing tower may not be adequate under complex loading conditions. Albermani and Kitipornchai [55] proposed a nonlinear analytical technique; the tower is modelled as an assembly of

beam-column elements. Linear, geometric and deformation stiffness matrices are used to describe the behaviour of a general thin-walled beam-column element in an updated Lagrangian framework. The method was employed to predict failure loads and failure modes of a number of tested towers. The results are in good agreement with those obtained from tests. Kitipornchai et al. [56] developed a model to assess the effect of bolt slippage on the structural behaviour of lattice structures. Due to insufficient reliable experimental data, the model cannot be used for practical purposes. Ungkurapinan et al. [57] studied the behaviour of joint slip in steel electric transmission towers. 36 joint tests were carried out and mathematical expressions to describe slip and load-deformation behaviour were developed. Values calculated from the expressions can be used in Kitipornchai et al.'s models [56] and the joint deformation should be incorporated in a second-order analysis. Shakourzdeh et al. [58] derived a numerical method to take into consideration the deformation of the joint connections in linear, nonlinear and stability of three-dimensional thin-walled space frames. The authors demonstrated the importance of connection behaviour for determining the overall stability and ultimate strength of framed structures through numerical examples.

Kang et al. [59] proposed a finite element model (FEM) in which member continuity, the asymmetrical sectional properties of members, the eccentricity of connections, and geometrical and material nonlinearities are considered. The proposed FEM is verified using experimental results. Kang et al. [59] pointed out that the pin-ended assumptions and the negligence of secondary bracing may be too conservative for a tower design. In fact, the connection rigidity of the bracing

members significantly affects the ultimate load capacity. Rigid connection increases the buckling capacity. However, it may not be realistic or involves a large amount of construction cost. In summary, in design a lattice tower, the assumption of connection rigidity should be realistic; otherwise, the buckling capacity of it will be either overestimated or underestimated, which would be consequently either uneconomical or dangerous.

Teh et al. [60] demonstrated the global buckling behaviour of high-rise steel storage rack frames is hardly revealed by commonly used two-dimensional (2D) buckling analyses as three-dimensional (3D) interaction modes are involved and not captured. It is shown that the monosymmetric upright columns of a high-rise rack frame fail in a flexural-torsional mode due to the shear-centre eccentricity of the sections, and that the 3D buckling analysis is more reliable in determining the critical member of a rack frame. However, in routine design, 2D analyses in the down aisle and in the cross-aisle directions are performed independently. Current steel storage rack design standards such as AS 4084 [61] combine independent 2D flexural buckling analyses and simplified flexural-torsional buckling analysis of individual columns to account for 3D behaviour. However, the use of the 2D design procedure based on the simple effective length factor of 1.0 for a braced frames results in overestimation for the elastic flexural-torsional buckling strength of the upright columns; while the effective length factor assumption of 1.7 for an unbraced frame results in underestimation of the strength of the frame, which are not consistent with 3D buckling analysis.

It can be seen from the literature review that second-order analysis of frames does not cover angle sections which are characterised by asymmetric cross section and eccentric connections. This thesis is devoted to fill this gap and to make the design method a valuable tool for analysis of this type of steel frames. As can be seen in the following chapters, the technique is calibrated against code recommendations and used for design of a practical angle trusses which are further compared against the hand calculation.

2.5 Concluding Remarks

The literature review consists of three parts. The first part focuses on the classical analysis of angle compression members which enables us to understand the structural behaviour of angle members loaded either concentrically or eccentrically. The second part focuses on the development of nonlinear analysis of steel structures of both symmetrical and asymmetrical sections. The second-order analysis gives us a better understanding on the structural behaviour of angle compression members in a more complex configuration and the structural response of steel framed systems. However, a great deal of time and money involved in computer analysis in the old days prohibited the widespread use of second-order analysis in routine design. In recent years, as computer technology advances, personal computers become popular and indispensable in our daily life. This provides a golden opportunity to adopt second-order analysis in routine design. The last part is a literature review of analyses of steel frames. There are a number of alternative approaches to assess the load carrying capacity of a steel framed system

on top of the traditional effective length factor method including the notional load method and the second-order analysis. Many researchers and engineers consider the second-order analysis is capable of capturing the true equilibrium path of the structure and produces a more rational design of steel structures.

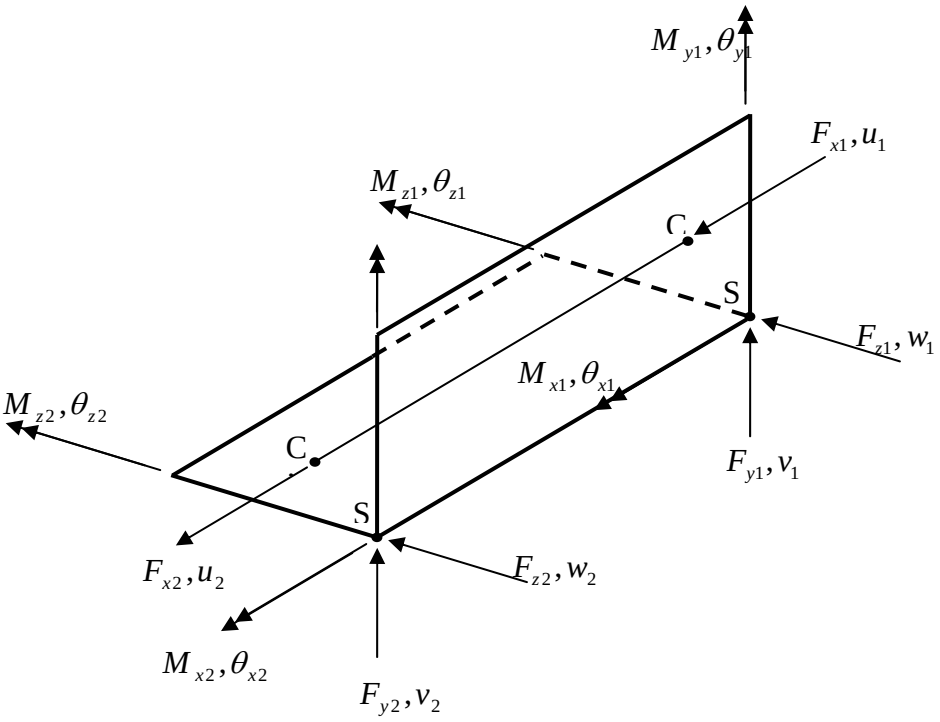

Fig. 2.1 A general angle element

Chapter 3 Review of Current Design Methods

3.1 Introduction

A review of literature shows that, depending on cross-sectional configurations, eccentricities and effective lengths, single-angle struts usually fail by the following modes:

- flexural buckling about the principal minor axis
- flexural buckling about the geometrical axes
- flexural-torsional buckling
- interaction between local and global buckling and
- local plate buckling

The design rules regarding flexural buckling were already well developed in many national codes. The effort required to solve for the cubic equation prohibits the consideration of flexural-torsional buckling mode in routine design, in addition to its assumption of elastic material behaviour. For stocky struts, flexural-torsional buckling may be more critical. So, the current design rules may be inadequate. This chapter gives a review of current design practice for eccentrically loaded angle struts. The national design codes being reviewed include the British Standard, Hong Kong Code, European Standard, American Standard and Australian Standard. In addition, the conventional design process will also be explained in details.

3.2 Current design methods for angle struts

3.2.1 British Standard

BS 5950 Part 1:2000 [3] states that for single-angle struts connected to a gusset plate or directly to another member at each end or by an equivalent welded connection may be treated as axially loaded with reduced compressive strength, ignoring the eccentricity due to the end connections and modifying the effective slenderness ratio. When, at end connections, two or more bolts are used in standard clearance holes in line along the angle, or by an equivalent welded connection, the slenderness λ should be taken as the greatest of:

$0.85\lambda_v$ but $\geq 0.7\lambda_v + 15$

$1.0\lambda_a$ but $\geq 0.7\lambda_a + 30$

$0.85\lambda_b$ but $\geq 0.7\lambda_b + 30$

where λ_v, λ_a and λ_b are the slenderness ratios about minor v-v axis, the a-a axis parallel to the attached leg and the b-b axis parallel to the outstanding leg as shown in Figure 3.1.

If a single bolt connection is used at each end, the compression resistance should be taken as 80% of the compression resistance of an axially loaded member and the slenderness λ should be taken as the greatest of:

$1.0\lambda_v$ but $\geq 0.7\lambda_v + 15$

$1.0\lambda_a$ but $\geq 0.7\lambda_a + 30$

$1.0\lambda_b$ but $\geq 0.7\lambda_b + 30$

3.2.2 European Standard

Eurocode 3 [41] allows the direct use eccentricities and end fixities in the design of angles as web members in compression provided that the chords provide appropriate and adequate end restraint to web members made of angles and the end connections of such web members supply appropriate fixity (at least two bolts if bolted). The slenderness ratio should be taken as the greatest of:

$$33\varepsilon + 0.7\lambda_v$$

$$47\varepsilon + 0.7\lambda_Y$$

$$47\varepsilon + 0.7\lambda_Z$$

where $\varepsilon = \sqrt{\frac{235}{p_y}}$

λ_v, λ_Y and λ_Z are respectively the effective slenderness ratios about minor v-v axis and the Y-Y and Z-Z axes which are parallel to the two legs as shown in Figure 3.2. However, when only one bolt is used for end connections of angle web members, the eccentricities should be taken into account considering the interaction of bending and axial force.

3.2.3 Hong Kong Standard

In Hong Kong Steel Code [62], for web members, buckling about principal axes and axes parallel to the legs should be considered. For angle sections connected by two or more bolts, the slenderness ratio should be calculated from the larger of the actual member length and the following:

$0.35 + 0.7\lambda_v / (93.9\varepsilon)$

$0.5 + 0.7\lambda_x / (93.9\varepsilon)$

$0.5 + 0.7\lambda_y / (93.9\varepsilon)$

where $\varepsilon = \sqrt{\frac{275}{p_y}}$ and λ is the effective slenderness ratio.

λ_v, λ_x and λ_y are respectively the slenderness ratios about minor v-v axis and the x-x and y-y axes parallel to the two legs. For a single bolt connection, 80% of the axial force compression resistance of the double bolt connection should be used. The code states that for short members, the effect of load eccentricity should be considered analytically. As an alternative, the buckling strength can be designed using the combined axial force and moment equation, or by a second-order analysis allowing for eccentric connections and member imperfections such as using an equivalent member imperfection giving the same compressive strength.

3.2.4 American Standard

In the AISC LRFD Specification for Single-Angle Members [63], the design strength of compression angle members shall be taken as $\phi_c P_c$

where $\phi_c = \text{resistance factor for compression} = 0.90$

$$P_c = A_g p_c \tag{3.1}$$

a. For $\lambda_c \sqrt{Q} \le 1.5$

$$p_c = Q\left(0.658^{Q\lambda_c^2}\right) p_y \tag{3.2}$$

b. For $\lambda_c\sqrt{Q} > 1.5$

$$p_c = \left[\frac{0.877}{\lambda_c^2}\right] p_y \tag{3.3}$$

where $\lambda_c = \frac{KL}{r\pi}\sqrt{\frac{p_y}{E}}$

$Q =$ reduction factor for local buckling

K is the effective length factor to accommodate the various end conditions. According to the Commentary on Section E2, Equations (3.2) and (3.3) are based on a reasonable conversion of research data into design equations. For members whose design is based on compressive force, the largest effective slenderness ratio preferably should not exceed 200. AISC LRFD [63] does not provide a simplified approach in designing eccentrically loaded angles, which should be designed as members in combined flexure and axial forces.

The interaction of flexure and axial compression applicable to specific locations on the cross section shall be limited by the following equations:

For $\frac{F_c}{\phi_c P_c} \geq 0.2$

$$\left|\frac{F_c}{\phi_c P_c} + \frac{8}{9}\left(\frac{M_y}{\phi_b M_{cy}} + \frac{M_z}{\phi_b M_{cz}}\right)\right| \leq 1.0 \tag{3.4}$$

For $\frac{F_c}{\phi_c P_c} \leq 0.2$

$$\left| \frac{F_c}{2\phi_c P_c} + \left(\frac{M_y}{\phi_b M_{cy}} + \frac{M_z}{\phi_b M_{cz}} \right) \right| \leq 1.0 \qquad (3.5)$$

where F_c = axial compression

M_y, M_z = maximum moment about y-y and z-z axes

M_{cy}, M_{cz} = compression capacity about y-y and z-z axes

ϕ_b = resistance factor for flexure $= 0.90$

The interaction equations shall be evaluated for the principal bending axes either by considering the sense of the associated flexural stresses at the critical points of the cross section, the flexural terms are either added to or subtracted from the axial load term.

3.2.5 Australian Standard

In AS 4100 [27], single angle web compression members in trusses which are connected with at least by two bolts or by welding at their ends and loaded through one leg shall be designed to satisfy the following:

$$\frac{F_c}{\phi P_c} + \frac{M_a}{\phi M_{cz} \cos\alpha} \leq 1 \qquad (3.6)$$

where M_a = the design end moment about a-a axis parallel to the attached leg

ϕ = the capacity factor

α = the angle between z-z and a-a axis

The design end moment M_a shall be taken as not less than $F_c \cdot e$, resulting from the out-of-plane load eccentricity e,

where $e = c_a - \frac{t}{2}$ for angles on the same side of the truss chord, or

$e = e_c + e_t$ for angles on opposite sides of the truss chord

(see Figure 3.3)

3.2.6 Summary

As a concluding remark, BS 5950 [3], Eurocode 3 [41] and Hong Kong Steel Code [62] provide a faster design approach for eccentrically load single angle compression members but seem to be overly simplified as the effects due to end restraints and load eccentricity are ignored. AISC LRFD [63] and AS 4100 [27] are more rational to consider the load eccentricity in design explicitly. However, the method of determining the effective length is still controversial for some time. The first three design codes assume that the two ends of the members are immovable. In the last two design codes the value of the member effective length factor are determined on the basis of the rotational and the translational restraints at the ends of the member. In addition, since many of the design rules in codes are developed based on minor axis flexural buckling, they may not be adequate especially for stocky members which are susceptible to flexural-torsional buckling.

3.3 Conventional design method

3.3.1 Design Procedure

The previously mentioned design codes, which are widely used today, were developed based on nonlinear analysis of simple idealized individual members. However, the conventional design procedure of structural steelwork is based on linear analysis with the nonlinear effects ignored which means an element of the structure is having a constant stiffness independent of the deformations and magnitude of member forces. Mathematically, this condition can be presented as:

$$F = K \cdot u \tag{3.7}$$

in which K is the element stiffness matrix, u is the displacement vector and F is the force vector of a structural system.

When designing a steel structure, first of all, a linear analysis is carried out to determine the internal forces and moments of all members under external loads. After that, the resistance of each individual member is determined according to the design rules given in the codes to account for the nonlinear effects. A sufficiently safe structure is having its resistance larger than the factored forces and moments according to this method. The relationship can be written as:

$$\phi R \geq \lambda F \tag{3.8}$$

in which ϕ is the material factor, R is the resistance of the structure, λ is the load factor.

The process of the conventional design is summarized schematically in Figure 3.4. A typical buckling resistance check equation is shown as follows:

$$\frac{P}{A_g p_c} + \frac{M_y}{S_y p_y} + \frac{M_z}{S_z p_y} \leq 1 \tag{3.9}$$

in which p_c is the design compressive strength, p_y is the design yield strength, P is the external force applied to the section, A_g is the gross cross-sectional area, M_y and M_z are the external moments about the y and z axes respectively and S_y and S_z are the section modulus about y and z axes respectively.

3.3.2 Advantages and disadvantages of linear analysis

A special feature of linear analysis is the validity of the principle of superposition of different load cases because of the assumption of constant element stiffness. Therefore, the force diagram of ultimate load of the structure can be simply obtained by summing individual force diagrams of various load cases. However, the linear theory is only applicable for structures with small displacements and a less severe degree of nonlinearity. In fact, the realistic structural behaviour is nonlinear. The nonlinear behaviour can be demonstrated by compressing a column of intermediate slenderness range. Because of the presence of initial geometric imperfection, bending occurs immediately when the load is applied instead of buckling at the elastic buckling load as shown in Figure 3.5. This type of nonlinearity can be regarded as the $P-\delta$ effect. In a linear analysis, the column is assumed to be perfect and will only shorten with the axial load applied and the calculated compressive stress is distributed evenly over the cross section; while, in

actual fact, the true compressive stress is distributed linearly over the cross section in the elastic range because of the bending action. In the design stage, in order to compensate compressive stress due to flexure, the compressive strength of the column is reduced from p_y to p_c according to the Perry-Robertson formula with the assumed effective length of the column. The effective length factor is largely dependent on the end conditions of the member. Therefore, the checking of the buckling resistance is carried out as an independent stage instead of an integrated part of design. Another nonlinear effect can be demonstrated by applying a point load at the mid-span of a beam as shown in Figure 3.6. Under the point load, the beam will deflect vertically and horizontally. However, the horizontal displacement is relatively small compared with the vertical displacement and is usually ignored in analysis. Although, it is sufficiently safe to ignore the horizontal displacement in a structural design if the horizontal displacement is small, it will be dangerous to exclude this effect for slender steel structures with large deflections. These types of simple elements rarely exist in real structure; in fact, the joints which an element is connected to may move and affect the compression capacity and the accuracy of the compressive strength estimated by the design codes is highly dependent on the assumptions of the effective length. If the assumed effective length is longer than the actual effective length, the design may be too conservative. Likewise, if the assumed effective length is shorter than the actual effective length, the design may be insufficiently safe. Consequently, any incorrect assumptions of effective length may lead to an uneconomical design or an unsafe design. This design procedure shows an inconsistency between analysis and design. The collective effect of the $P-\Delta$ and $P-\delta$ is best illustrated by a two-storey frame subject to two vertical

point loads at the top as shown in Figure 3.7. Globally, the local deflection and the global displacements in fact mutually affect each other and the structural response of the other members as well and should not be ignored in analysis. In a linear analysis, the interactions with buckling, connection behaviour and other second-order effects are always ignored. Therefore, this type of analysis is incorrect in calculating forces and moments. The best way to eliminate the inconsistency between analysis and design is to carry out a second-order analysis which is going to be described in details in Chapter 4.

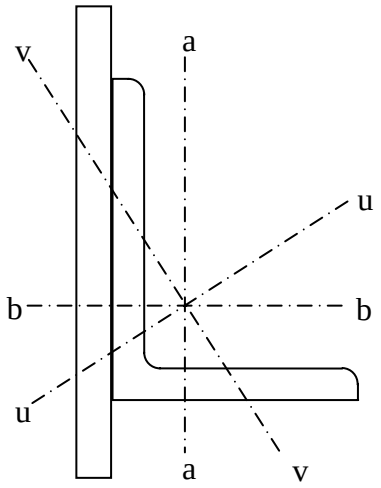

Figure 3.1 Axes of an angle section compliant with BS 5950

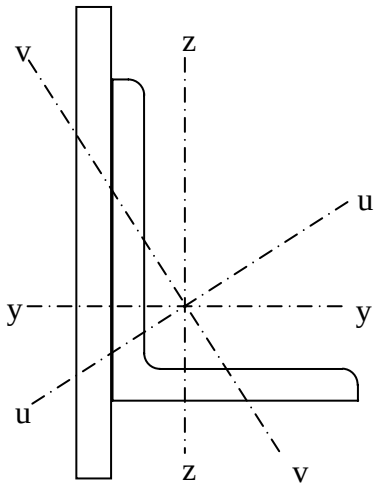

Figure 3.2 Axes of an angle section compliant with Eurocode 3

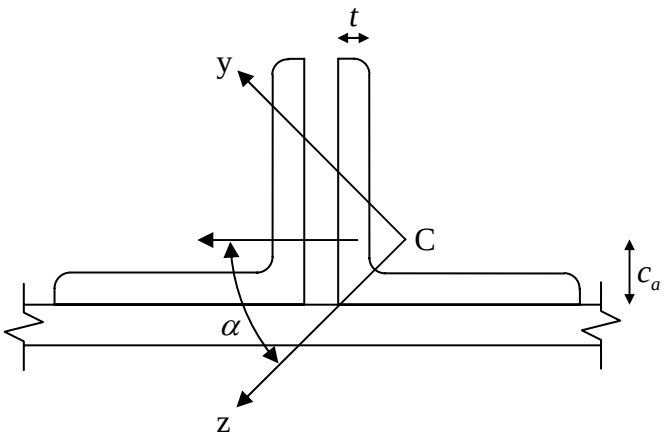

(a) Angles on same side

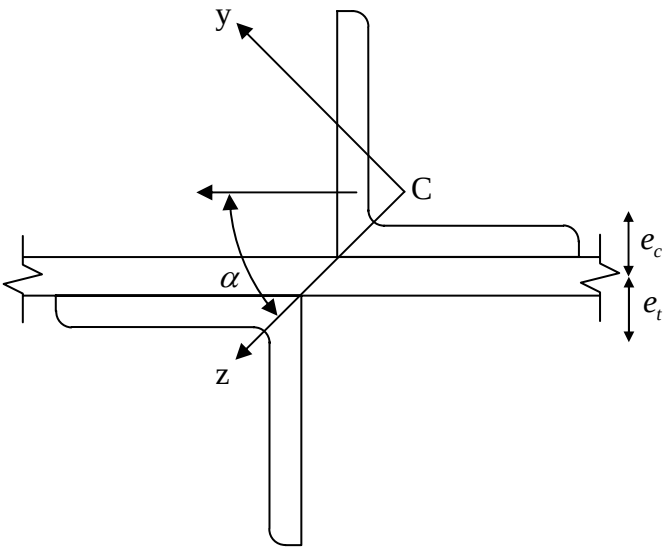

(b) Angles on opposite sides

Figure 3.3 Single angles loaded through one leg

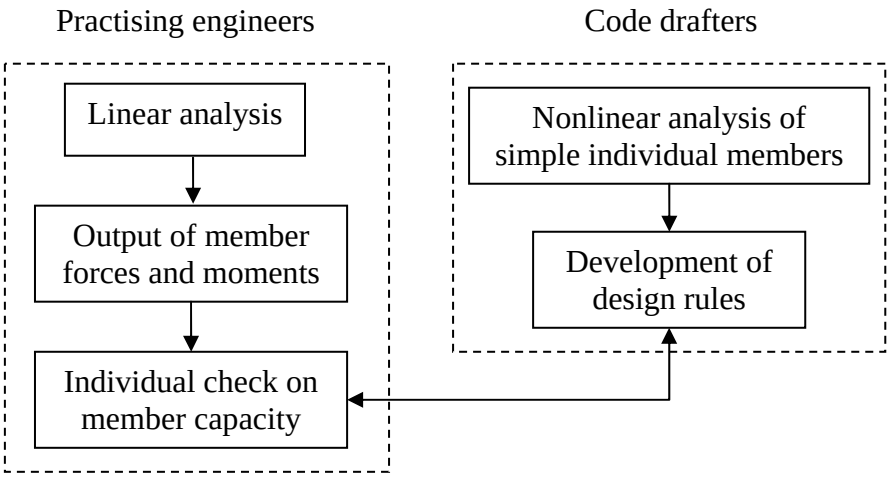

Figure 3.4 Conventional design procedure

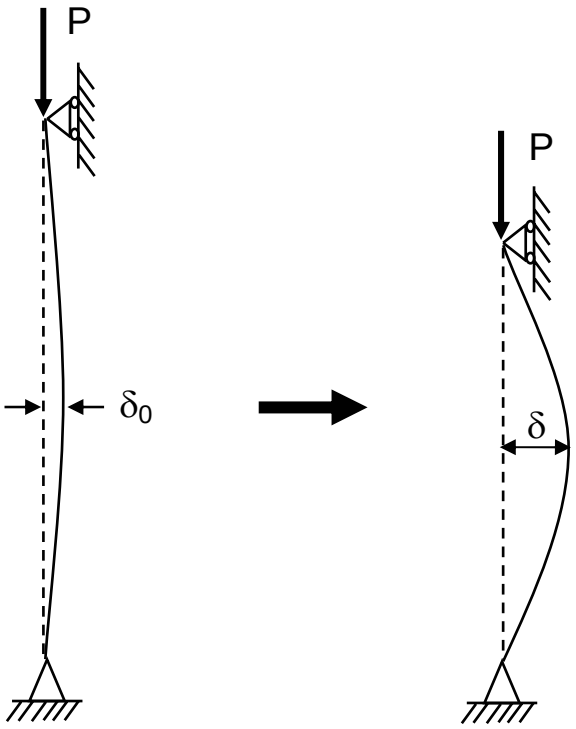

Figure 3.5 Bending of column due to presence of initial imperfection

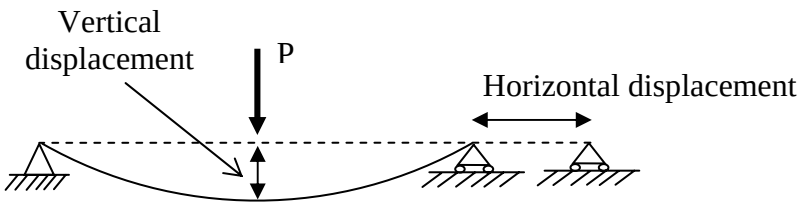

Figure 3.6 Shortening of beam due to lateral load

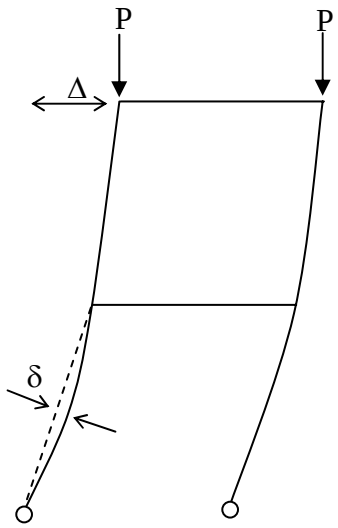

Figure 3.7 Change of structural geometry of a steel frame

Chapter 4 Second-order Analysis and Design using Incremental-iterative Numerical Methods

4.1 Introduction

The conventional design procedure has been widely used because during the pre-computer age when the computer time was expensive, linear analysis seemed to be the best choice of analysis as it requires the least amount of computer time and effort. Today, the prevalence of low-cost personal computers and the growing importance of environmental and economical concerns provide a golden opportunity to develop a second-order analysis method. In this method, which has been well-researched by Chen and Chan [47], Chan and Zhou [44], Chan and Chui [33], Chan [64], both the first-order and second-order effects are included during the analysis. In other words, the member deflection (δ), together with the global displacment (Δ), is taken into account so that section capacity check is adequate for strength design as follows:

$$\frac{P}{A_g p_y} + \frac{M_y + P(\delta_z + \Delta_z)}{Z_y p_y} + \frac{M_z + P(\delta_y + \Delta_y)}{Z_z p_y} = \phi \le 1 \qquad (4.1)$$

in which p_y is the design strength, P is the external force applied to the section, A_g is the cross-sectional area, M_y and M_z are the external moments about the y and z axes respectively and Z_y and Z_z are the section modulus about y and z axes respectively.

$P(\delta_z + \Delta_z)$ and $P(\delta_y + \Delta_y)$ are the moments due to the change of member stiffness under load and large deflection effects of which the consideration, incorporating the initial imperfections, allows for the effect of "effective length" automatically. In addition, the characteristics of realistic structure (e.g. initial imperfection and residual stresses) are also considered in the analysis so the design is completed readily with the analysis. The process of a non-linear analysis design is summarized in Figure 4.1. Equation (4.1) captures the essence of second-order analysis that a simple section capacity check equation with the $P-\delta$ and $P-\Delta$ moments considered is already enough for stability check. As such, it is unnecessary to use the reduced compressive strength, p_c to calculate the axial strength in the proposed second-order design method. In a theoretical term, the reduction of buckling strength for a more slender structure can hardly be understood in a simple engineering term unless we explain the phenomenon as an increase in $P-\delta$ and $P-\Delta$ effects. The effective length concept can hardly be established here since the relationship between the buckling resistance of a complex but slender structure and the effective length cannot be established numerically.

4.2 The tangent stiffness matrix

The element stiffness matrix allowing for the presence of axial force can be derived from the differential equilibrium equation directly using the stability function method. Alternatively, the element stiffness matrix can be derived from an assumed

displacement function using the total potential energy method. By the principle of stationary potential energy, the linear and geometric stiffness matrices can be derived by substituting the displacement function into the energy function and differentiating twice the energy function with respect to the degrees of freedom as

$$\frac{\partial^2 \Pi}{\partial x_i \partial x_j} = \left[k_L + k_G\right] \tag{4.2}$$

in which Π is the energy function, k_L is the linear stiffness matrix, k_G is the geometric stiffness matrix, and x_i, x_j are the nodal degrees of freedom.

The energy functional of a general beam-column element as shown in Figure 4.2 corresponding to the action of an axial force can be expressed as:

$$\Pi = \frac{1}{2}\int_0^L EI\left(\frac{d^2v}{dx^2}\right)^2 dx + \frac{P}{2}\left(\frac{dv}{dx}\right)^2 dx + M_1\theta_1 + M_2\theta_2 + F_1v_1 + F_2v_2 \tag{4.3}$$

A standard procedure of deriving an element stiffness matrix from an assumed cubic displacement function is shown as follows.

We should firstly establish a polynomial for the deflection of the element. If we have 4 degrees of freedom, namely the two displacement and the two rotational degrees of freedom, we use cubic polynomial as displacement function which has also 4 coefficients so that the coefficients can be solved. Thus,

$$v = a_0 + a_1x + a_2x^2 + a_3x^3 \tag{4.4}$$

The displacement function can then be solved with appropriate boundary condition. For demonstration purpose, the following simple boundary conditions of a simply supported column are used:

$$x = 0;\ \ v = 0;\ \frac{\partial v}{\partial x} = \theta_1 \tag{4.5a}$$

$$x = L;\ \ v = 0;\ \frac{\partial v}{\partial x} = \theta_2 \tag{4.5b}$$

Thus,

$$v = \left[x - \frac{2x^2}{L} + \frac{x^3}{L^2} \quad -\frac{x^2}{L} + \frac{x^3}{L^2} \right] \left[\theta_1 \quad \theta_2 \right] \tag{4.6}$$

The linear and geometric stiffness matrices can be derived by substituting Equation (4.6) into Equation (4.2) and differentiating twice the energy function with respect to the degree of freedom as

$$\left[k_L + k_G \right] = \frac{EI}{L} \begin{bmatrix} 4 & 2 \\ 2 & 4 \end{bmatrix} + P \begin{bmatrix} \frac{2L}{15} & -\frac{L}{30} \\ -\frac{L}{30} & \frac{2L}{15} \end{bmatrix} \tag{4.7}$$

Element stiffness matrices can also be derived with other assumed displacement functions in a similar fashion. The matrix in Equation (4.7) can also be used for bifurcation analysis. Mathematically, as described in Chapter 1, the structural system will buckle when the determinant of the matrix vanishes, i.e.

$$\left|k_L + \lambda k_G\right| = 0 \tag{4.8}$$

in which | | represents the determinant of the bracketed matrix.

Therefore, if only one single cubic polynomial is considered as a displacement function, the buckling load of a simply supported column can be found from manipulating Equation (4.7) as,

$$P = \frac{12EI}{L^2} \tag{4.9}$$

The percentage of difference between the buckling load in Equation (4.9) and the analytical Euler load is 21.6%. This illustrated that one element per member is not sufficient for second-order analysis using element derived from cubic displacement function. A higher accuracy can be achieved by using more elements per member. However, this bifurcation analysis is only based on a mathematical idealization that the structure deforms only in the loaded directions until the bifurcation load is reach which is not suitable for all kinds of structures. To predict more accurately the response of a structure under load, load-deflection analysis is needed which traced the true equilibrium path for the structure and the stresses and deflections are continuously updated.

4.3 The secant stiffness matrix

To illustrate load-deflection analysis, it is also necessary to derive the secant stiffness matrix. The secant stiffness relations between the moments and rotations

can be obtained by the first variation of the total potential energy given in Equation (4.3) as:

$$\Delta M_1 = \left(\frac{4EI}{L} + \frac{2PL}{15}\right)\Delta\theta_1 + \left(\frac{2EI}{L} - \frac{PL}{30}\right)\Delta\theta_2 \tag{4.10}$$

$$\Delta M_2 = \left(\frac{2EI}{L} - \frac{PL}{30}\right)\Delta\theta_1 + \left(\frac{4EI}{L} - \frac{2PL}{15}\right)\Delta\theta_2 \tag{4.11}$$

in which Δ represents the incremental form of the quantities, L is the deformed length.

The axial force can be obtained directly from the change in element length as

$$u_x = u_a + u_b \tag{4.12}$$

in which u_x, u_a and u_b are the total, the axial and the bowing shortenings respectively. u_a can be obtained directly by subtracting the deformed length by the initial length of the element calculated from the coordinates of the element nodes while u_b is given by:

$$u_b = \frac{1}{2}\int_0^L \left(\frac{\partial v}{\partial x}\right)^2 dx$$

$$= \frac{L\left(2\theta_1^2 - \theta_1\theta_2 + 2\theta_2^2\right)}{30} \tag{4.13}$$

The incremental form of Equation (4.13) can be obtained by taking a variation on the equations as:

$$\Delta u_x = L_{i+1} - L_i + \frac{L}{30}\left[4\Delta\theta_{y1}\cdot\theta_{y1} - \Delta\theta_{y1}\cdot\theta_{y2} - \theta_{y2}\cdot\theta_{y1} + 4\Delta\theta_{y2}\cdot\theta_{y2}\right] \tag{4.14}$$

With the secant stiffness relationships, the resistance of the element can be evaluated in an incremental manner.

4.4 The transformation matrices

Before carrying a second-order analysis, the element stiffness matrix $[k_L + k_G]$ must be transformed from the local system to the global system. If an element has 6 degrees of freedom, namely $\lfloor \delta_x \quad \theta_{y1} \quad \theta_{z1} \quad \theta_x \quad \theta_{y2} \quad \theta_{z2} \rfloor$, these 6 independent forces and moments are required to be expressed in terms of 12 degrees of freedom as:

$$[F] = [T][P] \tag{4.14}$$

in which

$[F]$ is the 12 × 1 local element force vector $[F_{x1} \quad F_{y1} \quad F_{z1} \quad M_{x1} \quad M_{y1} \quad M_{z1} \quad F_{x2} \quad F_{y2} \quad F_{z2} \quad M_{x2} \quad M_{y2} \quad M_{z2}]^T$

$[P]$ is the 6 × 1 elemental force vector $[F_x \quad M_{y1} \quad M_{z1} \quad M_x \quad M_{y2} \quad M_{z2}]^T$

$[T]$ is the transformation matrix as

$$[T]=\begin{bmatrix} -1 & 0 & 0 & 0 & 0 & 0 \\ 0 & 0 & 1/L & 0 & 0 & 1/L \\ 0 & -1/L & 0 & 0 & -1/L & 0 \\ 0 & 0 & 0 & -1 & 0 & 0 \\ 0 & 1 & 0 & 0 & 0 & 0 \\ 0 & 0 & 1 & 0 & 0 & 0 \\ 1 & 0 & 0 & 0 & 0 & 0 \\ 0 & 0 & -1/L & 0 & 0 & -1/L \\ 0 & 1/L & 0 & 0 & 1/L & 0 \\ 0 & 0 & 0 & 1 & 0 & 0 \\ 0 & 0 & 0 & 0 & 1 & 0 \\ 0 & 0 & 0 & 0 & 0 & 1 \end{bmatrix} \quad (4.15)$$

With the transformation matrix in Equation (4.15), the element stiffness matrix $[k_e]$ in the local coordinate system having the dimension of 12 × 12 can be obtained as:

$$[k_e]=[T][k_L+k_G][T]^T \quad (4.16)$$

The transformation matrices relating the element to the global coordinate axes can be evaluated as follows:

4.4.1 Rotational Transformation Matrix for principal axes

For asymmetric members such as angles, the principle axes are not parallel to the global axes as shown in Figure 4.3. In order to relate the sectional properties of the member in the principal axes to those parallel to the global axes, a rotational transformation matrix is required as shown as follows:

$$[L_3]' = \begin{bmatrix} 1 & & \\ & \cos\phi & \sin\phi \\ & -\sin\phi & \cos\phi \end{bmatrix} \tag{4.17}$$

and

$$[L_3] = \begin{bmatrix} [L_3]' & 0 & 0 & 0 \\ 0 & [L_3]' & 0 & 0 \\ 0 & 0 & [L_3]' & 0 \\ 0 & 0 & 0 & [L_3]' \end{bmatrix} \tag{4.18}$$

4.4.2 Translational transformation matrix

For eccentrically connected members, a translational transformation matrix is necessary to relate the member forces and displacements to those at the node. Figure 4.3 shows the correlation between the load axes and the local axes. The origin can be set to the point at which the load applies so that the moments due to eccentricity of the axial load can be considered automatically. By the rigid body kinematics, the translational transformation matrix can be written as:

$$[L_2]' = \begin{bmatrix} 1 & 0 & 0 & 0 & C_z & -C_y \\ 0 & 1 & 0 & -S_z & 0 & 0 \\ 0 & 0 & 1 & S_y & 0 & 0 \\ 0 & 0 & 0 & 1 & 0 & 0 \\ 0 & 0 & 0 & 0 & 1 & 0 \\ 0 & 0 & 0 & 0 & 0 & 1 \end{bmatrix} \tag{4.19}$$

and

$$[L_2] = \begin{bmatrix} [L_2]' & 0 \\ 0 & [L_2]' \end{bmatrix} \tag{4.20}$$

4.4.3 Local to global transformation matrix

In other to transform the stiffness matrix for the elements from the local coordinate system to the global coordinate system, the following transformation matrix is required:

$$[L_1]' = \begin{bmatrix} l_x & l_y & l_z \\ -\frac{l_x l_y}{Q} & Q & -\frac{l_y l_z}{Q} \\ -\frac{l_z}{Q} & 0 & \frac{l_x}{Q} \end{bmatrix} \tag{4.21}$$

and

$$[L_1] = \begin{bmatrix} [L_1]' & & & \\ & [L_1]' & & \\ & & [L_1]' & \\ & & & [L_1]' \end{bmatrix} \tag{4.22}$$

where l_x, l_y and l_z are the direction cosines of x, y and z axes

$$Q = \sqrt{l_x^2 + l_z^2} \tag{4.23}$$

When $|l_y| = 1$, the following matrix for $[L_1]'$ should be used.

$$[L_1]' = \begin{bmatrix} 0 & -l_y & 0 \\ l_y & 0 & 0 \\ 0 & 0 & 1 \end{bmatrix} \tag{4.24}$$

The global tangent stiffness matrix is given by:

$$[K_T] = [L]^T [{}_e k_T][L] \tag{4.25}$$

The transformation matrix $[L]$ can be considered as the product of the rotational, the translational and the local to global transformation matrices. That is,

$$[L] = [L_1][L_2][L_3] \tag{4.26}$$

4.5 Nonlinear analysis using the Newton-Raphson method

The Newton-Raphson method is the combination of the direct iterative method and the pure incremental method. In the direct iterative method, the displacements are computed with the tangent stiffness, which are then used to calculate the resistance with the second stiffness. The stiffness and thus the new displacements are recalculated. This process is continued until convergence is achieved. In the pure incremental method, the secant stiffness is not required and the incremental displacements are calculated with incremental applied force. However, this method will produce numerical drift-off error. The direct iterative method is more accurate since it satisfies the equilibrium conditions while the pure incremental method progresses along the load-deflection curve. Therefore, the Newton-Raphson method combines the goodness of the two methods. Figure 4.4 presents the flow chart for second-order analysis using the Newton-Raphson procedure and Figures 4.5(a) and 4.5(b) show the iterative schemes for the conventional and modified Newton-Raphson methods respectively. This is an incremental load method with an equilibrium check in every cycle. The numerical procedure iterates at a constant load level. In the conventional Newton-Raphson method the tangent stiffness matrix is continuously updated within one load cycle while in the modified one, the

tangent stiffness matrix is kept constant within a load cycle. The drawback of this method is there may exist divergence problem. The key steps of the Newton-Raphson procedure of the present analysis are as follows:

1. Apply incremental force vector $[\Delta F]$

2. Calculate the incremental global displacements $[\Delta u]$ for the structure

$$[\Delta u] = [K_T]^{-1}[\Delta F] \tag{4.27}$$

where $[K_T]$ is the global stiffness matrix

3. Update geometry $[x]_{i+1}$ and accumulate displacements $[u]_{i+1}$

$$[x]_{i+1} = [x]_i + [\Delta u] \tag{4.28}$$

$$[u]_{i+1} = [u]_i + [\Delta u] \tag{4.29}$$

4. Extract element displacement vector $[u_e]$ from global displacement vector and transform to local displacement vector $[u_l]$

$$[u_l] = [L][u_e] \tag{4.30}$$

where $[L]$ is the transformation matrix

5. Calculate the element resistance force vector $[F_l]$ and transform to global axes $[F_e]$

$$[F_l] = [k][u_l] \tag{4.31}$$

$$[F_e] = [L]^T [F_l] \tag{4.32}$$

where $[k]$ is the element stiffness matrix

6. Add up all element resistance force vectors to global resistance force vector $[R]$

$$[R] = \sum [F_e] \tag{4.33}$$

7. Compute the unbalanced forces $[\Delta R]$

$$[\Delta R] = [F] - [R] \tag{4.34}$$

where $[F]$ is the external force vector

This process is repeated until the unbalanced forces are eliminated to a sufficiently small error. To achieve this, it is necessary to revise the displacements and re-check the equilibrium condition. The convergence check is carried out using the following conditions:

$$[\Delta u]^T [\Delta u] < 0.1\% \cdot [u]^T [u] \tag{4.35}$$

$$[\Delta F]^T [\Delta F] < 0.1\% \cdot [F]^T [F] \tag{4.36}$$

After the convergence requirements are satisfied, a new load cycle begins with an updated tangent stiffness matrix and the whole previous process repeats. The whole incremental-iterative process is presented graphically in Figures 4.5(a) and 4.5(b). In the conventional Newton-Raphson method, the tangent stiffness is updated every iteration which makes the procedure take fewer iterations to achieve convergence; in the modified Newton-Raphson method, the tangent stiffness is kept constant within each load cycle which makes the computer time shorter as it is time-consuming to form and solve for the tangent stiffness matrix. A compromise of both methods may achieve the most optimal number of iterations. However, both methods may encounter divergence problem which is referred to as when the

applied incremental load approaches the limit point, the equilibrium errors in Equations (4.35) and (4.36) increases with the number of iterations until over-flow as shown in Figures 4.5(a) and 4.5(b).

4.6 Other numerical solution techniques

To improve this defect of divergence, the Newton-Raphson method is revised to be subjected to an additional constraint such as the arc-length distance or the minimum residual displacement norm. Further details can be found in Chan and Chui [33]. The basic formulations of the other solution techniques are shown as follows:

The incremental equilibrim equation can be written as:

$$[\Delta F] = [K_T][\Delta u] \tag{4.37}$$

The constraint equation with force vector parallel to the applied load vector can be written as:

$$\Delta\lambda[\Delta\bar{F}] = \Delta\lambda[K_T][\Delta\bar{u}] \tag{4.38}$$

in which $\Delta\lambda$ is a load corrector factor for imposition of the constraint condition, $[\Delta\bar{F}]$ is the force vector parallel to the applied load vector and of arbitrary length and $[\Delta\bar{u}]$ is the conjugated displacement vector of $[\Delta\bar{F}]$.

Superimposing Equations (4.37) and (4.38), the resulting incremental equilibrium equation becomes:

$$[\Delta F] + \Delta\lambda[\Delta\bar{F}] = [K_T]([\Delta u] + \Delta\lambda[\Delta\bar{u}]) \tag{4.39}$$

Therefore, in each iteration, the load and displacement can be updated as:

$$[F]_{i+1} = [F]_i + \Delta\lambda_{i+1}[\Delta\bar{F}] \tag{4.40}$$

$$[u]_{i+1} = [u]_i + [\Delta u]_{i+1} + \Delta\lambda_{i+1}[\Delta\bar{u}] \tag{4.41}$$

in which the subscript i refers to the i-th iteration number within a load cycle.

4.6.1 The arc-length method

In this method, the arc distance is kept constant in a particular load cycle. Figure 4.6 shows the graphical scheme for the method of controlling the arc-distance of displacements. The arc distance is taken as the dot product of the displacement vectors. Denoting the arc-distance as S, the constraint equation of a load cycle from Equation (4.41) can be obtained as:

$$([u]_{i-1} + [\Delta u]_i + \Delta\lambda[\Delta\bar{u}]_i)^T([u]_{i-1} + [\Delta u]_i + \Delta\lambda[\Delta\bar{u}]_i) = S^2 \tag{4.42}$$

4.6.2 The minimum residual displacement method

Chan [64] proposed a simple technique to search for a direction leading to the minimum value for the displacement error expressed as $[\Delta u]_{i+1} + \Delta\lambda_{i+1}[\Delta u]$. This can be done by differentiating the residual displacement with respect to the parameter $\Delta\lambda_i$ as follows:

$$\frac{\partial\left\{\left(\left[\Delta u\right]_i + \Delta\lambda_i\left[\Delta\bar{u}\right]\right)^T\left(\left[\Delta u\right]_i + \Delta\lambda_i\left[\Delta\bar{u}\right]\right)\right\}}{\partial\Delta\lambda_i} = 0 \tag{4.43}$$

Simplifying and rearranging, we have

$$\Delta\lambda_i = -\frac{\left[\Delta\bar{u}\right]^T\left[\Delta u\right]_i}{\left[\Delta\bar{u}\right]^T\left[\Delta\bar{u}\right]} \tag{4.44}$$

The graphical scheme is shown in Figure 4.7.

Other methods have been proposed to vary the value of to a certain constraint but it has been reported by Clark and Hancock [65] that the arc-length and the minimum residual displacement methods are the best among these varied versions of nonlinear numerical methods and other similar methods will not be elaborated further here.

4.7 Second-order analysis with NIDA

NIDA (Nonlinear Integrated Design and Analysis) [66] was coded with an aim for second-order nonlinear analysis and design meeting the code requirement for strength and stability design. The program follows the concept associated with the ultimate limit state design code with the “first-plastic-hinge” limit load criterion used in AS 4100 [27] and BS 5950 [3]. The element stiffness matrix allowing for initial imperfection derived by Chan and Zhou [44] and Chan and Gu [46] are used.

The program provides a variety of choices of nonlinear solution techniques including those introduced previously.

In this thesis, software NIDA [66] is extended to include angle members for second-order elastic and plastic analysis and design of structures made of angles, like the transmission line towers and the light-gauge trusses. The modifications involve inclusion of an asymmetric element and development of yield surface of angle sections. The developed numerical tool is valuable in analyzing structures made of angle members without the need of assessing the effective length L_E which carries great uncertainty in towers, trusses and frames.

4.8 Concluding remarks

This chapter introduces the physical concept of second-order analysis. To trace the load-deflection path, or the equilibrium path, of a structure, the stiffness matrix for an element is derived and then transformed and assembled to form the global stiffness matrix for the complete structure for the finite element analysis. To solve the displacements of the nodes, a non-linear solution technique is required. The Newton-Raphson method is probably the most common technique used today. The essence of this method is its incremental-iterative scheme with efficiency and accuracy. It performs iterations until an equilibrium point is reached in each incremental load cycle. However, the Newton-Raphson method may cause divergence problem after the limit point. Therefore, other nonlinear solution

techniques such as the arc-length method and the minimum residual displacement method are introduced.

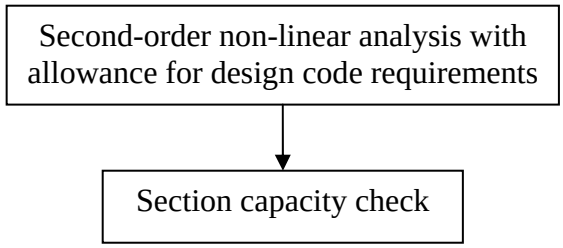

Figure 4.1 Non-linear analysis design procedure

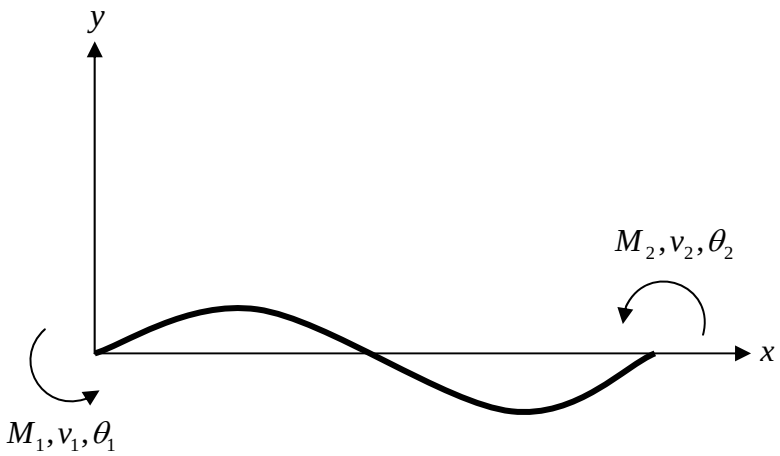

Figure 4.2 A two-dimensional beam-column element

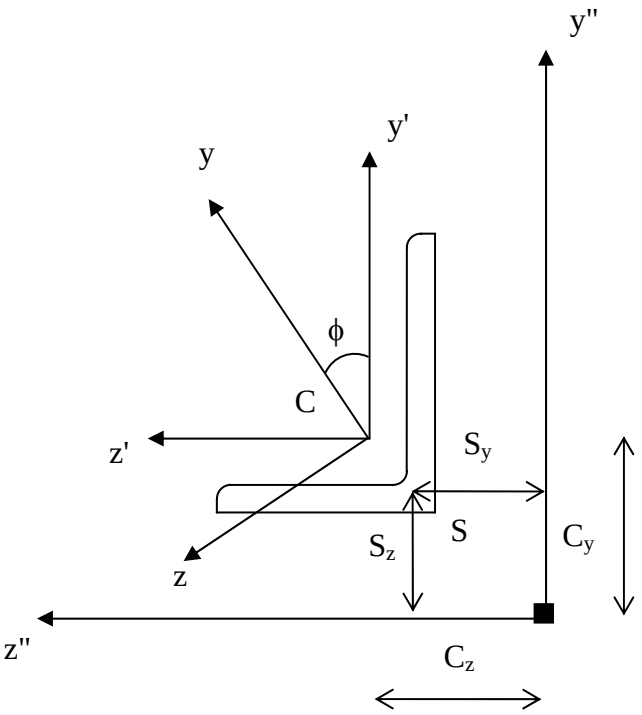

Figure 4.3 Local coordinate axes in element cross section

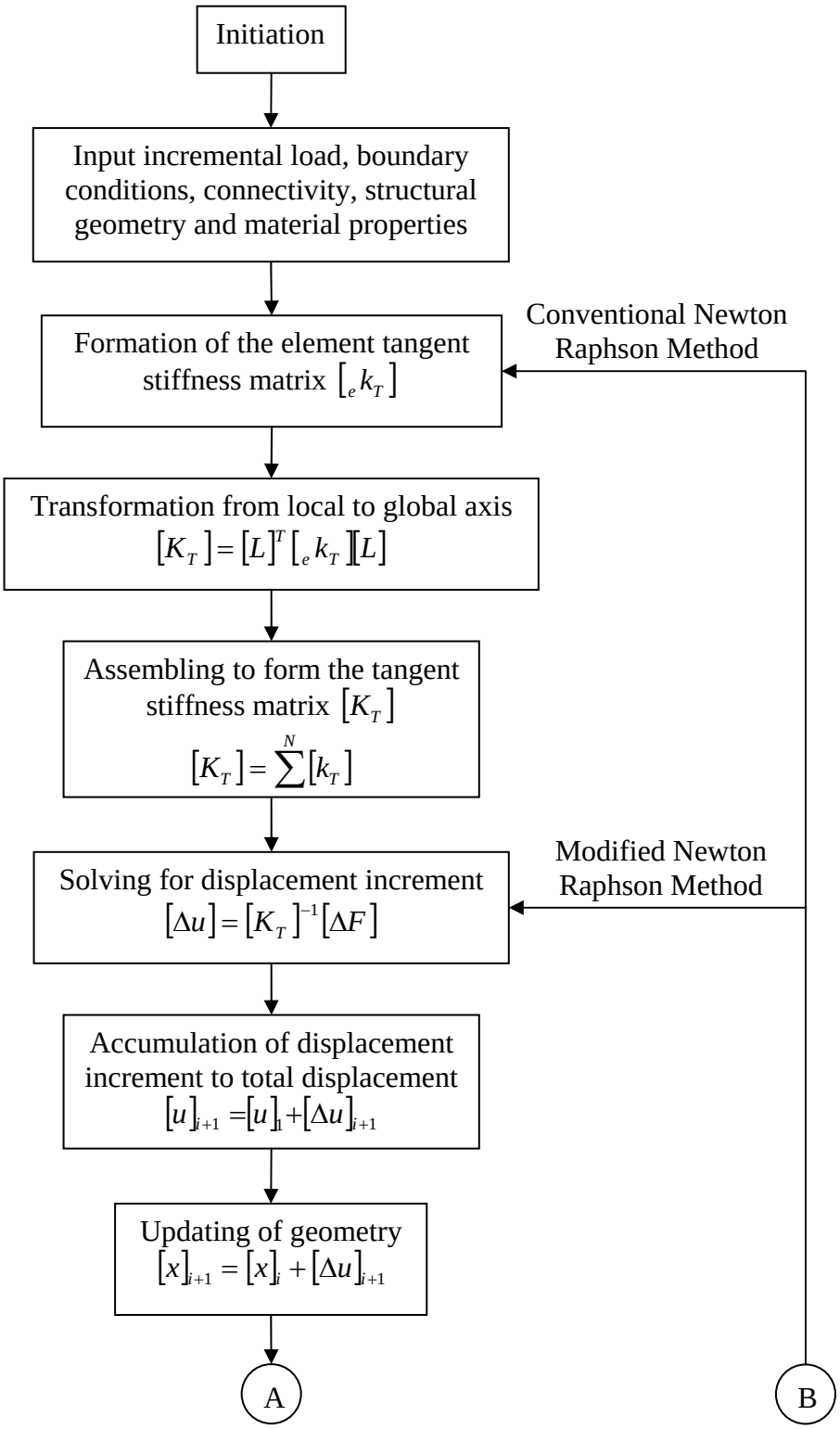
Initiation
Input incremental load, boundary conditions, connectivity, structural geometry and material properties
Formation of the element tangent stiffness matrix $[{}_e k_T]$
Conventional Newton Raphson Method
Transformation from local to global axis
$[K_T] = [L]^T [{}_e k_T][L]$
Assembling to form the tangent stiffness matrix $[K_T]$
$[K_T] = \sum^N [k_T]$
Solving for displacement increment
$[\Delta u] = [K_T]^{-1}[\Delta F]$
Modified Newton Raphson Method
Accumulation of displacement increment to total displacement
$[u]_{i+1} = [u]_1 + [\Delta u]_{i+1}$
Updating of geometry
$[x]_{i+1} = [x]_i + [\Delta u]_{i+1}$
A
B

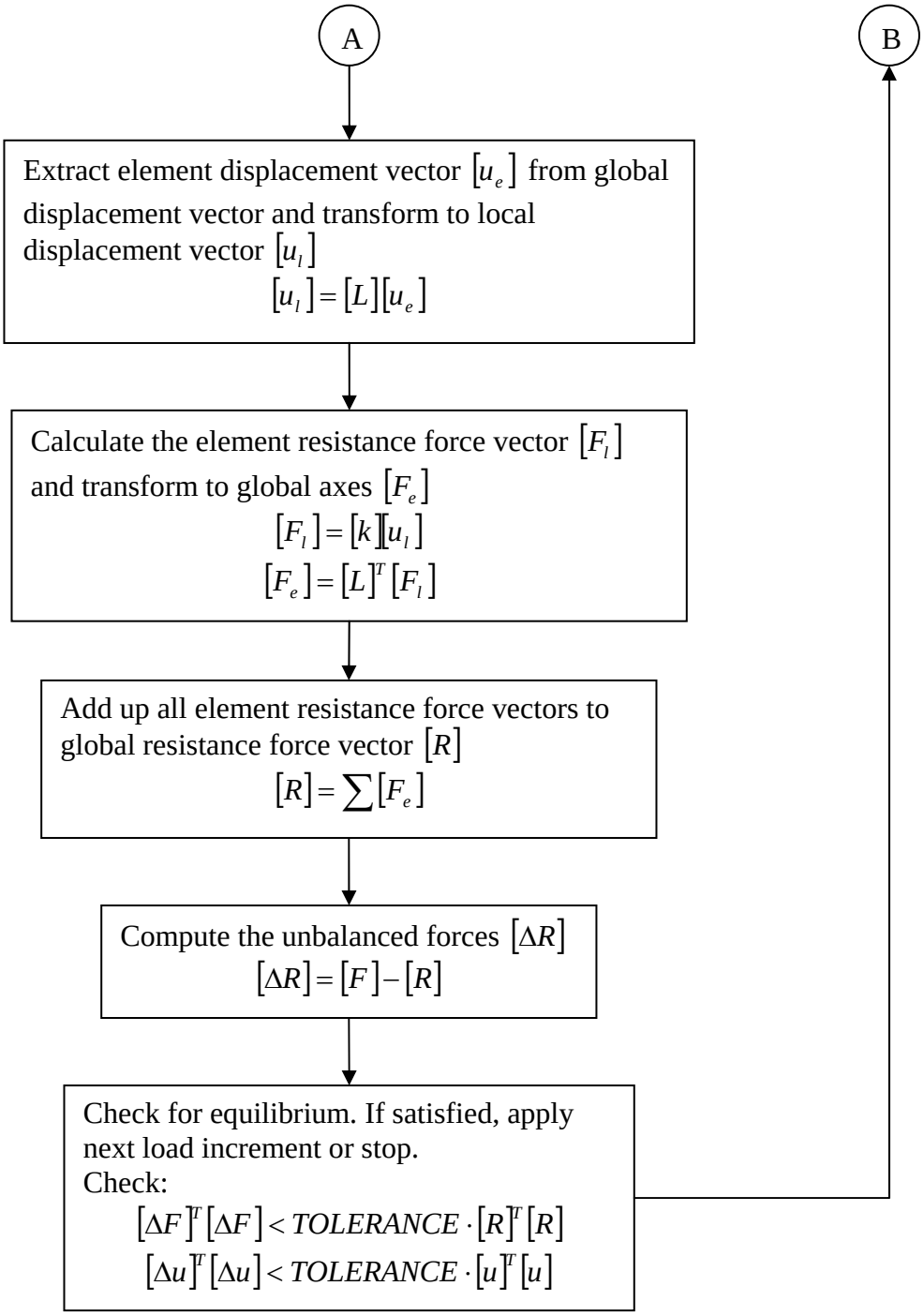

Figure 4.4 Flow chart for second-order analysis using the Newton-Raphson procedure

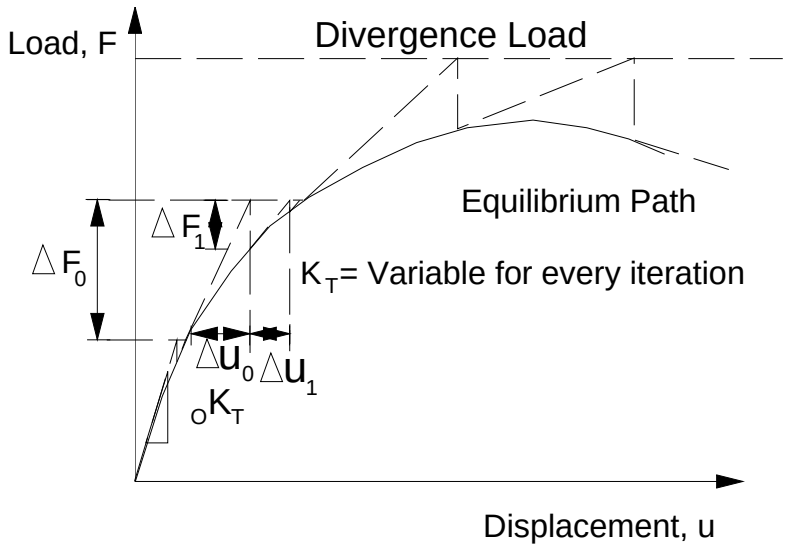

(a) Conventional Newton-Raphson method

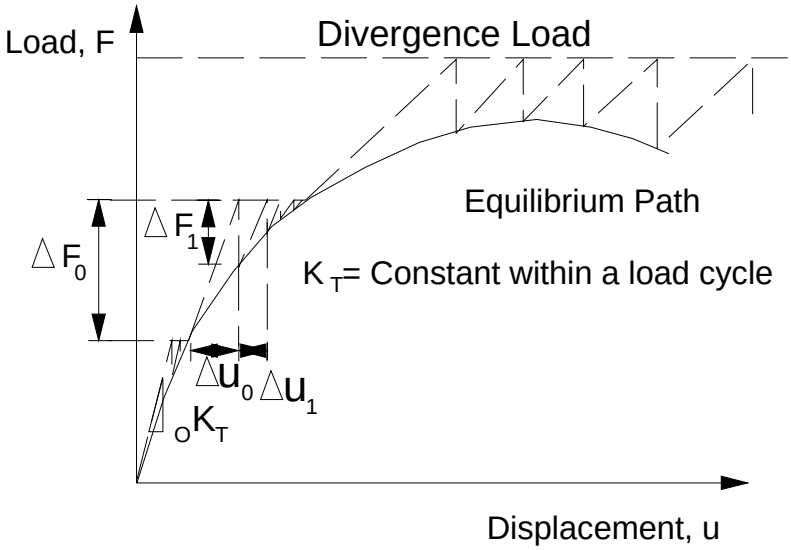

(a) Modified Newton-Raphson method

Figure 4.5 The Newton-Raphson method

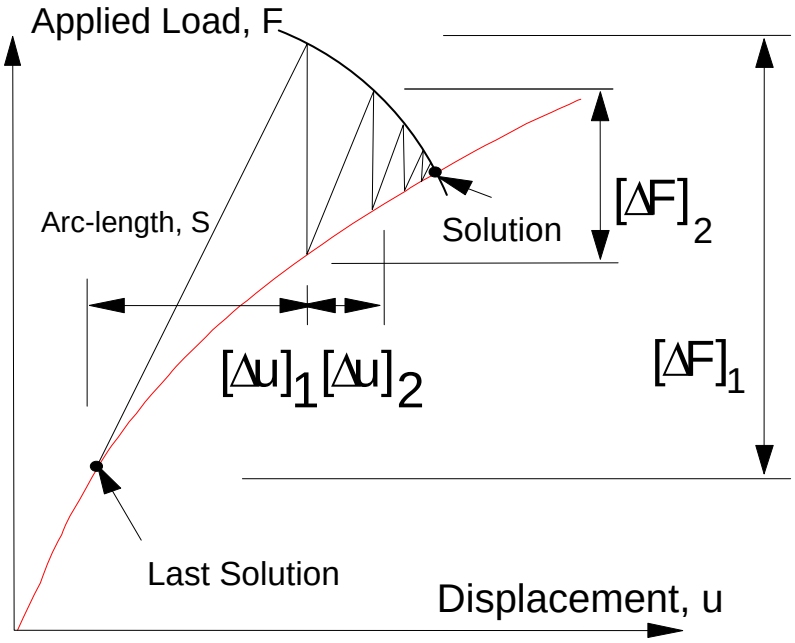

Figure 4.6 The arc-length method

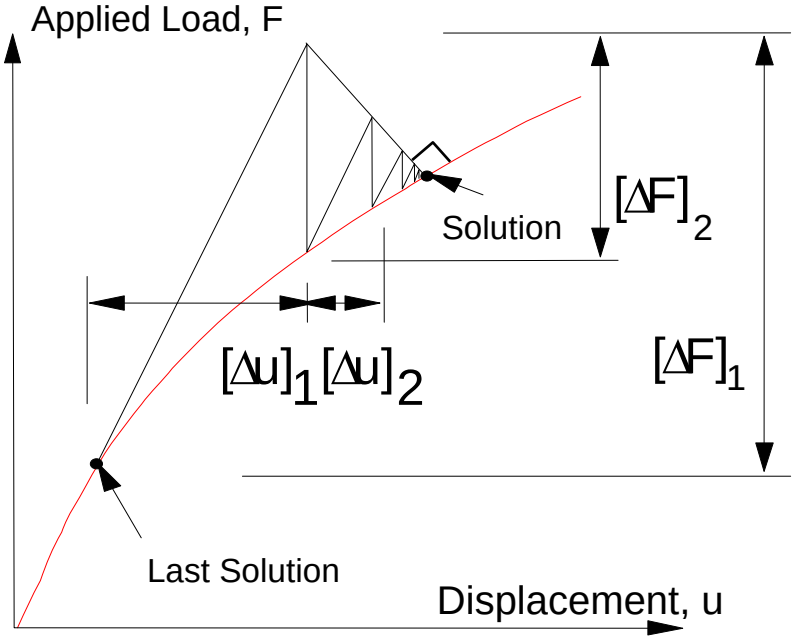

Figure 4.7 The minimum residual displacement method

Chapter 5 Second-order Elastic Analysis and Design of Angle Frames and Trusses

5.1 Introduction

As mentioned previously in Chapter 1, real members are far from ideally perfect owing to the presence of initial curvature, load eccentricity, residual stresses and the realistic stress-strain behaviour of the material. Rational analysis incorporating all these imperfections can be carried out by computer modelling. However, it is a time consuming process and rarely used in routine design. Instead, some national codes [3,41,62] may allow a simplified design approach which was developed from the results of computer modelling and correlations with experimental data available in the literature. In this chapter, a computer modelling of a single angle strut will be carried out. Based on the results, two design approaches dealing with single-angle using second-order elastic analysis are proposed. The first proposed method is based on the simplified approach given in BS 5950 [3] with the effects due to load eccentricity and end restraint ignored i.e. the equivalent imperfection approach. The second proposed method is modified from the equivalent imperfection approach with the exact end moments and joint stiffness considered during the analysis i.e. the exact end moment approach. Both methods take the first yield load or the load causing the member to fail in the first-plastic-hinge design as the ultimate failure load.

5.2 Computer modelling of a single angle strut

5.2.1 Description of model

The model used in the investigation is a simple initially curved column under compressive load as shown in Figure 5.1 as a replacement for a real member. Using the PEP element [44], one element per member is sufficient to produce satisfactory accuracy. The initial curvature is amplified so as to model the collective effect of all the aforementioned imperfections. The lower end is a pin support and the upper end is a roller support so that the buckling length, or the effective length, is simply equal to the member length. The compressive force acts at the centroid of the section. The imposition of initial curvature is important for the analysis as it triggers bending at the connection when an axial force is applied and the column will fail before the Euler buckling load is reached. If the initial curvature is absent, only axial shortening will occur under compression which is unable to tell the actual compressive stress the column is taking. In design codes, the values of imperfection-to-length ratio (δ_0/L) vary from section to section and to be determined for both equal and unequal angles so that the same compressive strength given in BS 5950 [3] and Eurocode 3 [41] can be obtained. The compressive strength curves of these sections of slenderness ratios ranging from 10 to 350 are generated using NIDA [65]. Comparisons are made between these curves and those given in BS 5950 [3] and Eurocode 3 [41] to ensure they are consistently close but conservative to the code requirements in order that the result can be safely used in practical design.

5.2.2 Model assumptions

There are a few assumptions for the model used in the analysis. First, the element is prismatic and homogeneous. Second, the compressive load is applied precisely at the centroid of the section. Third, the material is perfectly elastic. Fourth, the initial curvature of the element forms a perfect half sine curve though it was found that the actual initial shape has little effect on the end result. Fifth, the assumed failure mode is bending about the principal minor axis. Therefore, the initial imperfection is imposed along the plane of the principal major axis so that bending about the principal minor axis is initiated. This assumption is valid for slender members. For stockier members, other failure modes may occur, such as bending about geometric axis and flexural-torsional buckling which are not directly considered in the investigation but they may be considered implicitly in the analysis by using the proposed equivalent imperfection. In addition, compression members containing thin-plate elements such as angles are vulnerable to local buckling of the cross-section which reduces the buckling strengths of the members. The effect of local buckling is ignored here. In other words, only Class 3 semi-compact sections in which as defined by BS 5950 [3] only the extreme fibre in compression can be loaded to the design strength angle sections are considered in this paper. However, if slender sections are used, the effective cross-sectional area and the effective section modulus can be used to determine the effective cross sectional geometrical parameters and the proposed method here can be applied. As an alternative, reduced design strength may be used.

5.2.3 Equivalent initial curvature

An equivalent initial curvature is the value of the amplified initial curvature which, when used in a second-order analysis, can reproduce the buckling strength of the member the same as the buckling strength given in BS 5950 [3] and Eurocode 3 [41]. For a hypothetic initially curved element, the initial curvature relates to the compressive strength p_c in the form the Perry-Robertson formula given by:

$$p_c = \frac{p_y + (1+\eta)p_E}{2} - \sqrt{\left(\frac{p_y + (1+\eta)p_E}{2}\right)^2 - p_E p_y} \tag{5.1}$$

The Perry factor η is given by:

$$\eta = \frac{\delta_0 \cdot y}{r^2} \tag{5.2}$$

where y is the distance from the extreme fibre in compression to the centroidal axis of the cross section

Equation (5.2) can be re-written as:

$$\eta = \frac{\delta_0}{L} \cdot \frac{y}{r} \cdot \frac{L}{r} = \frac{\delta_0}{L} \cdot \frac{y}{r} \cdot \lambda \tag{5.3}$$

As can be seen from Equation (5.2) the Perry factor depends on the initial curvature-to-length ratio, the slenderness ratio and the dimensionless term y/r from the cross-sectional properties. y/r may not have any physical meaning except it is a ratio between geometrical properties across a section; however, for

each section type the values of y/r are roughly constant and therefore each sectional type can be assigned a typical value of y/r.

5.2.3.1 Initial curvature to BS 5950

The Perry factor η in BS 5950 [3] is modified based on computer modelling and experimental results and is given by:

$$\eta = 0.001a(\lambda - \lambda_0) \tag{5.4}$$

where a is the Robertson constant

λ_0 is the limiting slenderness ratio $= 0.2\sqrt{\pi^2 \frac{E}{p_y}}$

a is equal to 5.5 for both equal and unequal angle sections. λ_0 is a limiting slenderness to account for the stocky column effect which is insensitive to initial imperfections. To determine the equivalent value of initial imperfection fulfilling BS 5950 [3], we have,

$$\eta = \frac{\delta_0}{L} \cdot \frac{y}{r} \cdot \lambda = 0.001a(\lambda - \lambda_0) \tag{5.5}$$

Therefore,

$$\frac{\delta_0}{L} = \frac{0.001a(\lambda - \lambda_0)}{y/r \cdot \lambda} \tag{5.6}$$

The equivalent δ_0/L can be calculated by Eqn. (5.6) with known slenderness ratio and the dimensionless term y/r . Alternatively, a conservative design value for the equivalent δ_0/L can be used by omitting the limiting slenderness ratio. For most practical purposes, angles of intermediate and slender range are commonly used and the design of stockier angle columns is unaffected by buckling and therefore the ignorance of λ_0 is unimportant again. The effect of ignoring the limiting slenderness ratio λ_0 is insignificant for comparatively slender columns. Therefore, the expression of δ_0/L can be simplified to:

$$\frac{\delta_0}{L} = \frac{0.001a}{y/r} \tag{5.7}$$

5.2.3.2 Initial curvature to Eurocode 3

In Eurocode 3 [41], the modified Perry factor is given by:

$$\eta = \alpha\sqrt{\frac{p_y}{\pi^2 E}}(\lambda - \lambda_0) \tag{5.8}$$

where $\alpha =$ imperfection factor $= 0.34$ for angle sections

The equivalent initial curvature to Eurocode 3 [41] can be worked out by a similar approach using Equations (5.3) and (5.8) as,

$$\frac{\delta_0}{L} = \frac{\alpha\sqrt{\frac{p_y}{\pi^2 E}}(\lambda - \lambda_0)}{y/r \cdot \lambda} \tag{5.9}$$

Neglecting the limiting slenderness term, Equation (5.9) can be simplified as,

$$\frac{\delta_0}{L} = \frac{\alpha}{y/r}\sqrt{\frac{p_y}{\pi^2 E}} \tag{5.10}$$

When calculating the compressive strength of an eccentrically loaded member, NIDA [65] takes the eccentricities, residual stresses and initial imperfections into account simply by means of this equivalent initial curvature. Therefore, these effects are controlled by the value of δ_0/L which is derived as follows.

5.2.4 Compressive strength curves to BS 5950 and Eurocode 3

The compressive strength of an angle strut to BS5950 [3] and Eurocode 3 [41] can be traced via the imposition of the equivalent initial imperfection using the Newton-Raphson procedure as described in Chapter 4. The value of δ_0/L can be calculated precisely using Equations (5.6) and (5.9) or conservatively using Equations (5.7) and (5.10). For similar geometrical cross-sections, the values of y/r are roughly constant; so are the values of δ_0/L. Therefore, the values of δ_0/L for all angle sections will only slightly vary. Having mentioned that the effect due to local buckling will not be accounted for directly in the analysis, sections having the leg length-to-thickness ratios larger than the limiting value for Class 3 semi-compact sections will not be considered in the investigation. Since Eurocode 3 [41] has a more stringent requirement on the limiting value than the BS 5950 [3], we will adopt the Eurocode 3 requirement. The angle sections for investigation are covered in BS EN 10056 [67] with steel grade S275 and young modulus 205

kN/mm^2. Careful consideration must be taken to identify which extreme point of the section in compression is critical i.e. having the least value of section modulus. For equal angles, it is found that the critical situation happens when the angle heel is in compression and their corresponding y/r values range from 2.031 to 2.241. For unequal angles, the critical situation happens when the toe at the shorter leg in compression and their corresponding y/r values range from 2.281 to 2.854. As the value of δ_0/L is inversely proportional to the value of y/r, the most conservative value of δ_0/L can be obtained when the smallest of these y/r values is substituted into Equation (5.7) for BS 5950 [3] and Equation (5.10) for Eurocode 3 [41]. The sections having the smallest values of y/r for equal and unequal angle sections and their calculated δ_0/L values are summarized in Table 5.1.

The next step is to generate the design curves using NIDA [66] by inputting these values of δ_0/L for the worst cases. Figures 5.2 and 5.3 show the buckling curves of equal and unequal angles of steel grade S275 derived from the basis of the equivalent initial imperfections in Table 5.1. Generally, the results generated by the proposed method agree well with the design code BS 5950 [3] and Eurocode [41]. The discrepancies between the present curves and the design code curves will be less than 9% for the BS 5950 [3] and the Eurocode 3 [41], the curves tend to converge to the same value when the slenderness ratio is high. It is because when the member is slender, the effect of neglecting the limiting slenderness is relatively insignificant.

5.3 The equivalent initial curvature approach

When designing trusses of various serial sizes of angles to BS 5950 [3] or Hong Kong Steel Code [62] by the proposed second-order analysis method, it is suggested the initial imperfection per member length tabulated in Table 5.1 should be imposed to compensate for the effect due to load eccentricity and other imperfections such as initial curvature, residual stresses and material non-linearity. This proposed method is modified from the conventional simplified methods which are normally employed with the assumptions that the loads are applied to the trusses at the joints and transferred to the members concentrically and all connections are pinned and can freely rotate so no moments are created. In fact, these assumptions are hardly true because the joints are almost always bolted or welded away from the centroid. However, in general, the error due to these assumptions will not cause the structure to have a lower than expected safety margin. In the conventional method, the second-order effects are considered only in the design stage as an independent step after the analysis; while in the second order analysis, the second-order effects are included during the analysis as an integral part with design. For truss members with single-bolted connections, the failure load of the truss calculated should be reduced to 80% as required by BS5950 [3] and Hong Kong Steel Code [62]. However, such simplified approach is not allowed in Eurocode 3 [41] as when only one single bolt is used, the end moments induced by the load eccentricities should be considered by an axial force-moment interaction equation. For double-bolted connection, in many design codes normally the effective length of the member is reduced to account for the restraining effect due to the connection. For example, an effective length factor of 0.85 is used in BS

5950 [3]. In the proposed method, this effective length assumption is omitted because this assumption is based on immovable end nodes of the members which are non-existent in practical scenario. Since the effect of local plate buckling is neglected in the investigation, this method can be used for Class 4 slender sections in which plate elements under compression not meeting the limits for class 3 semi-compact sections defined in BS 5950 [3] should have an appropriate reduction in section properties or design strength to design codes by the effective width or the effective stress method. However, this modified method is still inadequate to consider the directions of the end moments. These end moments may be adverse or beneficial to the overall structure and the equivalent initial curvature approach cannot truly reflect the end condition that a practical angle is subject to.

5.4 The exact end moment approach

The exact end moment approach was further modified from the equivalent initial curvature approach by Chan and Cho [68]; the end moments and the rotational stiffness due to the end conditions are considered during analysis. The end moments due to load eccentricity are considered by connecting the angle web members at each end to the chord members by rigid arms. The rigid arm will be the element joining the centroid and the point of load application so that the magnitude and the direction of the end moments due to load eccentricity can be taken into account immediately during the analysis. For single-bolted connection, the connection joints are allowed to rotate freely. For double-bolted connection, rotational springs are inserted to the joints connecting rigid arm elements to the

angle web member element in the in-plane direction so that the couples due to the double-bolted connection can be considered. The end condition is symbolized by rotational spring elements inserted at the ends of the member. Therefore, the rotational stiffness due to the double-bolted connection can be considered at an early stage of the analysis rather than at the design stage as in the linear analysis and effective length design method. The value of the rotation spring stiffness depends on the arrangement of the bolt group and its material properties. Only the rotational deformation of the connection spring element is considered for design because the effects of the axial and shear forces in the connection deformations are small when compared with that of bending moments. The merit of this approach over the purely equivalent imperfection approach is that it considers the direction of the end moments so that the aforementioned effect can be reflected during analysis. The spring stiffness of a rotational spring can be calculated in the following steps.

As shown in Figure 5.4, the couple, M_R, formed by the pair of bolts is given by:

$$M_R = F_R \cdot d = S_R \theta \tag{5.11}$$

The shear stress, τ, across the cross-section, A_S, of the bolt is:

$$\tau = \frac{F_R}{A_S} \tag{5.12}$$

in which A_S is the shear area and can be taken as 0.9 of the cross sectional area recommended in most design codes like the Hong Kong Steel Code [62].

The shear strain, γ, of the bolt shank is:

$$\gamma = \frac{2\delta}{l} = \frac{d \cdot \theta}{l} = \frac{\tau}{G} \tag{5.13}$$

Rearranging terms, the rotational stiffness, S_R, due to the double-bolted connection will be given by:

$$S_R = \frac{GA_S d^2}{l} \tag{5.14}$$

where F_R is the shear force exerted on the bolt; d is the distance between the centroids of the two bolts; θ is the rotation of the bolt group; δ is the displacement of the bolt; l is the length of the bolt shank; G is the shear modulus of elasticity. From the above equation, it can be seen that the spring stiffness S_R is directly proportional to the shear area of the bolt shank and the square of the bolt spacing and inversely proportional to the shank length of bolts.

To account for the rotation stiffness of the spring element in the analysis, the following incremental tangent stiffness matrix is superimposed to the element stiffness matrix.

$$\begin{bmatrix} M_e \\ M_i \end{bmatrix} = \begin{bmatrix} S_c & S_c \\ -S_c & S_c \end{bmatrix} \begin{bmatrix} \theta_e \\ \theta_i \end{bmatrix} \tag{5.15}$$

in which M_e and M_i are the incremental external and internal moments at two ends of a connection. The external node refers to the one connected to the global node and the internal node is joined to the angle element. The stiffness of the

connection, S_c , can be related to relative rotations at the two ends of the connection spring as:

$$S_c = \frac{M_e}{\theta_e - \theta_i} = \frac{M_i}{\theta_i - \theta_e} \tag{5.16}$$

in which θ_e and θ_i are the conjugate rotations for the moments M_e and M_i.

The incremental force is assumed in the software and the incremental displacement is solved. The basic element stiffness is modified by addition of the tangent stiffness of the connection spring modeled as a dimensionless spring element in a computer analysis as:

$$\begin{bmatrix} S_1 & -S_1 & 0 & 0 \\ -S_1 & k_{11}+S_1 & k_{12} & 0 \\ 0 & k_{21} & k_{22}+S_2 & -S_2 \\ 0 & 0 & -S_2 & S_2 \end{bmatrix} \begin{bmatrix} \Delta\theta_{1e} \\ \Delta\theta_{1i} \\ \Delta\theta_{2i} \\ \Delta\theta_{2e} \end{bmatrix} = \begin{bmatrix} \Delta M_{1e} \\ \Delta M_{1i} \\ \Delta M_{2i} \\ \Delta M_{2e} \end{bmatrix} \tag{5.17}$$

in which S_1 and S_2 are the spring stiffness for simulation of semi-rigid connections at ends; k_{ij} is the stiffness coefficients of the element; θ_{1e}, θ_{1i}, θ_{2e} and θ_{2i} are respectively the rotations at two sides for the two ends of an element shown in Figure 5.5.

5.5 Worked examples

5.5.1 Example 1 – Design of an angle roof truss

A roof truss is normally sloped to drain rainwater away. The vertical height of trusses varies usually from one fifth to one quarter of the span length, giving a

slope varying between 21.5° and 26.5°. A typical roof truss is shown in Figure 5.6. From economical point of view, the spacing of roof trusses normally ranges from 4 m to 7.5 m depending on the span length of the roof truss. In this example, the error due to joint assumptions is illustrated. Design of the roof truss with both single-bolted and double-bolted conditions are carried out using the conventional approach, the equivalent initial curvature approach and the exact end moment approach. In the conventional method, a linear analysis is carried out to determine the internal forces of the truss. The buckling resistance of individual members is then determined using formulae given in BS 5950 [3].

Particulars of the design scheme:

- Span length of trusses: 18 m
- Height of trusses: 3.6 m
- Spacing of trusses: 4 m
- Material used: Grade S275 steel with Young's modulus of 205kN/mm^2
- Assume that purlins are at node points of the trusses and the weight of the sheeting and purlins is 0.25 kN/m^2
- Assume a self-weight for the truss of 0.1 kN/m^2 on slope
- Assume the live load is 0.50 kN/m^2 on slope

The forces in roof truss members are worked out as follows:

Total dead load $= 1.4 \times (0.25 + 0.1) = 0.49\ kN/m^2$

Total live load $= 1.6 \times 0.5 = 0.80\ kN/m^2$

Total load on a rafter $= (0.49 + 0.80) \times 4 = 5.16\ kN/m$

Load per node $= 5.56 \times 3.23 = 16.7\ kN$

Note that the load at the end point is half of that on the intermediate points.

Table 5.2 shows the forces in the roof truss members. Due to symmetry, only half of the floor truss is considered. Assume that the rafters will be 80×60×6 double angles ($I_x = 49.0cm^4$, $I_y = 234.0cm^4$ and $A = 16.08cm^2$) with the long legs attached to the gusset plates. BS 5950 [3] Clause 4.7.10.3 requires the following check:

For x-x axis,

$$\lambda_x = 0.85\frac{L_x}{r_x} \text{ but not less than } 0.7\frac{L_x}{r_x} + 30$$

In this case $\lambda_x = 0.85 \times 323/2.51 = 109 < 0.7 \times 323/2.51 + 30 = 120$

Therefore, the critical slenderness ratio is 120

For y-y axis

$$\lambda_y = \left[\left(\frac{L_y}{r_y}\right)^2 + {\lambda_c}^2\right]^{0.5} \text{ but not less than } 1.4\lambda_c$$

where λ_c is the slenderness of the single component about its weakest axis, i.e. $\lambda_c = L_v/r_v$

If there are 6 interconnections between two angles forming the strut, then:

$$\lambda_v = \frac{323}{1.28 \times 6} = 42$$

$$\lambda_y = \left[\left(\frac{323}{3.81} \right)^2 + 42^2 \right]^{0.5} = 131 > 1.4 \times 42 = 59$$

Therefore, the critical axis in this case is x-x where the slenderness ratio is 131. From Table 24(c) of BS 5950 [3], $p_c = 85\,N/mm^2$, the axial load capacity P_c is given by:

$$P_c = 85 \times 16.08/10 = 136.7kN$$

Assuming the internal bracing members will be 75×50×8 angle ($I_u = 60.1cm^4$, $I_v = 10.9cm^4$ and $A = 9.44cm^2$) with the long leg attached to the gusset plates, according to Clause 4.7.10.2 of BS 5950 [3], the critical slenderness ratio of the single angle struts for single-bolted connection and double-bolted connection are 224 and 191 respectively and their corresponding axial load capacities are $25.2kN$ and $42.5kN$. Assume the lower chord members will be L75×50×8 angle ($I_u = 60.1cm^4$, $I_v = 10.9cm^4$ and $A = 9.44cm^2$). The slenderness ratio is 238 and the axial load capacity is 28.7kN. Results show that for single bolted connection, the internal web member CI will yield first and the load factor, which is the ratio of failure load to design load, will be 1.01 and for double bolted connection, the rafter BC will fail first and the load factor will be 1.22. When using the equivalent initial curvature approach, the internal web members are assumed to be pin-jointed and

the other components are assumed to be continuous, the initial imperfection-to-length ratio is amplified to 1/414 for all unequal angles. The internal member CI yield first for both single and double-bolted connection and the load factors are 1.00 and 1.24 respectively. When using the exact end moment approach, on top of the imposition of the initial imperfection, the internal members of the truss are offset and the joint stiffness is imposed in each end node so that the load eccentricities and the rotational restraints due to connection are considered in the analysis. It can be observed that both single and double-bolted connection, the internal member BC will fail first and the load factor will be 1.67 and 1.76 respectively.

The results are summarized in Table 5.3. It can be seen that for different connection assumptions yielding of material will start at different members which may affect the overall loading capacity of the structure. The equivalent initial imperfection method can achieve a more rigorous design than the BS 5950 [3]. This is expected since the members are assumed pinned and the imperfections are equivalent to the values in BS 5950 [3]. However, the method has an distinctive advantage on the efficiency of completing a design with an analysis. The exact end moment method provides a more rational alternative which carefully consider the load eccentricities and rotational restraints of web members. Since the $P-\Delta$ and the $P-\delta$ effects due to the change of structural geometry and the deflection along a member respectively after loads are already included during the analysis via geometry update and the use of initial imperfection, the section capacity is adequate for strength design which can be completed at the same time when the

analysis is completed. Obviously, the present method is much more efficient since separated member check is not needed. A conventional analysis and design assumes all connections are pinned which is in contrast with the actual scenario.

5.5.2 Example 2 – Design of a tower truss

This example illustrates the error due to effective length assumptions. The planar 1.0m×3.0m tower truss as part of a braced web portal frame is subject to two vertical forces shown in Figure 5.7. The internal segment is designed based on an assumed effective length. According to BS 5950 [3], in order to allow for the effects due to lack of verticality, a notional horizontal force of 0.5% of the vertical load is applied at the same level. The design load, F, of the truss is determined in this example. The material design strength is 275N/mm^2 and Young's modulus is 205kN/mm^2, and the angle is of size L40×40×4 ($I_v = 1.89cm^4$ and $A = 3.09cm^2$). When designing according to BS 5950 [3], different engineers may make varied assumptions of effective length and discrepant results will be obtained. As summarized in Table 5.4, if $L_E = 1.0L$, where L is the distance between bracings, the failure load will be 52.8kN; if $L_E = 0.85L$, the failure load will be 67.2kN; and if $L_E = 0.7L$, the failure design load will be 85.2kN . When using the second-order analysis, the initial imperfection-to-length ratio is amplified to 2.781×10^{-3} for equal angles and the failure load is 83.4kN. Without assuming any effective length, the failure load can be computed as the $P-\Delta$ effect is automatically considered by geometry update and the $P-\delta$ effect by member bowing.

Comparing the BS 5950 [3] design method and the proposed method, if the effective length is taken as $1.0L$, the failure load calculated according to BS 5950 [3] is about one-third lower than that calculated by the proposed method; if the effective length is taken as $0.85L$, the failure load calculated by the BS 5950 approach is still about 20% lower than that calculated by the proposed method. But, when the effective length is taken as $0.7L$, the BS 5950 method and the proposed method will give almost the same result. In this example, it is shown that the conventional design method appears to be unreliable for the reason that a small difference in effective length can lead to a sizeable difference in design load. Unfortunately the assessment of effective length is sometimes uneasy and unreliable, leading to over-design of some members and occasional under-design of others. However, the second-order analysis avoids the error associated with the assumption of effective length.

5.5.3 Example 3 – Design of a large transmission tower

This example demonstrates the practical application of second-order analysis of a moderately large structure made of angle sections via the use of equivalent initial curvature. A transmission tower with a height of 45m and a base of 10m × 10m is to be built on the top of Cloudy Hill in Hong Kong in order to cater the launch of a digital terrestrial television (DTTV) service in Hong Kong in 2007.

5.5.3.1 Project requirements

The transmission tower is located at 444m above sea level. The overall height is 45m. The foundation of the tower is a concrete footing. The wind speed

requirement is 90 m/s which is much higher than the minimum required wind speed of 59.5 m/s for normal structures in Hong Kong.

5.5.3.2 Load path

The wind load acting on the individual members, antenna dishes and panels and the self weight of the transmission tower are transferred to the concrete footings. The bracings are added to restrain the main members from buckling.

5.5.3.3 Design codes used

Hong Kong Steel Code [62], Hong Kong Wind Code [69] and the PNAP 45 [70] are used. PNAP means Practice Note for Authorised Persons in full and this is a set of statutory notes published by the Buildings Department of the Hong Kong Special Administrative Zone Government requesting the project engineers, architects or surveyors to follow as a minimum building standard in Hong Kong. These documents can be downloaded from the following website:

http://www.bd.gov.hk/english/documents/index_crlist.html

Interestingly, some of these like the PNAP 106 for curtain wall testing are referenced and used in China which admires the building safety standard in Hong Kong. PNAP 45 [70] is used to check against dynamic effects. The non-linear second-order analysis method is allowed in Chapter 6 of the Code of Practice for Structural Uses of Steel in Hong Kong 2005. Therefore, this example on a real structure is designed to the code requirement and finally approved for actual

construction which appears to be the first in the world of second-order analysis for an angle tower without any assumption of effective length.

5.5.3.4 Design assumptions

1. The bracing members are assumed to be pin-jointed.
2. At each support, the displacements of the three directions are restrained while the rotations about the three directions are free.
3. The assumed dead load of platform is 0.75kPa.
4. The assumed live load on platform is 2.0kPa according to the Hong Kong Building Ordinance [71].
5. Steel grade S355 is used for all steel angle members. For steel thickness greater than 16mm, the design strength should be reduced accordingly to Code of Practice for Structural Uses of Steel Hong Kong 2005. For slender sections, design strength should be reduced to account for local buckling. Steel grade Q345 is used for all steel hollow members. The material properties are shown in Table 5.5.
6. Both ultimate limit state and serviceability limit state are considered.
7. All connections unless otherwise stated are bolted connections with bolts of M-24 ISO grade 10.9.

5.5.3.5 Member sizes

The overall view of the transmission tower consisting of various sizes of members is shown in Figure 5.8. A total tonnage of 42.9 of steel has been used.

5.5.3.6 Individual load cases

There are 4 major groups of individual load cases.

1. Wind load acting to members

Wind speed of 90 m/s is used and it gives the basic wind pressure p_w as,

$$p_w = \frac{\rho v^2}{2} = 0.6v^2 = 4860\text{Pa} = 4.86\text{kPa}$$

in which ρ is the air density equal to 1.2 kg/m^3 and v is the wind speed in m/s.

As the design wind pressure is 4.86 kPa which is greater than the required basic wind pressure in HK Wind Code 2004, it satisfies the BD's requirement. According to the Hong Kong Wind Code Appendix E2, the total pressure coefficient C_p for individual members of an open framework building shall be taken as 2.0. Therefore the total wind pressure shall be determined by the following equation:

$$p_p = C_p\, p_w = 2 \times 4.86 = 9.72\text{kPa}$$

2. Wind load acting on antennae

The dish antennas will contribute wind point loads to the tower. The antennas are tilted to an angle and their corresponding axial forces and shears are calculated by a programme, ANTWIND, which are available at www.andrew.com. On the other hand, the antenna panels will contribute uniformly distributed load the tower. Assuming a width of 30 cm, each column of antenna panels will contribute wind load of

$$4.86 \times 0.3 = 1.46 \text{ kN/m}$$

For antenna panels hanging from 469m to 489m, assuming that there are effectively two columns of panels subject to wind load, and the distributed wind load should be

$$1.46 \times 2 = 2.92 \text{ kN/m}$$

The wind load acting on the antenna dishes and panels are shown schematically in Figure 5.9.

3. Live Load

Live load is distributed uniformly on platforms which is 2.0 kPa as assumed.

4. Dead load

Dead load includes the self weight of the steel, which is 0.75 kPa as assumed, and the self weights of the antennas provided by the supplier.

5.5.3.6 Combined load cases

There are 7 combined load cases which have been considered:

1. 1.4 WL + 1.0 DL in X direction
2. 1.4 WL + 1.0 DL in Y direction
3. 1.4 WL + 1.0 DL in diagonal direction
4. 1.2 WL + 1.2 LL + 1.2 DL in X direction
5. 1.2 WL + 1.2 LL + 1.2 DL in Y direction
6. 1.2 WL + 1.2 LL + 1.2 DL in diagonal direction
7. 1.6 LL + 1.4 DL

Note: WL = wind load

DL = dead load

LL = live load

5.5.3.7 Resonant dynamic response

PNAP 45 [69] is used to check against dynamic effects. The calculation is shown as follows:

The natural frequency of the antenna is calculated as follows:

$$f = \frac{500 \times 2D}{h^2} = \frac{500 \times 2 \times 0.457}{10^2} = 4.57Hz$$

The critical velocity is:

$$v_{cr} = 5D \cdot f = 5 \times 0.457 \times 4.57 = 10.44m/s$$

$$\therefore v_{cr} < v = 90m/s$$

$$C = 0.6 + K\left[\frac{10D_t^{\ 2}}{W} + \frac{1.5\Delta}{D}\right]$$

$$= 0.6 + 3.0\left[\frac{10 \times 0.457^2}{133} + \frac{1.5 \times 3.034 \times 10^{-2}}{0.457}\right] = 0.946$$

$$\because C < 1$$

$\therefore$ severe oscillation is unlikely.

5.5.3.8 Analysis results

In the analysis by NIDA which is the only software accepted by the Buildings Department in Hong Kong for second-order analysis, second-order iterative

analysis and design is carried out for each load case individually. In all the analysis, an elastic buckling (Eigen-buckling) analysis is first carried out to identify the buckling mode and global frame imperfection of one-500th of tower height is then inserted before the design loads are applied to the structure for analysis and design. The required time for the seven load cases using a personal computer of 1.6 MHz is 70 seconds which is likely to be less than 1% required design time by hand method. Even when using the computer-assisted method speeding up the manual design time, one cannot be sure of the effective length factor of various members since the sway effect can hardly be identified.

The output by NIDA is printed on a spreadsheet for easy checking. The maximum section capacity factor ϕ in Equation 4.1 is tabulated in Table 5.6 indicating no member fails under all assumed load cases. From the analysis, the most critical combined load case, as expected, will be:
1.4 WL +1.0 DL in diagonal direction or 45^0 to the X- or Y-axis.

A simple comparison with the linear analysis and design shows that the discrepancy is moderate and the present method consumes about 20% less steel.

5.6 Concluding remarks

This chapter proposed two methods for designing angle trusses, namely the equivalent initial curvature approach and the exact end moment approach. The advantage of the first approach is its simplicity but it may underestimate the failure

load of the structure especially for the double-bolted single angles. The advantage of the second approach is its rational consideration of the effects due to load eccentricities and end restraints which may produce a less conservative design. However, it requires more effort to consider the magnitudes of the load eccentricities and the stiffness of the rotational spring. The axial stress at every extreme point must be checked as the maximum bending stress about each axis is not necessarily coincides. The first approach is currently used in designing the digital terrestrial television transmission tower in Hong Kong. It does not require assumption on effective length, which is determined separately in each combined load case, so that the error due to gross estimation of effective length can be eliminated with safety improved and design made more efficient.

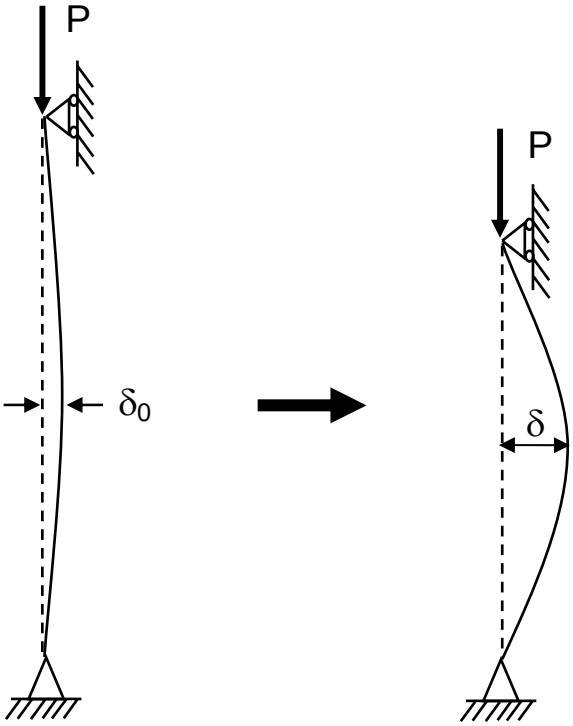

Figure 5.1 Element model used in the analysis

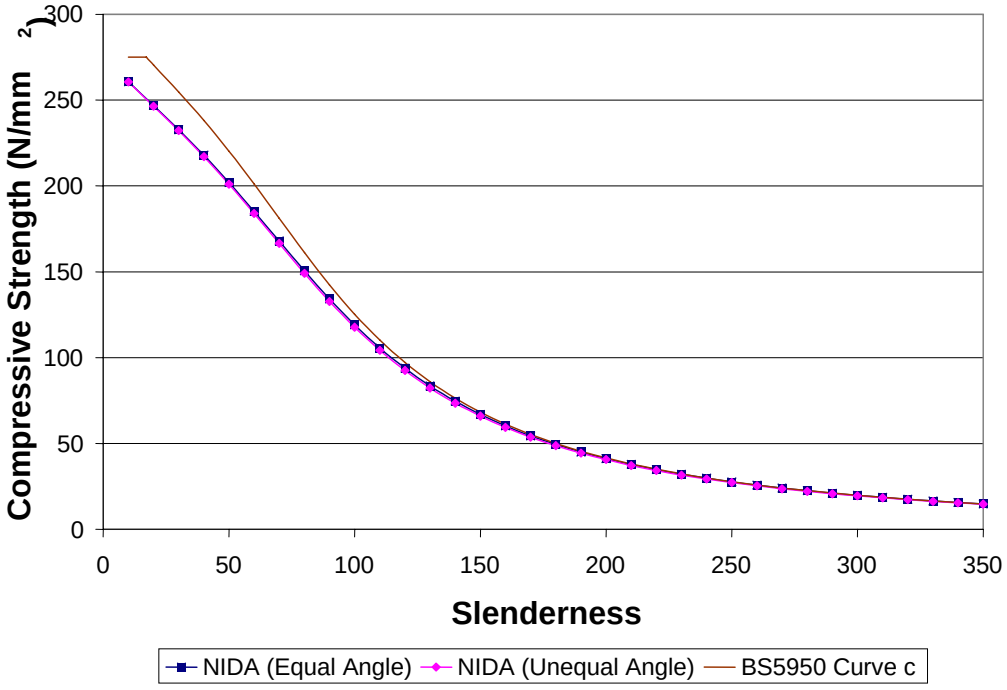

Figure 5.2 Compressive strength curves to BS5950 Curve c

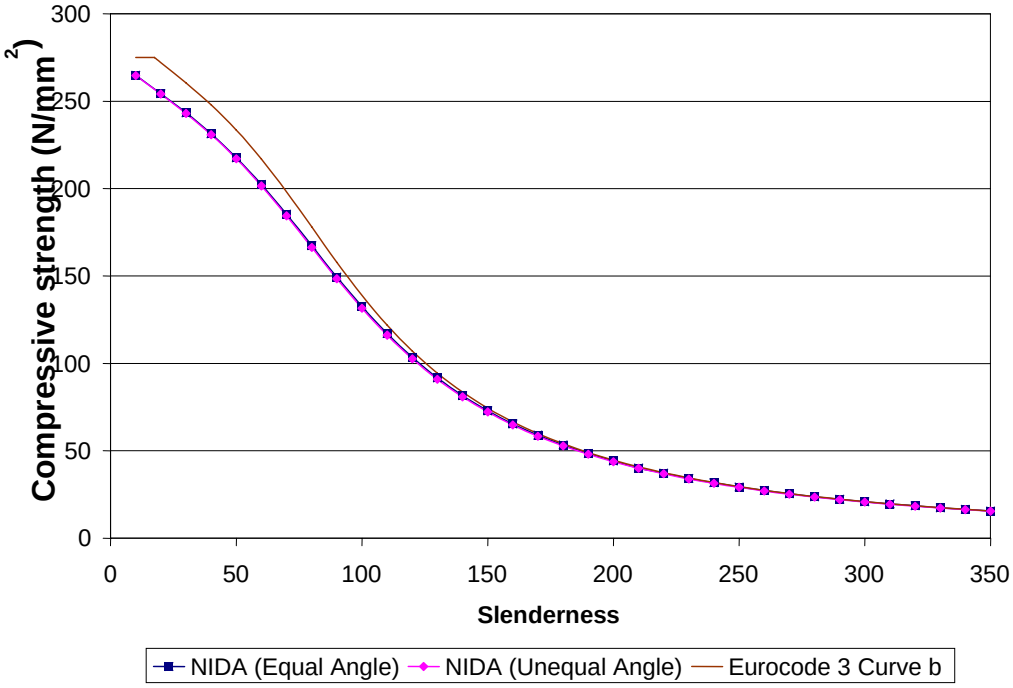

Figure 5.3 Compressive strength curves to Eurocode 3 Curve b

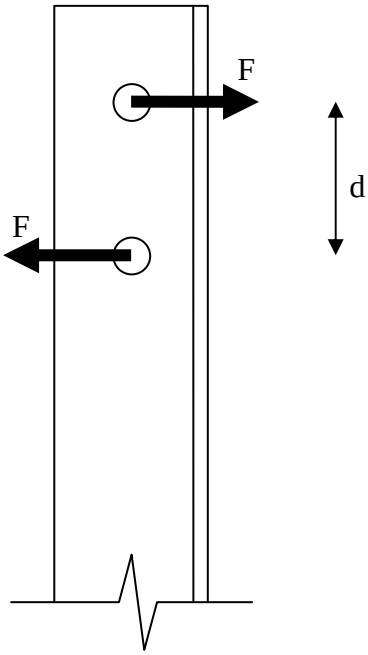

Figure 5.4 Couple formed by shear forces of two bolts

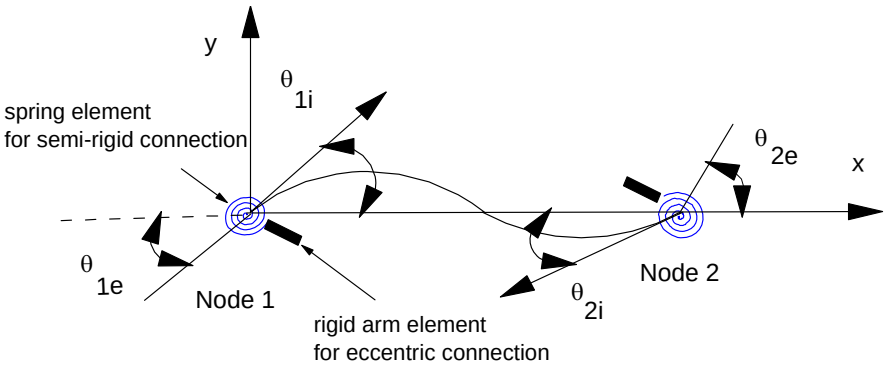

Figure 5.5 The external and internal rotations

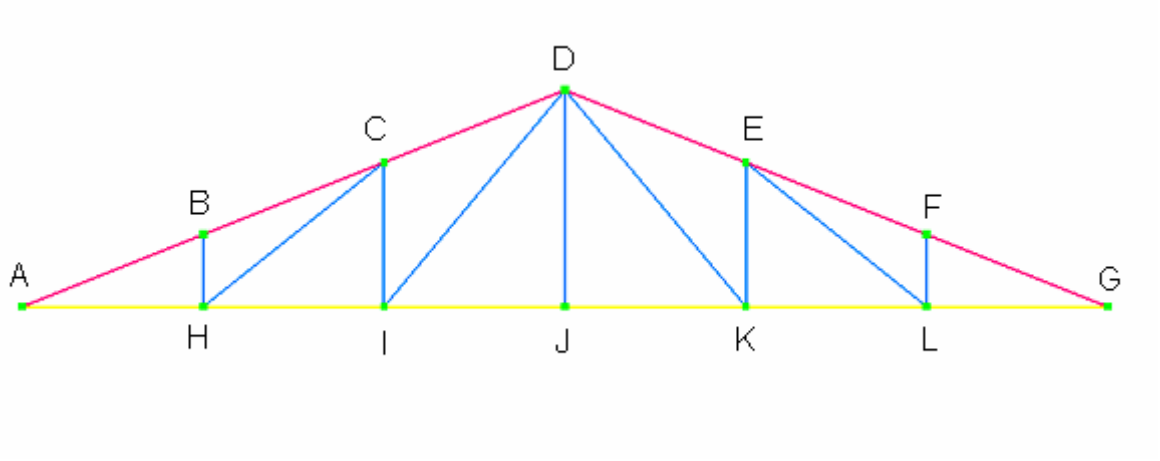

Figure 5.6 A typical roof truss

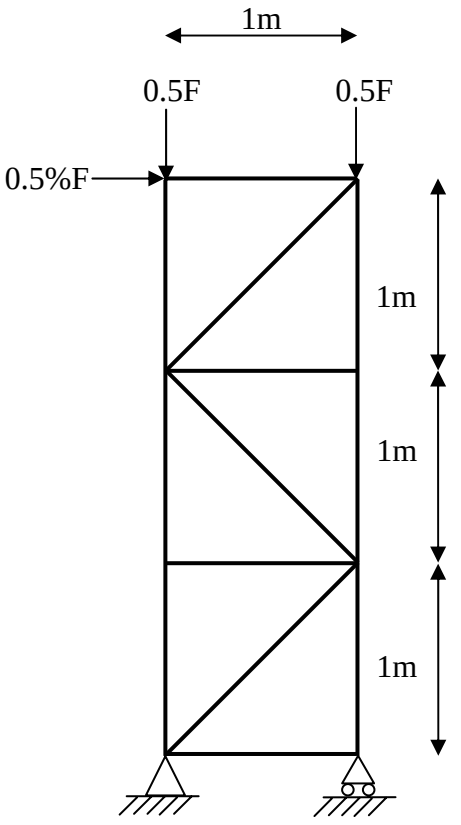

Figure 5.7 A tower truss

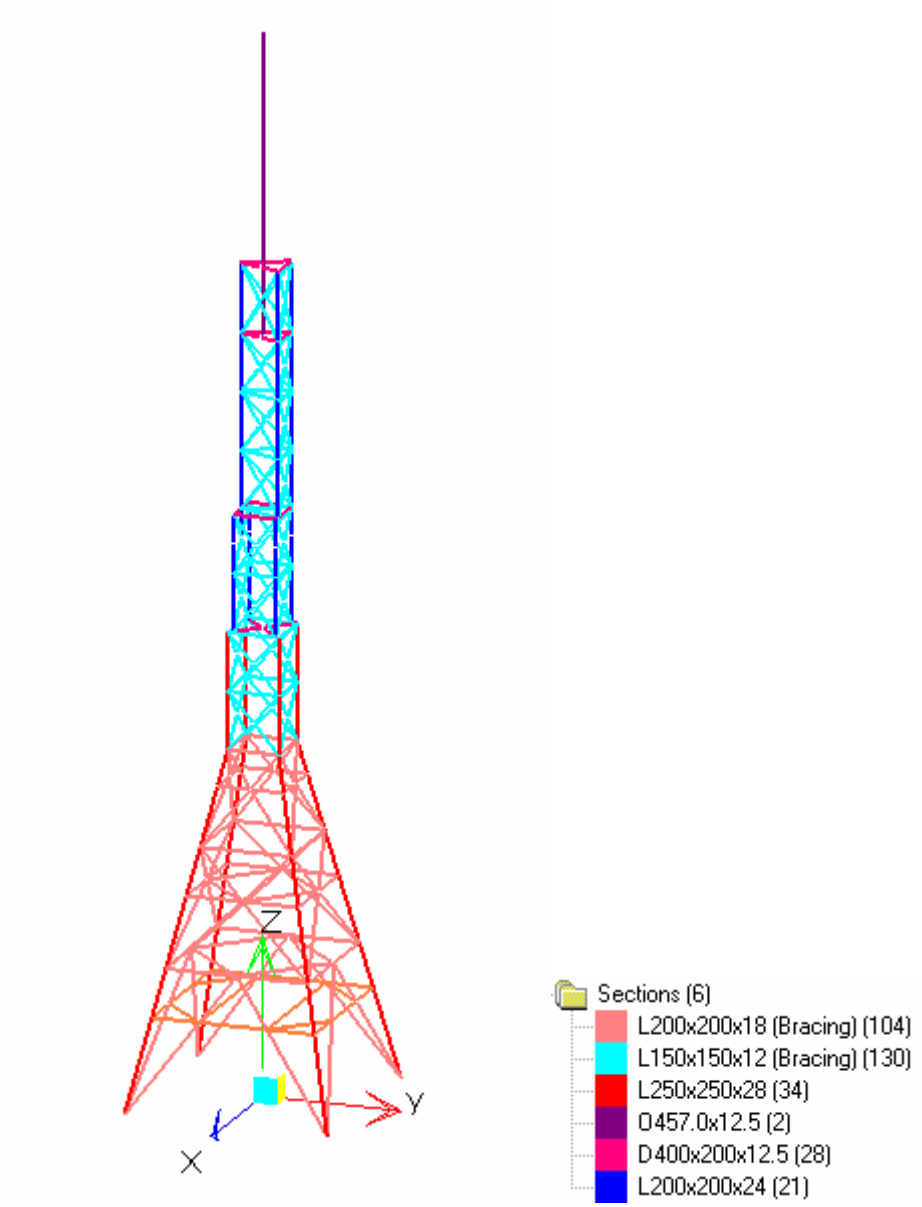

Fig. 5.8 Overall view of the tower

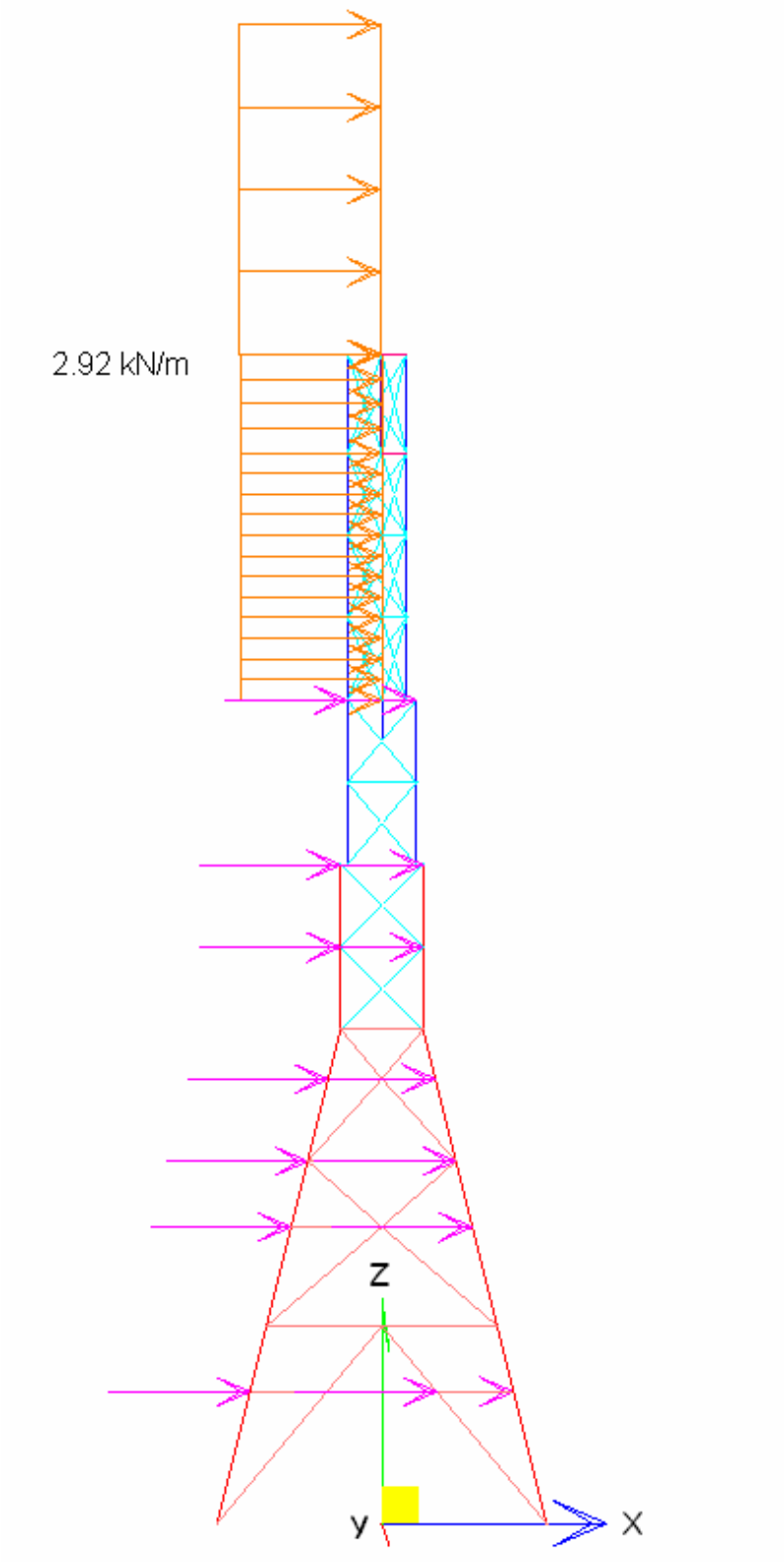

Fig. 5.9 Wind load acting on antennas (X Direction)

Table 5.1 Summary of design values of δ_0/L

	Section	y/r	δ_0/L **to BS 5950**	δ_0/L **to Eurocode 3**
Equal angle	L30×30×3	2.031	1/369	1/512
Unequal angle	L80×60×7	2.281	1/414	1/575

Table 5.2 Internal member forces of the roof truss

Member	**Force (kN)**	**Member**	**Force (kN)**
AB	-112.0	CI	-25.0
BC	-112.0	DI	+32.5
CD	-89.7	AH	+20.7
BH	-16.7	HI	0
CH	+26.5	IJ	-20.8

Table 5.3 Results of various analysis types

	Single Bolt		Double Bolt	
	Load Factor	**Failure Member**	**Load Factor**	**Failure Member**
BS 5950	1.01	Web	1.22	Rafter
Second-order 1	1.00	Web	1.24	Web
Second-order 2	1.67	Web	1.76	Web

Note: Second-order 1 means equivalent initial curvature method

Second-order 2 means exact end moment method

Table 5.4 Comparison between BS5950 and the proposed method

Effective Length	**BS5950 Load (kN)**	$\frac{P}{P*}$ **(1)**
1.0L	52.8	0.633
0.85L	67.2	0.806
0.7L	85.2	1.022

(1) $\frac{P}{P*}$ refers to the ratio of the BS5950 load to the load calculated by the proposed method.

Table 5.5 Material properties

Steel Grade	**Young modulus (kN/m^2)**	**Yield stress (kN/m^2)**	**United weight (kN/m^3)**
S355	2.05×10^8	3.55×10^5	76
Q345	2.05×10^8	3.15×10^5	76

Table 5.6 Section capacity factors

Section	Section capacity factors
L200x200x18 (Bracing)	0.836
L150x150x12 (Bracing)	0.761
L250x250x28	1.000
O457.0x12.5	-0.795
D400x200x12.5	0.709
L200x200x24	-0.658

Chapter 6 Advanced Plastic Analysis and Design of Angle Frames and Trusses

6.1 Introduction

In Chapter 5, the second-order elastic design and analysis of single angle members is developed and employed to design a practical tower. However, the design equations of these two design methods are developed based on the first yield of the material. It is obvious that complete failure or collapse of a structure is unlike when only the yield stress is reached at the outermost fibre as some portion of the material remains elastic and is able to sustain more loads. In fact, the section before loaded may have already yielded by residual stress due to welding that this elastic design is not rational. In general, the overall loading resistance of a structure is normally greater than the elastic design load resistance based on the first yield. For studies of progressive collapse and true ultimate load analysis, the elastic analysis may be not adequate. A frame can allow constituting members to have sections sustaining a load beyond its full plasticity in the process of carrying loads. In this case, the failure is irreversible. In this chapter, the proposed design method is extended to a second-order plastic design method. The reduced full plastic moment capacities of angle sections under axial force and biaxial bending are developed with interactive moment-axial force equations formulated. Using the set of interactive equations, more general software for second-order plastic or advanced analysis of typical frames made of members with symmetrical cross sections is modified and extended to the advanced analysis of angle trusses and frames. Research on the advanced analysis for this type of structures appears to be

unavailable in literature and the proposed method is believed to be among the original contribution on the important topic of advanced analysis of frames composed of asymmetrical cross sections like angles.

6.2 Assumptions

The proposed design method is based upon a number of basic assumptions about the material behaviour. Normally, steel exhibits upper and lower yield points and strain-hardening characteristics. In our proposed plastic design method, similar to other currently used design methods, the assumed material has the following behaviour:

1. Lower yield is assumed for the yield stress of material.
2. The yield stress in tension and compression are assumed equal
3. Strain-hardening is ignored; thus once the material has yielded, the stress is assumed to remain constant throughout any further deformation.

6.3 Full plastic moment capacities

With the above assumptions, it is now possible to determine the plastic bending moment capacity of an angle section at a fully plastic stage. Considering an angle section with unequal legs $b \times t$ and $\beta b \times t$, to simplify calculations, the section is idealized by assuming the material is concentrated at the centerline of the section and the actual round corners are replaced by sharp corners as shown in Figure 6.1. For the fully plastic section, different from the elastic neutral axis, the plastic

neutral axis must be the area bisector of the cross section so that the force equilibrium condition is satisfied. According to Trahair [72], if the points of intersections of the plastic neutral axis with the legs are defined by $\gamma_1 b$ and $\gamma_2 b$ as shown in Figure 6.2, then:

$$\gamma_2 = \frac{1+\beta}{2} - \gamma_1 \tag{6.1}$$

Theoretically,

$$0 \le \gamma_1 \le 1 \tag{6.2}$$

$$\frac{1-\beta}{2} \le \gamma_2 \le \frac{1+\beta}{2} \tag{6.3}$$

The full plastic moment M_{pY} about the geometric Y-axis can be calculated by taking moments of the fully plastic stress distribution about the axis through the horizontal leg of the angle section and is given by:

$$M_{pY} = p_y b^2 t \cdot \left(\frac{\beta^2}{2} - \gamma_1^{\,2} \right) \tag{6.4}$$

Similarly, the full plastic moment M_{pZ} about the Z-axis is given by:

$$M_{pZ} = p_y b^2 t \cdot \left(\frac{1}{2} - \gamma_2^{\,2} \right) = p_y b^2 t \cdot \left[\frac{1}{2} - \left(\frac{1+\beta}{2} - \gamma_1 \right)^2 \right] \tag{6.5}$$

To transform the moments about the rectangular axes to the moments about the principal axes, the following transformations are used.

$$M_{py} = M_{pY}\cos\theta + M_{pZ}\sin\theta \tag{6.6}$$

$$M_{pz} = -M_{pY}\sin\theta + M_{pZ}\cos\theta \tag{6.7}$$

in which θ is the principle angle.

6.4 The effect of axial load on moment capacities

To simplify calculations, angles with equal legs are considered, i.e. $\beta = 0$. With the presence of axial force, the full plastic moment is reduced. An angle section with arbitrary stress distribution with compressive stress at the heel and tensile stress at the toes is shown in Figure 6.3 $\gamma_1 b$ and $\gamma_2 b$ are the location where the plastic neutral axis intersects the angle legs but not an area bisector. Let n be the axial force ratio which is the ratio of axial load to its squash load. The section must be in force equilibrium. In other words, n can be worked out as:

$$n = 1 - (\gamma_1 + \gamma_2) \tag{6.8}$$

The centroid of an equal angle is approximately located at (0.25, -0.25) from the intersection of the two legs. The reduced moment capacities about the Y- and Z-axes are given by:

$$M_Y = p_y b^2 t \cdot \left[(1-\gamma_1) \cdot \left(\frac{1+\gamma_1}{2} - 0.25 \right) - \gamma_1 \cdot \left(\frac{\gamma_1}{2} - 0.25 \right) + (2\gamma_2 - 1) \times 0.25 \right]$$

$$= p_y b^2 t \cdot \left(\frac{\gamma_1 + \gamma_2}{2} - \gamma_1^{\,2} \right) \tag{6.9}$$

Similarly,

$$M_Z = p_y b^2 t \cdot \left(\frac{\gamma_1 + \gamma_2}{2} - {\gamma_2}^2 \right) \tag{6.10}$$

Applying rotational transformation matrix with $\theta = 45°$, the reduced moment capacities about the principal axes are given by:

$$M_y = \frac{\sqrt{2}}{2} p_y b^2 t \cdot \left[(\gamma_1 + \gamma_2) - ({\gamma_1}^2 + {\gamma_2}^2) \right] \tag{6.11}$$

$$M_z = \frac{\sqrt{2}}{2} p_y b^2 t \cdot \left[(\gamma_1 + \gamma_2) \cdot (\gamma_1 - \gamma_2) \right] \tag{6.12}$$

Using Equations (6.4) to (6.7), the full plastic moment capacities of an equal angle with the absence of axial force about the principal y- and z-axes can be calculated as follows:

$$M_{cy} = \frac{\sqrt{2}}{4} p_y b^2 t \tag{6.13}$$

$$M_z = \frac{\sqrt{2}}{2} p_y b^2 t \cdot \tag{6.14}$$

Therefore, Equations (6.13) and (6.14) can be rewritten and rearranged as:

$$\frac{M_y}{M_{cy}} = 2 \cdot \left[(\gamma_1 + \gamma_2) - ({\gamma_1}^2 + {\gamma_2}^2) \right] \tag{6.15}$$

$$\frac{M_z}{M_{cz}} = (\gamma_1 + \gamma_2) \cdot (\gamma_1 - \gamma_2) \tag{6.16}$$

From Equations (6.8) and (6.16),

$$\gamma_2 = (1-n) - \gamma_1 \tag{6.17}$$

$$\gamma_1 = \frac{1}{2} \cdot \left[\frac{M_z}{M_{cz}} \cdot \frac{1}{1-n} + (1-n) \right] \tag{6.18}$$

Eliminating γ_1 and γ_2 in Equation (6.15) will result in an interaction equation of axial force and biaxial moments:

$$n^2 + \frac{M_y}{M_{cy}} + \left(\frac{M_z}{M_{cz}} \cdot \frac{1}{1-n} \right)^2 = 1 \tag{6.19}$$

Geometrically, both γ_1 and γ_2 are limited from 0 to 1, Equation (6.19) is valid provided that:

$$\left| \frac{M_z}{M_{cz}} \right| \le 1 - n^2 \text{ for } n < 0 \tag{6.20}$$

$$\left| \frac{M_z}{M_{cz}} \right| \le (1-n)^2 \text{ for } n > 0 \tag{6.21}$$

For the section with tensile stress at the heel and compressive stress at the toes, a similar interaction equation can be worked out:

$$n^2 - \frac{M_y}{M_{cy}} + \left(\frac{M_z}{M_{cz}} \cdot \frac{1}{1+n} \right)^2 = 1 \tag{6.22}$$

Provided that

$$\left|\frac{M_z}{M_{cz}}\right| \le (1-n)^2 \text{ for } n < 0 \tag{6.23}$$

$$\left|\frac{M_z}{M_{cz}}\right| \le 1-n^2 \text{ for } n > 0 \tag{6.24}$$

6.5 Applications with second-order analysis

Equations (6.19) and (6.22) are modified and incorporated in a second-order analysis and design program NIDA [66].

$$\varphi_1 = n^2 + \frac{M_y}{M_{cy}} + \left(\frac{M_z}{M_{cz}}\right)^2 \frac{1}{(1-n)^2} \tag{6.25}$$

$$\varphi_2 = n^2 - \frac{M_y}{M_{cy}} + \left(\frac{M_z}{M_{cz}}\right)^2 \frac{1}{(1+n)^2} \tag{6.26}$$

Equations (6.21) and (6.22) are the yield functions of the section. At every load cycle, the section capacity of each member is checked. If M_y is positive, which means the heel is in compression, Equation (6.21) is adopted; if M_y is negative, which means the heel is in tension, Equation (6.22) is adopted. The analysis differs from the previously proposed elastic method in Chapter 5 is that if φ in Equation (6.21) or (6.22) reaches 1.0, the section achieves full plasticity; the young modulus of the material of the member is reduced to 0.1% of its elastic value and the internal member forces are replaced by those from the last load cycle. Therefore, no additional incremental forces and moments can be resisted by the member and

further moments are redistributed to the other members so that the load-deformation behaviour of the overall structure is still valid though one or more of its members yield.

The numerical method for second-order plastic analysis method is similar to the its elastic counterpart, except that the member resistance written in terms of the internal resistance vector with six components as $\lfloor F \quad M_{y1} \quad M_{z1} \quad M_x \quad M_{y2} \quad M_{z2} \rfloor^{\mathrm{T}}$, in which the alphabets represent respectively the axial force, bending moment about minor and major axes at two ends and the torsional moment, remain unchanged once the force and moment in the member reach the failure surface. The collapse load is then defined as the maximum load that the structure can withstand after which the load deflection curve declines and reaches the post-buckling stage.

To prevent the failure surface being violated, a small load step is applied and if the material factor φ defined in Equations (6.25) and (6.26) is greater than 1.0, the resistance vector is kept constant with the resistance normalized to 1.0 by dividing these 6 component force and moment by the material factor which is slightly greater than one if the load step is sufficiently small. Normally the recommended load step is 0.5% of the ultimate design load or the expected failure load for the angle truss. Numerical convergence through the use of minimum residual displacement iterative method [64] can normally be achieved when the load step is not too large and the structure does not form a mechanism. The approach has been

found to be an effective and reliable means of locating the ultimate load resistance of a steel structure or an angle truss.

6.6 Worked examples

Three examples are selected to verify the theory and the computational procedure. The first example is to compare the results against the code under various boundary conditions and the second example is to evaluate the theory against single member test for angles. The last example is to re-check the present theory against the tested result reported in the thesis of an undergraduate student..

6.6.1 Example 1 – comparisons with past experimental results

Experimental results from past research [14] are compared with theoretical results which are generated using NIDA. Each test specimen of size 2×2×1/4 in. ($A = 0.9375in^2$, $I_u = 0.5518in^4$, $I_v = 0.1434in^4$) was welded to a standard structural Tee of 8 in. long and 0.42 in. of stem thickness as shown in Figure 6.4. The young modulus and the yield stress of the material are 2.94×10^3 ksi and 50.9 ksi respectively. The test specimens are categorized into three groups according to their end conditions:

(a) Both ends are fixed in both directions as shown in Figure 6.5(a). However, the flexibility of the Tee stem allows out-of-plane rotation so it behaves as if elastically restrained in the out-of-plane direction.

(b) The strut ends in the direction of the outstanding leg of the angle can rotate freely, but the strut ends can not rotate in the plane of the Tee stem as shown in Figure 6.5(b).

(c) Opposite to end condition (b), the strut ends can not rotate in the direction of the outstand leg of the angle, but the strut ends can rotate in the plane of the Tee stem as shown in Figure 6.5(c). Similar to condition (a), the flexibility of the Tee stem allows out-of-plane rotation.

When using NIDA, the end eccentricities are considered by adding end moments at the end nodes and for end conditions (a) and (c) the flexibility of the Tee stem is modelled by two rotational springs added to the two end nodes. The stiffness of the rotational spring is given by:

$$k = \frac{k_A k_B}{k_A + k_B} \tag{6.27}$$

k_A and k_B are the rotation stiffness of the Tee stem alone and the Tee stem with the angle respectively as shown in Figure 6.6. The test results and the theoretical results with both elastic and plastic analyses are compared by plotting the failure load–slenderness relationship in Figures 6.7(a), (b) and (c) corresponding to three different end conditions. The predicted loads by NIDA using elastic analysis are always conservative to the test failure loads. The imposition of initial curvature magnifies the $P-\delta$ effect which allows the effects of residual stresses, other failure modes such as geometric axis flexural buckling and flexural-torsional buckling considered implicitly and gives design which fulfils the BS 5950 [3]

requirements. Comparatively, the predicted failure loads by NIDA using plastic analysis are closer to the experimental failure loads but not necessarily lower. This can be due to the experimental factors like quality of specimens, load application details and restraint etc. This shows that NIDA can give reliable result when dealing with biaxial bending, twisting and end restraint problems with the elastic solution ready for use for conventional design and the advanced analysis solution for collapse analysis in which not the design load, but the collapse load is of more interest.

6.6.2 Example 2 – Design of a floor truss

Figure 6.8 shows a four-bay indeterminate floor truss using 80×80×8 angles ($A = 12.2cm^2$, $I_u = 115cm^4$, and $I_v = 29.9cm^4$) as chord members and 50×50×5 angles ($A = 4.8cm^2$, $I_u = 17.4cm^4$, and $I_v = 4.55cm^4$) as web members. The material used is grade S275 steel with Young's modulus of 205kN/mm^2. An external force of 10 kN is added on each node on the upper chord. The floor truss is studied by three approaches, namely the traditional code method, the second-order elastic analysis method and the second-order plastic analysis method. Table 6.1 shows the internal forces in the floor truss members if all joints are assumed to be pinned. Due to symmetry, only half of the floor truss is considered. The critical failure member would be the compression diagonal web member in the first bay. According to the BS 5950 [3], the compression resistance of the member is 46.1kN and the design load factor is 3.15 which means when the load is increased by this factor of 3.15, the structure reaches its capacity limit. Using the proposed elastic

analysis method, the load factor is 4.72, 50% higher than that of the conventional method. When advanced plastic analysis is adopted, with the resistance vector remains unchanged once the force and moment in the member reach the failure surface, the load factor will be 5.69, which shows a further increase of 20%.

6.6.3 Example 3 – Design of a simple portal frame

The advanced plastic analysis method can be used alternatively without Equation (6.25) and (6.26). The accuracy of the proposed approach using imperfect element has been demonstrated and the advantage of the present method over the conventional effective length method is illustrated in the example here. As a demonstration, a very simple portal braced by a pair of angle members is studied by the two approaches, the code method based on a linear analysis and the second-order plastic analysis. As shown in Figure 6.9, the portal is 2m high by 3m wide with beams and columns of the same section of 305x305x240 UC ($A = 3.05 \times 10^3 cm^2$, $I_z = 6.42 \times 10^4 cm^4$ and $I_y = 2.031 \times 10^4 cm^4$) of S275 steel grade. The bracing angles are taken as sections 120x120x10 angles ($A = 23.2 cm^2$, $I_u = 497 cm^4$ and $I_v = 129 cm^4$) grade S275 steel of slenderness ratio around 150 with both ends pin-connected to the columns by a single bolt. For simplicity, the gusset plate is assumed thin with negligible flexural stiffness so that rotational spring at connection is ignored. The portal is pinned to ground and the beam is pinned to column, which represents the simplest case of simple construction with beams simply supported on columns and lateral force resisted by a bracing system.

In conventional linear analysis, the compressive angle member may be ignored in actual practice because of its high slenderness. Thus, two linear analyses were carried out with and without considering the presence of compression member for comparison. For second-order analysis, imperfection of L/360 is used in the analysis. Equation (6.25) and (6.26) are not applied. Instead, a linear interaction equation is adopted. In all design, the design load is assumed when the first member fails except in an elastic-plastic analysis where analysis is continued until the load cannot further be increased with increment of displacement. The failure loads calculated from various analysis methods are summarized in Table 6.2. From the results, the following observations have been made.

1. The conventional approach ignoring bracing members in compression yields a much higher loading capacity than considering bracing members in compression

2. However, second-order elastic analysis with allowance for their strength and stiffness reductions due to high slenderness and imperfections showed that this may be incorrect to ignore the compression bracing member as most compressive members are able to take consideration loads. The conventional approach ignoring compression bracing members may result in considerable over-designing.

3. If second-order plastic analysis is used, the loading capacity of the portal frame can be further increased considerably by 64%

The superiority of the present method over the conventional linear analysis is obvious in this example. The contribution of the compression member can be considered when using the second-order analysis and the actual failure mode in the structure can be manifested, both of the considerations are not possible to consider in a linear analysis with the effective length method.

6.7 Concluding remarks

It has been well known that failure of a member may not necessarily lead to the collapse of the complete structure and the reserve in strength after first member buckling can only be exploited when a second-order plastic analysis is carried out. Sequel to Chapter 5, this Chapter reports the method for advanced or second-order plastic analysis and design of angle trusses. A useful yield surface for angle section is proposed for incorporation into second-order analysis software such that the design of angle trusses and frames can be carried out efficiently, accurately and directly without empirical assumption of an effective length. The concept underlying the proposed theory can be extended to other sections like channels and unequal angles. The proposed work is aimed for putting second-order elastic and plastic analysis to practical design of structures composed of angle sections. So far, this proposed advanced plastic design method has not been used nor recommended for practical structures. However, it can be treated as the last resort to the sudden increase of ultimate load.

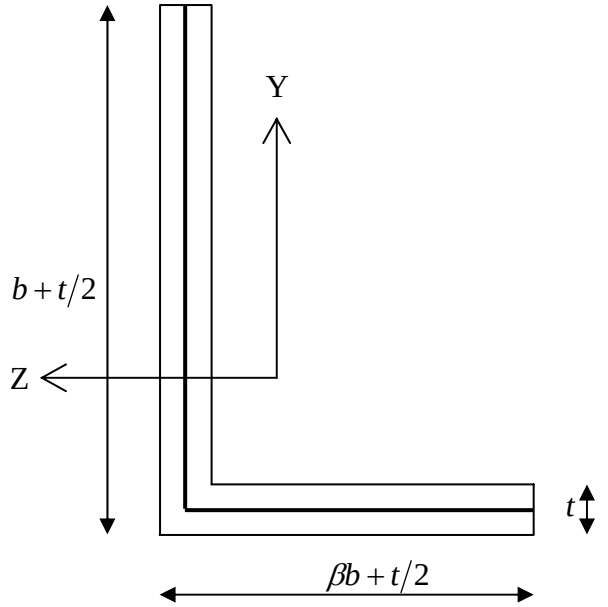

Figure 6.1 Midline idealization of an angle section

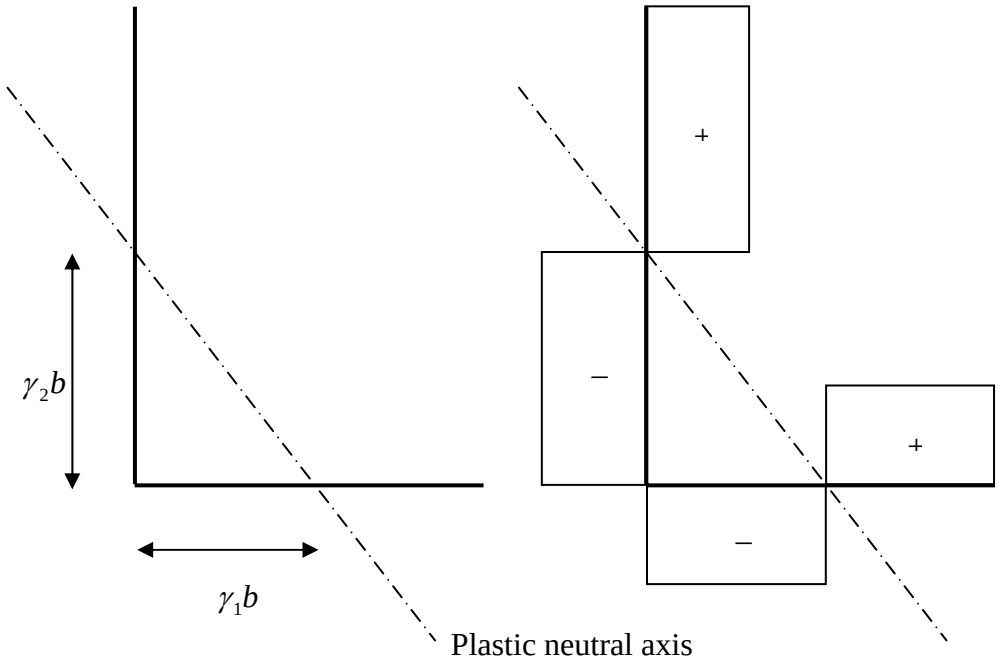

Figure 6.2 A fully plastic angle section without axial force

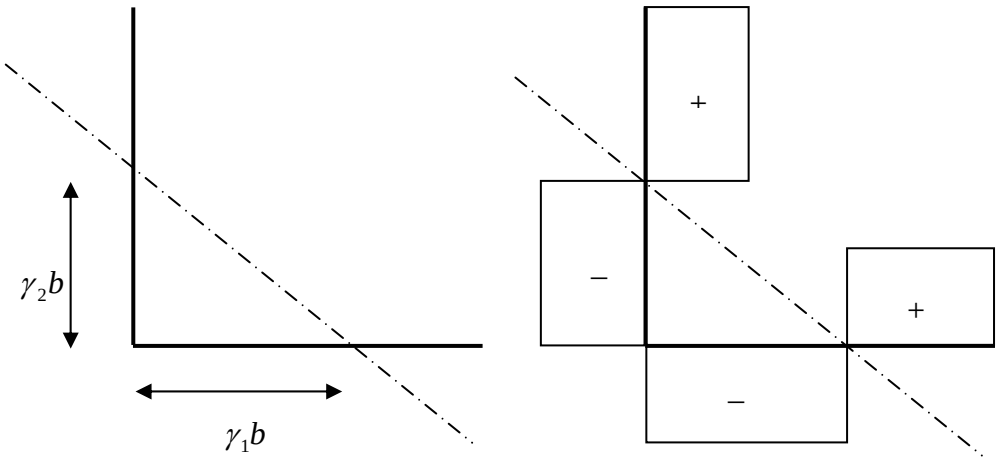

Figure 6.3 A fully plastic equal angle section with axial force

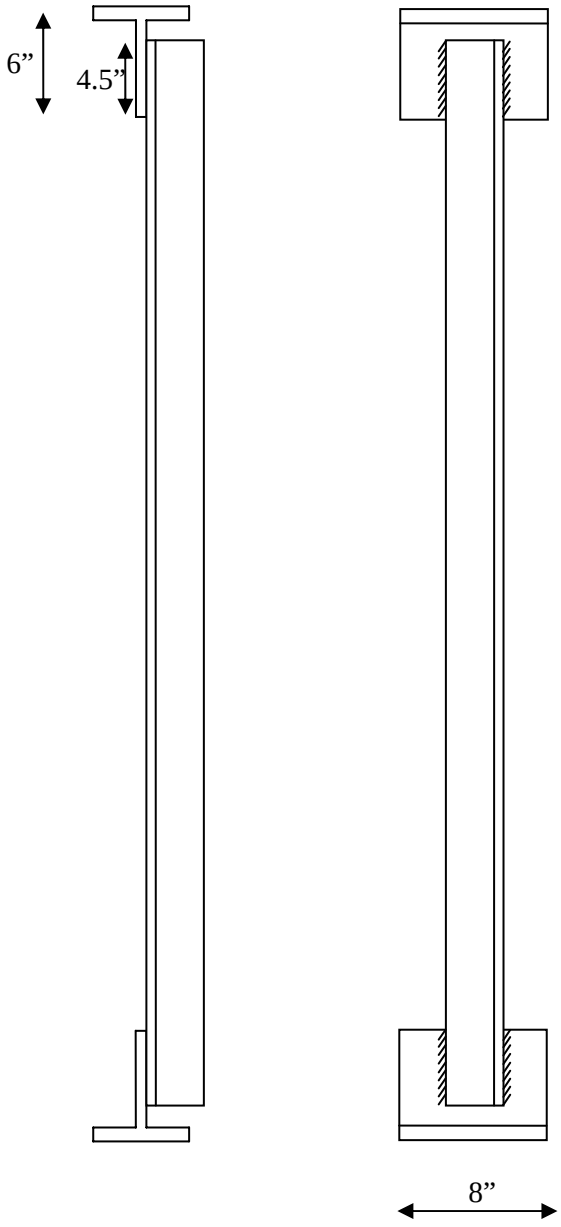

Figure 6.4 Front and side view of test specimen

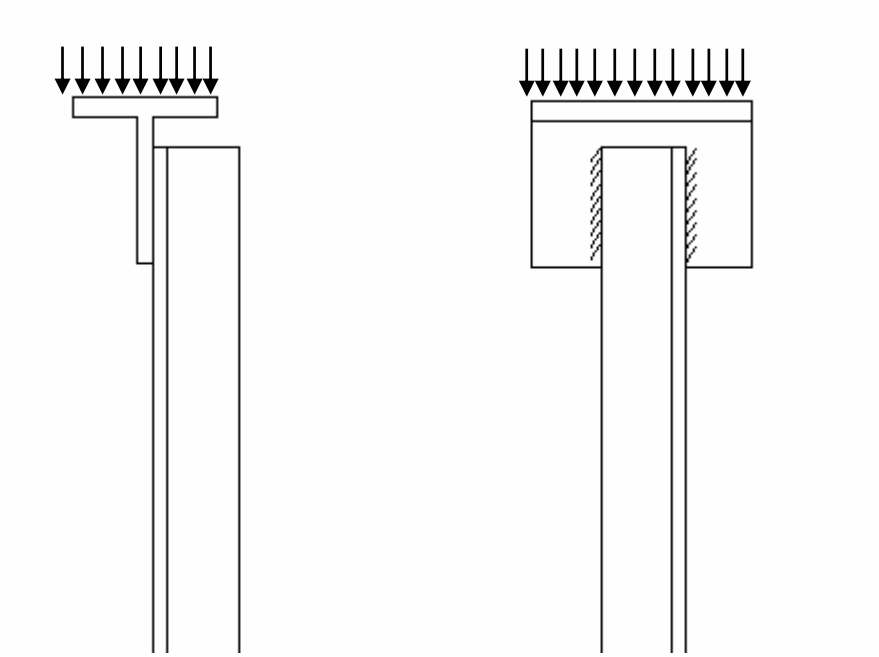

End condition (a)

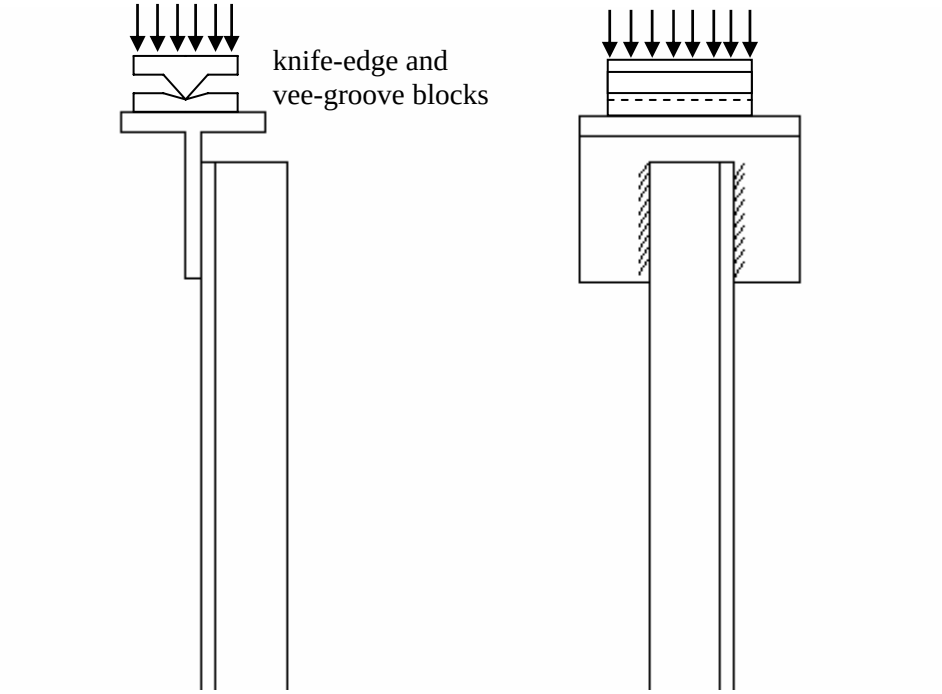

End condtion (b)

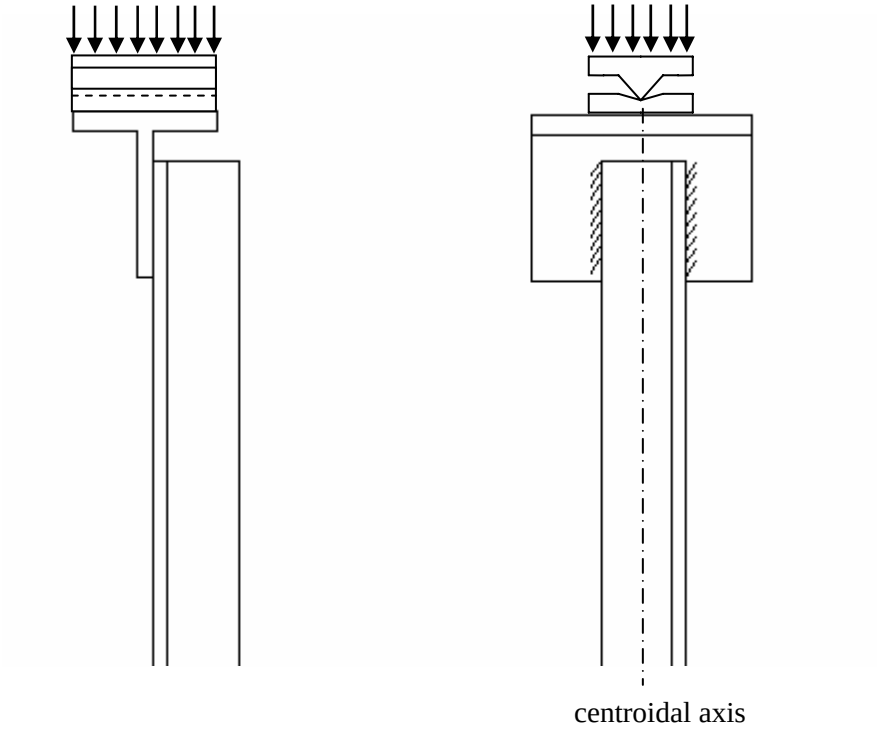

End condition (c)

Figure 6.5 Front and side view of end conditions

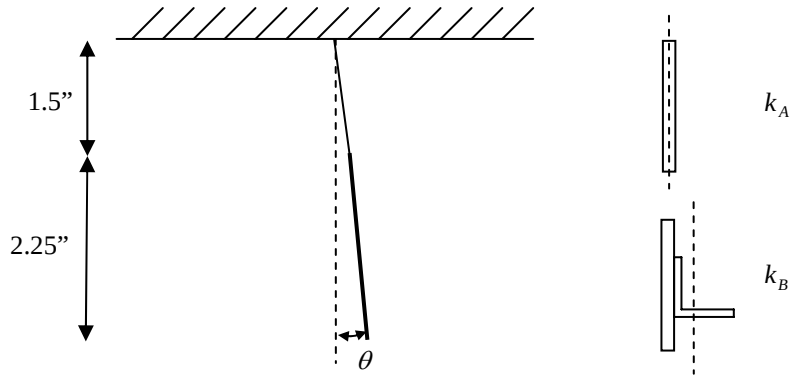

Figure 6.6 Idealization of rotation spring

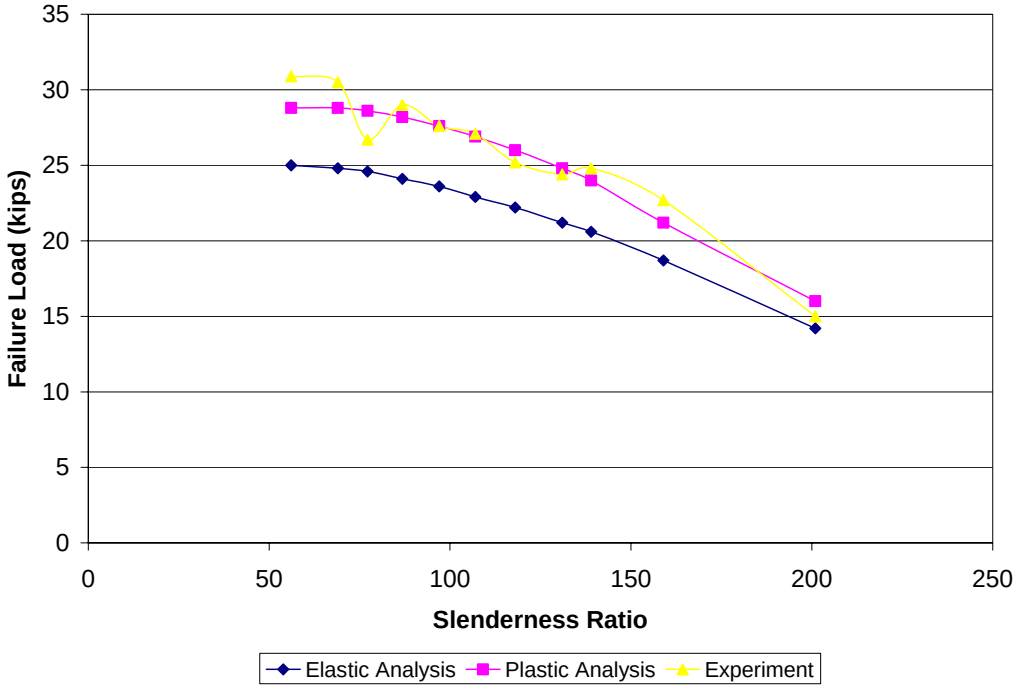

End condition (a)

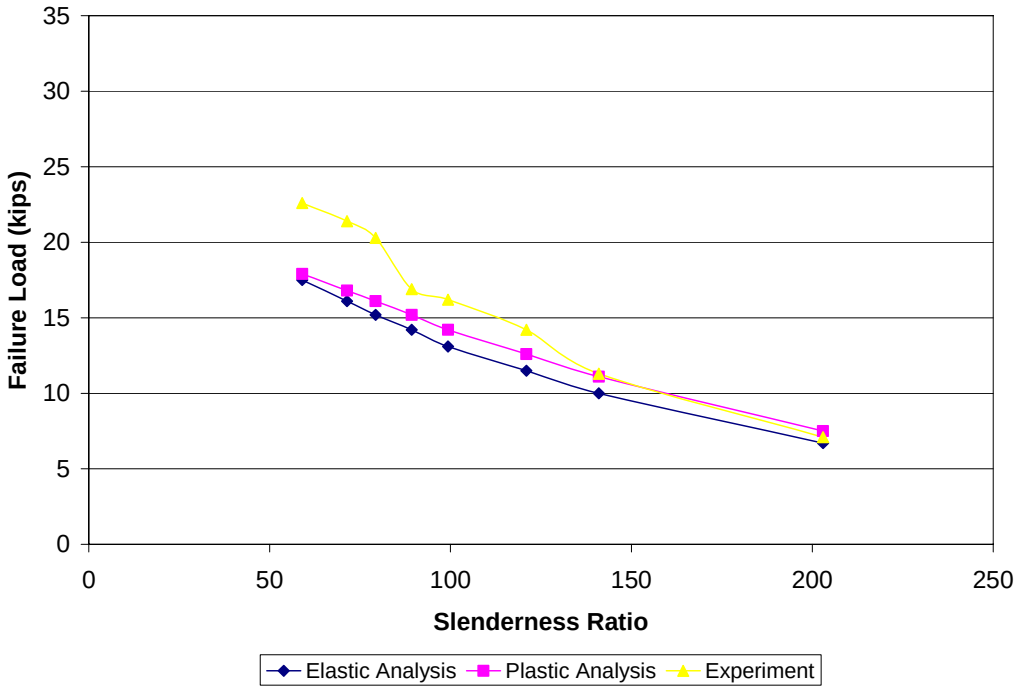

End condition (b)

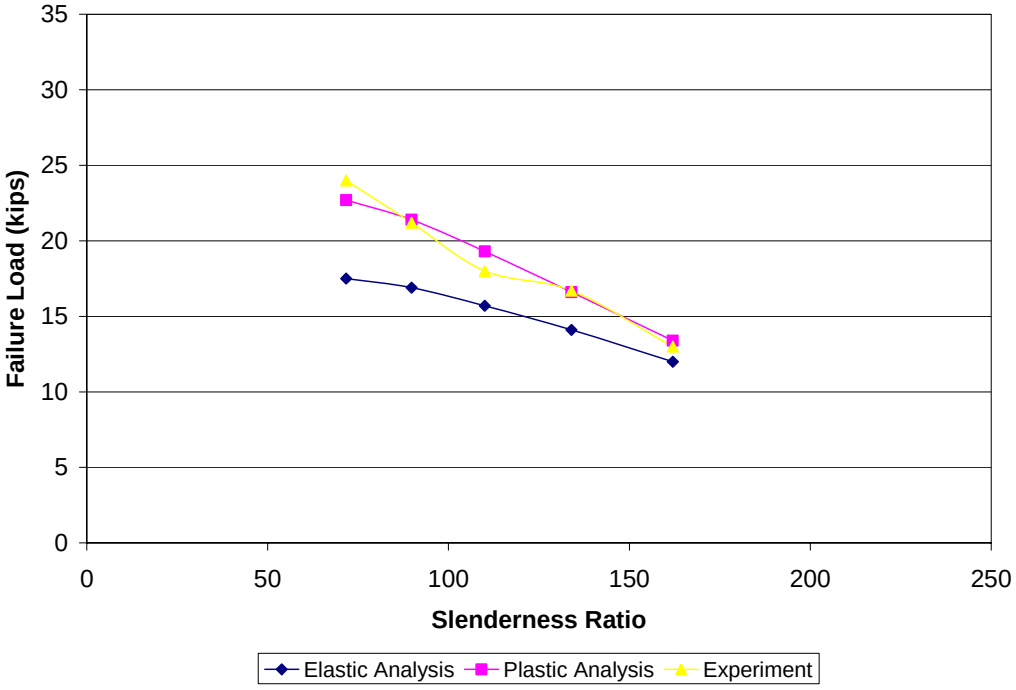

End condition (c)

Figure 6.7 Failure load vs Slenderness Ratio

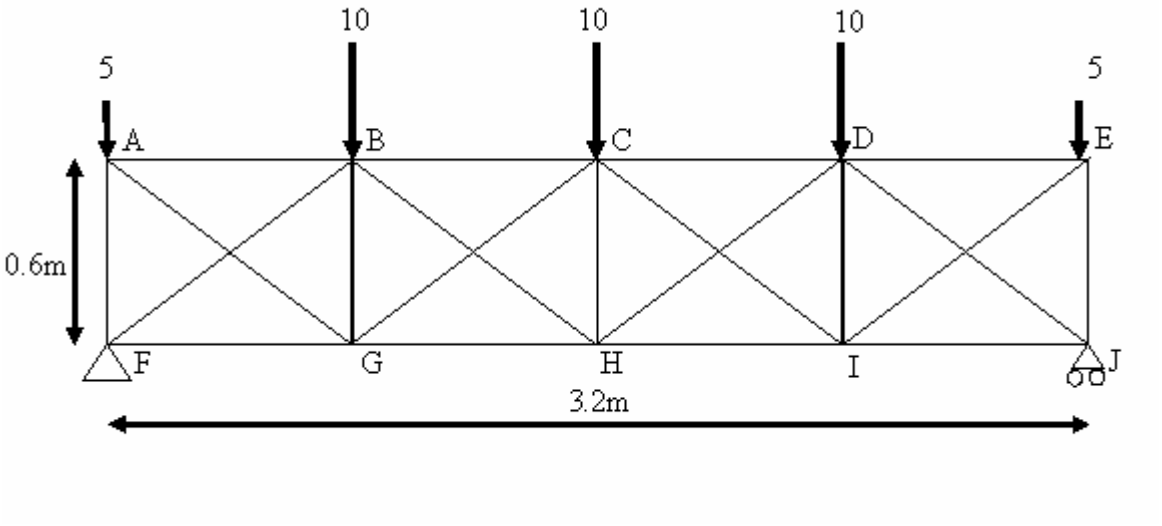

Figure 6.8 A typical floor truss

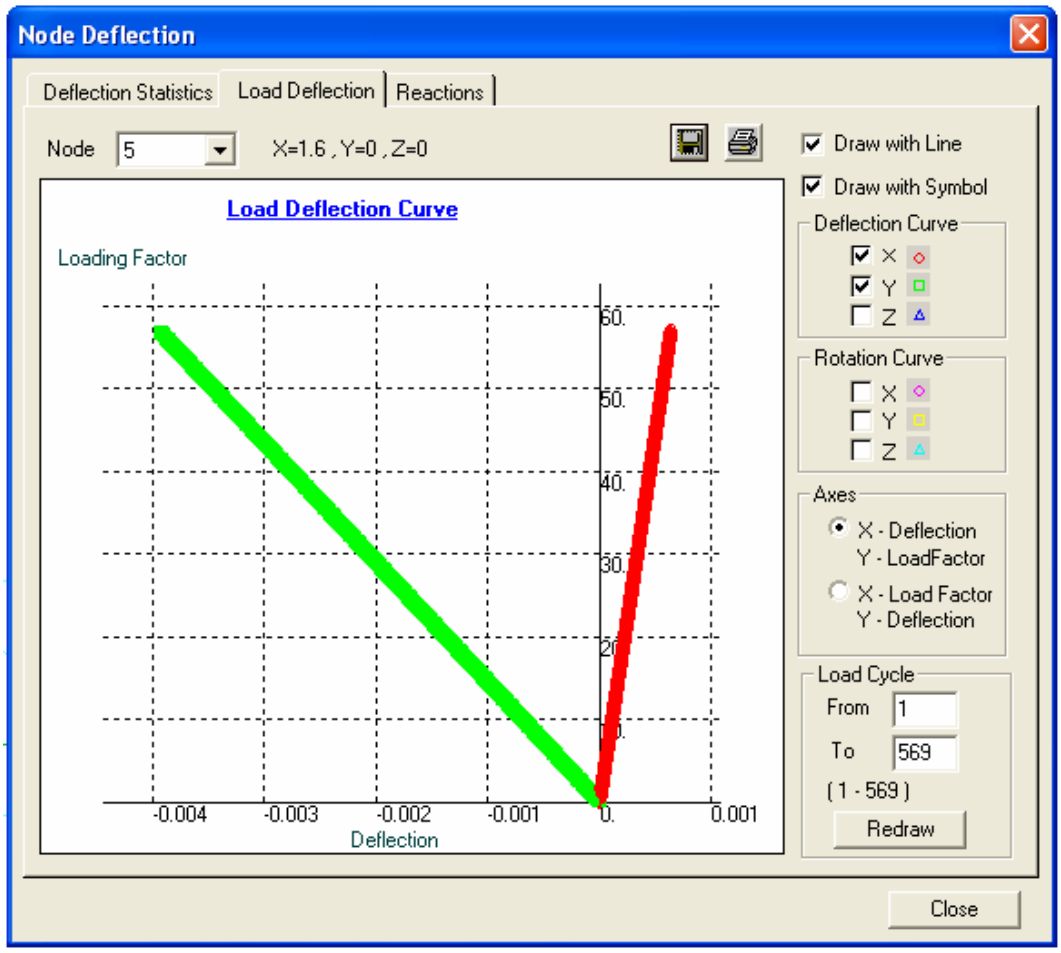

Figure 6.9 Load deflection curve of Node H in Example 2

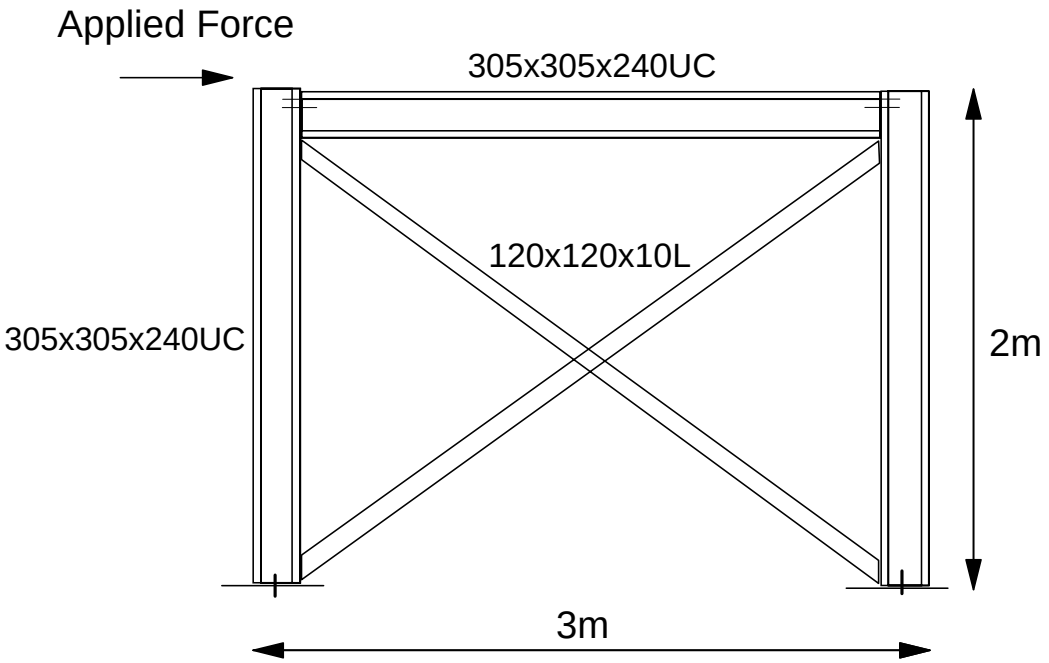

Figure 6.10 A simple portal

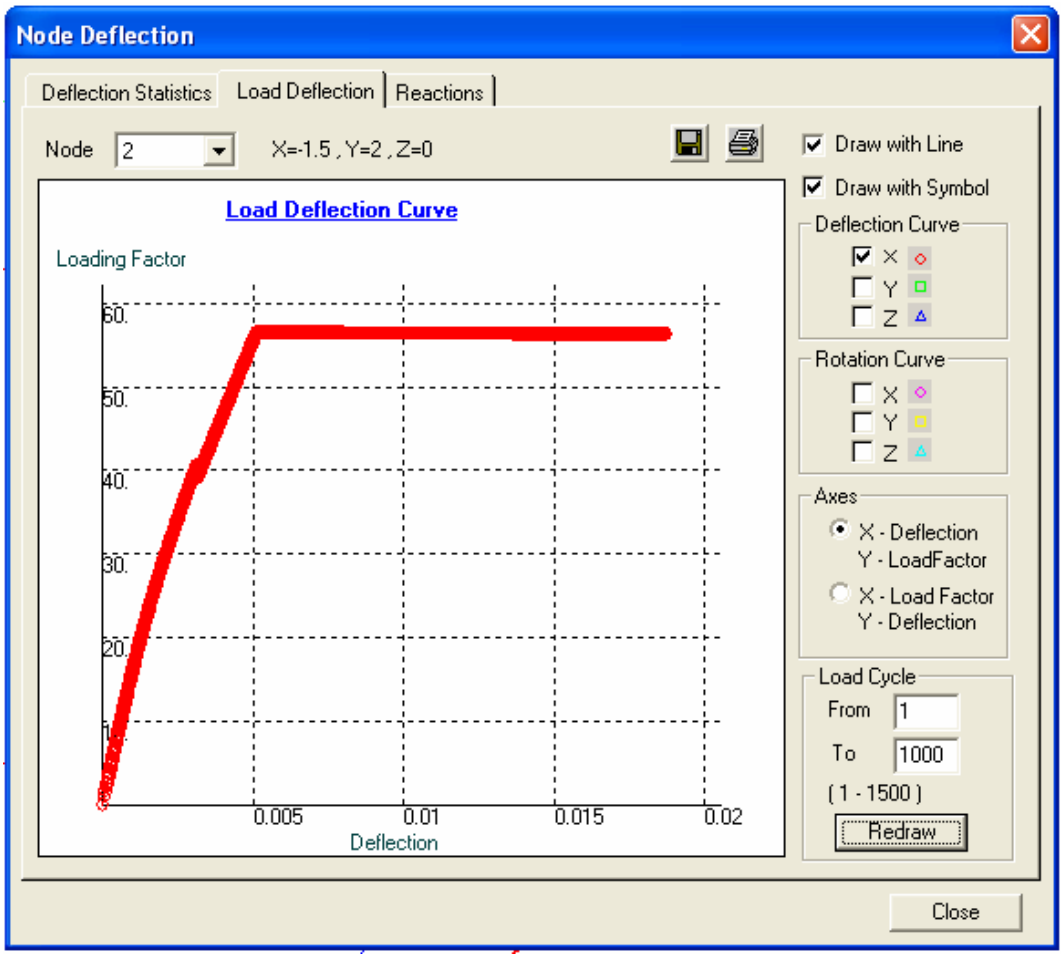

Figure 6.11 Load deflection curve at the point of load application in Example 3

Table 6.1 Internal member forces of floor truss in Example 2

Member	**Force (kN)**	**Member**	**Force (kN)**
AB	-8.3	CH	-3.8
BC	-22.5	AG	+10.4
FG	+11.7	BF	-14.6
GH	+24.2	BH	+3.1
AF	-11.2	CG	-5.2
BG	-3.1		

Note: + means tension
- means compression

Table 6.2 Design load of various types of analysis

Analysis Type	Design Load at First Yield [1](kN)	Corresponding Force at Compression Brace [2] (kN)	Corresponding Force at Tension Brace [2] (kN)
Linear analysis with design load assumed at failure of compression brace	205.0	123.0	123.0
Linear analysis ignoring the presence of compression brace	534.0	-	640.8
Second-order elastic analysis	282.4	118.4	221.6
Second-order plastic analysis	464.0	116.8	441.6

Note:

1. Design load, which is taken as the lateral load causing the bracing member to yield.
2. The compression or tension force at the design load
3. The design load calculated from the recommended imperfection in this paper.
4. Elastic-plastic buckling load obtained by simple maintenance of the maximum resistance of the compressive brace with the external load continues to increase until a mechanism is reached.

Chapter 7 Experimental Investigation

7.1 Introduction

In order to verify the models used in Chapters 5 and 6 and study the structural behaviour of a slender angle web member of a truss under predominately axial force, laboratory tests of angle trusses were carried out. Four single angle struts with slenderness ratio about 150 were tested as web members of a two-dimensional truss, which involves single-bolted and double-bolted connection and web members connected on one side or on alternative both sides. Although the truss is two dimensional, the failure modes of all test specimen were out-of-plane buckling. The ratios of failure load to squash load ranged from 0.219 to 0.303. The results will be compared with the theoretical and the design values in the followings.

7.2 Test Programme

Two series of tests involving four single angle struts as web members of a two-dimensional truss were carried out. The truss shown in Figure 7.1 is simply supported at its two ends with one end pinned and one end roller. The dimensions of the truss are carefully measured through its centre line. In the first series, the web members of the truss are connected to the chord members on the same side. Figure 7.2 shows the connection details of the specimen with webs connected on the same side with double-bolted connection. In the second series, the tests are repeated with the web members connected to the chord members on alternative sides. The specimens are of Grade S275 and two metres in length, making the

slenderness ratio (L/r) around 150. The leg length-to-thickness ratio meets the BS 5950 [3] requirements so that local buckling can be ignored. Each end of the member is connected to a gusset plate. The test included single and double bolted connections. Other details of the specimens are listed in Table 7.1.

7.2.1 Experimental set-up and instrumentation

The trusses were loaded in pair and sufficient lateral restraints were provided to ensure out-of-plane buckling at connecting nodes between chords and webs is fully avoided. Load was applied at the upper joint of the target failure member through a hydraulic jack. As shown in Figures 7.3 and 7.4, twelve strain gauges were mounted evenly at the mid-length of the targeted member and the tested truss was so designed that the targeted member fails first so that all measuring devices like displacement transducers and strain gauges can be mounted on the member which first fails. At the targeted member, two displacement transducers were positioned in the in-plane and out-of-plane directions and transducers were also used to monitor the movements of the top and the bottom joints of the targeted member so that the movement of the target member relative to the truss can be measured. The test was performed in a load-control manner. At the beginning of the test, the readings were recorded at an interval of 3kN. When the applied load was close to the estimated failure load, the interval was reduced to 1kN. At the load where the targeted member buckled or failed, the deformations of the remaining parts of the truss were small and reversible. Thus, after each test, the failed member was replaced by a new specimen so that the next test could be conducted under almost identical condition.

7.2.2 Testing procedure

1. The truss was fabricated.
2. Strain gauges were mounted on the mid-span of the test specimens as shown in Figure 7.3.
3. The test specimen was fixed on the truss.
4. The transducers were installed as shown in Figure 7.4.
5. The transducers were connected to the data logger and checked if they were properly connected.
6. The specimen was pre-loaded to 5 % of the estimated failure load through a manual hydraulic jack.
7. Load was applied on the specimen through a manual hydraulic jack and the load cell and transducer readings were recorded through the data logger at specified intervals.
8. Any observations, including the failure modes, during the test were recorded.
9. The test was stopped gradually after failure was observed.
10. The truss was unloaded gradually.

7.3 Test Results

7.3.1 Failure modes

The major failure modes are flexural buckling about the principal minor axis as shown in the photos (Figures 7.5 and 7.7). Figure 7.5 shows the buckled shape of

Specimen 1a, of which each end is connected to the gusset plate with single bolt, making it behave more like pin-ended in the in-plane direction as shown in Figure 7.6. In the meantime, the gusset plate provides some flexibility in the out-of-plane direction. Figure 7.7 shows the buckled shape of Specimen 1b, of which each end is connected to the gusset plate by two bolts. The double bolt connection at each end provides some flexibility making it behave as if partially restrained in the in-plane and out-of-plane directions as shown in Figure 7.8.

7.3.2 Load-deflection curves

The global displacements of the truss were measured by the transducers placed at the in-plane and out-of-plane directions at the mid-span and also at the upper and the lower joints of the targeted member. The relative movement to the truss can thus be calculated by these readings. Figures 7.9 and 7.10 respectively show the in-plane and out-of-plane deflections of the four specimens. The slope of each curve indicated the stiffness of the specimen. A steeper slope implies a stiffer structure. As can be seen from the curves, generally, their response patterns are similar with the out-of-plane deflections always more severe than the in-plane deflections and the double-bolted specimen having stiffer slopes than the single-bolted counterparts.

7.3.3 Failure loads

Table 7.2 listed the member failure loads and the corresponding failure load of the truss (taken as 50% of the total applied load) which are calculated using numerical integration of the stress over the cross-sectional area. The ratios of failure load to

squash load ranged from 0.219 to 0.303. It can be seen that the load capacities of the specimens with double bolt end connections are 9% to 15% higher than the counterparts with single bolt end connections. For the same end conditions, specimens with alternate side web arrangement will have the load capacities 15% to 20% lower that those with same side web arrangement. The alternately opposite side arrangement of the web members will make the end moments due to eccentric connections more severe.

7.4 Coupon Tests

In order to validate comparisons among loading tests carried out on different specimens, theoretical loads calculated by BS 5950 [3] and NIDA [66], the properties of the steel used in the test specimens should be established by means of coupon tests. Four coupons were therefore cut from flat, unyielded areas of the test specimens after completion of the load testing. The dimensions of the coupons were measured accurately using a Vernier caliper. The yield strength and the Young modulus of the steel were determined by tensile testing following the procedure given in BS EN 10002-1 [73]. Figure 7.11 shows the tensile test machine. The averaged results of the coupon tests are summarized in Table 7.3. Coupons 1a, 1b, 2a and 2b were cut from Specimens 1a, 1b, 2a and 2b respectively. All measured yield stresses exceeded the nominal yield strength ($275N/mm^2$) while all of the Young's moduli were in line with the nominal value ($205kN/mm^2$). Figure 7.12 shows the stress-strain curve of Coupon 1a.

7.5 Comparisons

7.5.1 Comparisons with BS 5950

BS 5950 [3] provides a simplified method for designing struts composed of single angles as mentioned previously in Chapter 3. They may be treated as axially loaded members with reduced compressive strength with ignoring the eccentricities at end connections. Using the measured material properties, the results calculated from the simplified method are summarized in Table 7.4. Although this method is easy and simple to use, it is not able to show the difference between the same side arrangement and alternately opposite side arrangement of web members. In other words, provided that the materials are identical in two sets of tests, the predicted failure load using this method would be also the same. As can be seen from the results, this method provides overly conservative (45.9 to 61.8%) estimates for angle struts with single-bolted connection, especially with webs connected on the same side, implying that taking 80% of the compressive resistance is too conservative in this case. On the other hands, it provides less conservative (10.4 to 14.5%) estimates for the double-bolted counterparts meaning the assumption of effective length factor of 0.85 is reasonable in this case.

7.5.2 Comparisons with NIDA

The failure loads are predicted by NIDA with the end moments and end rotational restraints taken into account during the analysis. This can be done by adding rigid arms to the element to simulate the eccentricity and adding rotational spring elements at the element joints to simulate the end restraints. The length or the rigid arm is taken as, which is equal to the distance between the centroid of the angle

strut and the node. The value of the rotational stiffness k is calculated from the flexural stiffness of the gusset plate and approximated as 1000 kNm/radian. This value is close to the rigidly fixed condition achievable for use with preloaded bolts. In the present case of using non-preloaded bolts, the value of k is taken as 10% of the calculated value. It should be noted that the currently using section capacity check equation in NIDA is not suitable for angle sections because the equation was derived primarily for doubly symmetric sections of which maximum bending stresses about each principal axis occurs at the four corners simultaneously. However, for angle sections, as they are mono-symmetrical or asymmetric, the points of maximum bending stress about both principal axes do not necessarily coincide. As a consequence, the loading capacities of the sections calculated are usually underestimated. In the present studies, the axial stress is checked against every extreme point of the section.

The computed results using second-order elastic analysis are summarized in Table 7.5. Compared with the conventional design method using BS 5950 [3], the nonlinear analysis and design method provides more economical or less conservative estimates for the single-bolted specimens (14.1 to 20.9%) and narrowly more conservative estimates for the double-bolted specimens (16.1 to 17.2%) for double-bolted specimens. The computed results using second-order plastic analysis are summarized in Table 7.6. It can be seen that the theoretical failure loads calculated by the advanced plastic analysis method are barely conservative with discrepancy from 1.0% to 11.8% of the experimental failure loads, which means that the member is likely to fail in a plastic mode.

7.6 Discussion

Comparing the laboratory test results with the traditional BS 5950 design method and the proposed NIDA design method, the following conclusions can be made. First, while the BS 5950 method cannot take the web arrangement (same side or alternate sides) into consideration. The design method provides conservative predictions of the failure loads of the truss. Second, for compression members with single-bolted end condition, NIDA provided more rational predictions as it allows for end restraint stiffness. Third, for compression members with double-bolted end condition, BS5950 provided less conservative predictions. It is seen that the factor of 0.8 used in calculating the compression resistance of a single-bolted compression member is too conservative for some range of slenderness ratio. Although the BS 5950 method was noted to have a more accurate prediction for the failure loads of the double-bolted compression members using an effective length factor of 0.85, the joint and web arrangement details cannot be incorporated directly into the effective length method such what the present second-order analysis approach does. It is suggested that the discrepancy between the test results and the NIDA [66] results can be further minimized by considering the rotational stiffness due to the presence of the gusset plates and accurate calculation of the rotational stiffness of the joints at the two ends of the member.

7.7 Concluding remarks

This chapter reports the experimental investigation of single angle webs in compression in a form of two-dimensional truss. The experimental results are

compared with the failure loads calculated by the BS 5950 [3] and NIDA [66] by applying both second-order elastic and second-order plastic analysis with the load eccentricities and the end restraints considered. It is found that the laboratory test results agree well with the theoretical results with accuracy acceptable for design purpose.

Figure 7.1 Truss before test (webs on alternate sides)

Figure 7.2 Connection details (web on same side, double-bolted)

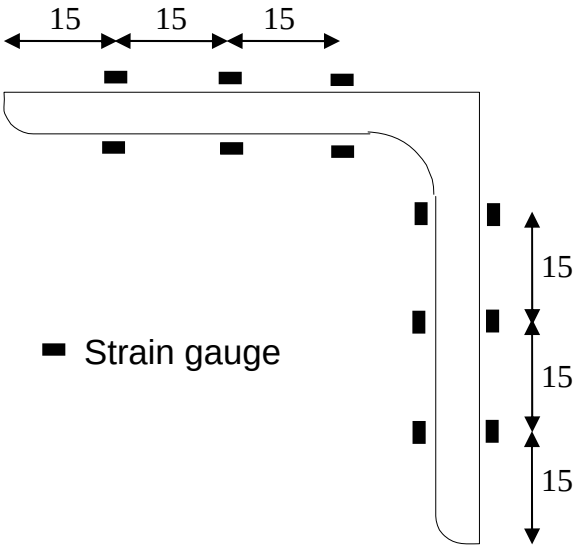

Figure 7.3 Locations of strain gauges

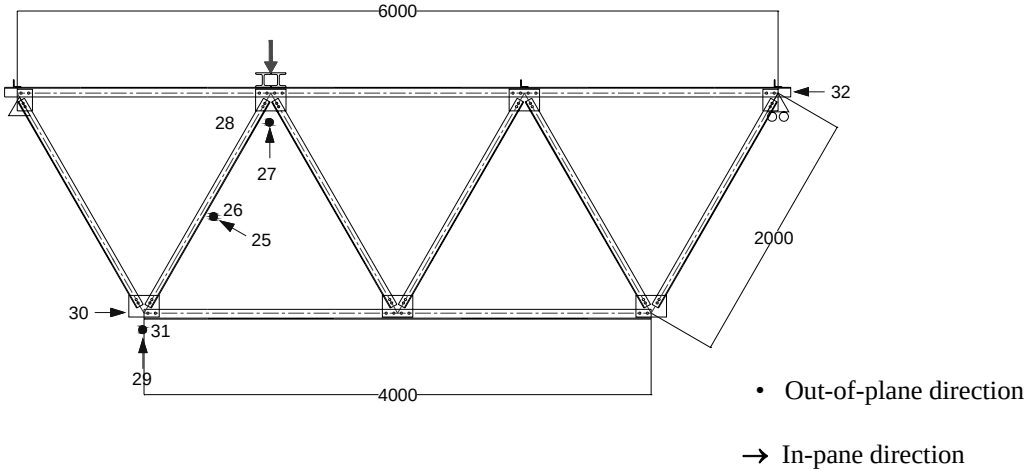

Figure 7.4 Locations of transducers

Figure 7.5 Weak-axis buckling mode (webs on same side, single-bolted)

Figure 7.6 Rotation of the specimen at the connection

(webs on same side, single-bolted)

Figure 7.7 Weak-axis buckling (webs on same side, double-bolted)

Figure 7.8 Rotation of the specimen at the connection

(webs on same side, double-bolted)

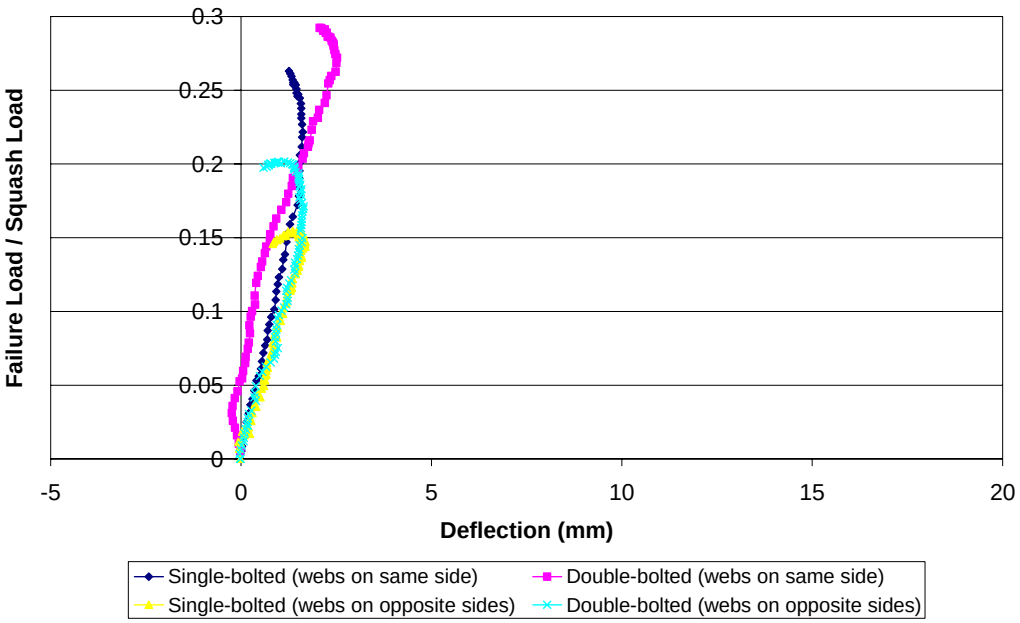

Figure 7.9 Experimental in-plane deflections of the specimens

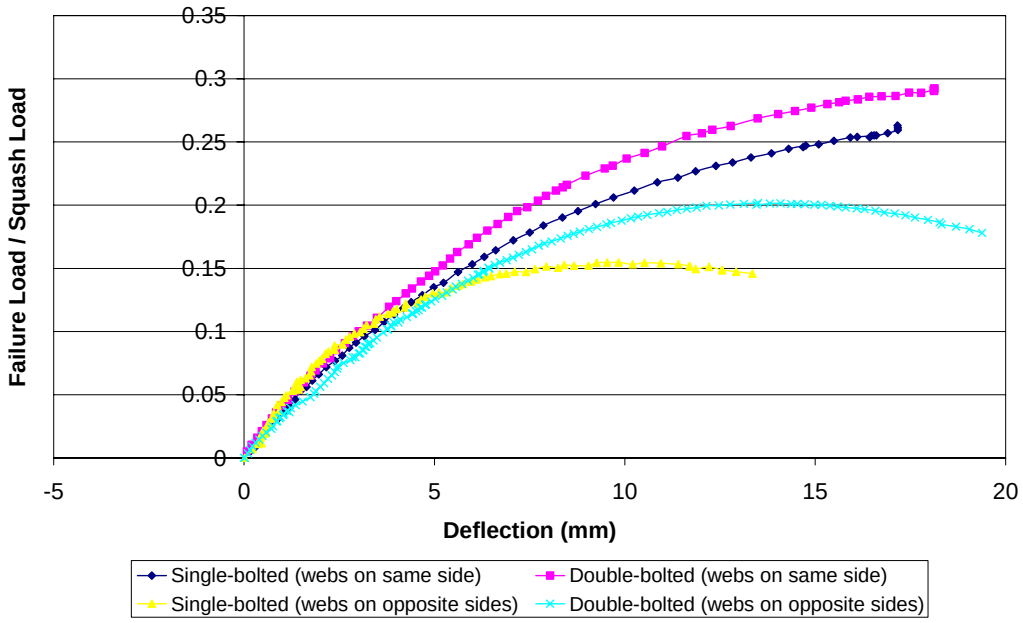

Figure 7.10 Experimental out-of-plane deflections of the specimens

Figure 7.11 Tensile test machine

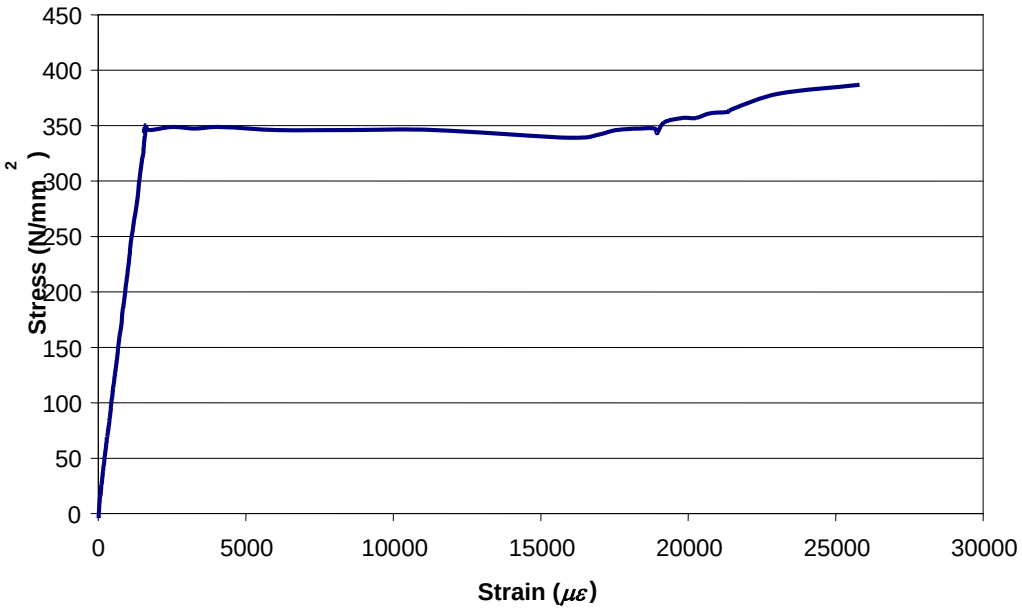

Figure 7.12 Stress-strain curve of coupon test (Coupon 1a)

Table 7.1 Details of test specimens

Specimen	Size	Web Arrangement	End conditions	Gusset Dimensions
1a	L65×65×6	Same Side	Single Bolt	240×180×8
1b	L65×65×6	Same Side	Double Bolt	240×180×8
2a	L66×66×6	Alternate Sides	Single Bolt	240×180×10
2b	L66×66×6	Alternate Sides	Double Bolt	240×180×10

Table 7.2 Experimental failure loads

Set	Specimen	Failure Load (kN)	Failure Load/ Squash Load	Failure Load of the Truss
1	1a	67.2	0.260	91.2
	1b	78.4	0.303	98.4
2	2a	57.5	0.219	68.4
	2b	72.1	0.275	78.9

Table 7.3 Coupon test results

Set	**Coupon**	**Young's modulus, E (kN/mm^2)**	**Yield stress, σ_y (N/mm^2)**
1	1a	216.9	347.0
	1b	211.8	347.6
	Average	214.4	347.3
2	2a	194.5	348.6
	2b	185.6	344.9
	Average	190.0	346.7

Table 7.4 BS5950 failure loads

Set	**Specimen**	**BS5950 Load (kN)**	**Test Load/ BS5950 Load**
1	1a	41.5	1.618
	1b	68.5	1.145
2	2a	39.4	1.459
	2b	65.3	1.104

Table 7.5 NIDA failure loads – Second-order elastic analysis

Set	Specimen	NIDA Load (kN)	Test Load/ NIDA Load
1	1a	55.6	1.209
	1b	66.9	1.172
2	2a	50.4	1.141
	2b	62.1	1.161

Table 7.6 NIDA failure loads – Second-order plastic analysis

Specimen	Theoretical Failure Load (kN)	Experimental Failure Load (kN)	Experimental Load / Theoretical Load
1a	60.1	67.2	1.118
1b	77.4	78.4	1.013
2a	54.3	57.5	1.059
2b	71.4	72.1	1.010

Chapter 8 Conclusions and Recommendations

8.1 Conclusions

The design of structures consisting angle sections have been controversial for some time because of the complexity arisen from the asymmetry of the section. Different national codes give considerably varied recommendations on the computation of design load resistance of angle struts. In spite of the lack of consistent design of this sectional type, it is practically very convenient to fabricate an angle structure by attaching one angle to another or through a gusset plate by connection through one leg. As a consequence, the load applied to the section is commonly eccentric and results in a pair of end moments. In the meantime, the connection may provide some degree of end fixity. Structural engineers may design this type of structures with the end moments and the end restraints considered in the analysis. However, to facilitate design process, some national codes such as BS 5950 [3], Eurocode 3 [42] and Hong Kong Steel Code [62] provide a simplified method which ignores the effects due to load eccentricities and the connections. In the simplified method, the compression resistance of an angle member is simply controlled by the "effective length" of the member. To adopt this method, a linear analysis method is carried out first to calculate the internal forces of the structure. In the analysis, all loads are assumed to be applied at the centroid of the sections and all connections are assumed to be pinned. In the second stage, the compression resistances of the members are calculated according to their slenderness ratios and their connection details. Although the design procedure is sped up by these simplified assumptions, the first-order linear analysis and design method appears to be too conservative in

cases where the nodes do not displace and may be dangerous when the ends of an angle strut moves considerably. Not only the load eccentricities and end restraints are ignored in the linear analysis used with the design code, but also the arrangement of the web members on one or alternate sides of a truss is overlooked.

In other national codes such as AISC LRFD [52,63], although the end moments are considered in the interaction equations, the end restraints are considered in terms of "K-factors", the failure loads are always underestimated because the interaction equation is basically derived for a symmetrical section of which the four corners are critical for moments about both principal axes simultaneously. However, for angle sections, as they are monosymmetric for equal-leg angle or asymmetric for unequal-leg angle, the points having maximum bending stress about both principal axes usually do not coincide. As a consequence, the loading capacities of the sections calculated from these interaction equations are underestimated. It is suggested that the axial stress is checked against every corner point of the section.

In the last decades, methods of second-order analysis and advanced analysis have been extensively and actively researched for doubly symmetrical sections. However, second-order analysis for unsymmetrical sections is still unsophisticated. For examples, those factors that have been mentioned in the first paragraph affecting the compression resistances of the angles are not included in the analysis. To widen the application of second-order analysis for practical steel design, this thesis is aimed to propose and to develop a second-order analysis design method for angle frames and trusses which allows the design to be completed within a short

time and the effect of buckling is considered automatically and relatively more rigorously than the current effective length method. In Chapter 5, two second-order elastic design methods have been proposed, namely the equivalent initial curvature approach and the exact end moment approach. In the first approach, the effects due to load eccentricities and end restraints are considered in the form of equivalent initial curvature. The second approach considers the end moments and the rotational stiffness of the connection explicitly by rigid arm and end spring in the analysis. The advantage of the first approach is on its simplicity but it may underestimate the failure load of the structure. The advantage of the second approach is its consideration of the effects due to load eccentricities and end restraints which may produce a more economical design. However, it requires more effort to consider the magnitudes of the load eccentricities and the stiffness of the rotational spring. In Chapter 6, a second-order plastic design method is introduced. It is obvious that failure of a member may not necessarily lead to the collapse of the complete structure. The proposed second-order plastic design method can exploit the reserve in strength after first member buckling. A useful yield surface for an equal angle section is proposed for incorporation into second-order analysis software such that the design of angle trusses and frames can be carried out efficiently and accurately with the load eccentricities and end restraints considered directly.

Chapter 7 reported the experimental investigation of single angle webs in compression in a form of two-dimensional truss. The experimental results are compared with the failure loads calculated by the BS 5950 [3] and NIDA [66] by

applying both second-order elastic and second-order plastic analysis with load eccentricities and end restraints considered. The results show that the failure loads calculated by the BS 5950 [3] were too conservative, especially for webs with single-bolted end condition and connecting on the same side. The second-order elastic analysis is able to give reasonable estimates of the actual failure load for both single-bolted and double-bolted end conditions and webs connected on one side and both sides. The second-order plastic analysis is capable of predicting the failure loads more accurately and rationally allowing for stress and force re-distribution after the yielding of first member.

8.2 Recommendations for future work

Undoubtedly, design of angle structures and towers is complex and quite many tower made of angle members fail when wind is close to the design wind speed. Every year hundreds of angle structures like transmission line towers are constructed in different parts of the world and the wind speed is ever increasing in the world, possibly due to the effect of global warming resulting in more latent energy from sea. The design of this dangerous types of structures requires a careful re-visit and the research on this topic appears to have been over-looked by many researchers who focus more on symmetrical sections like circular, square, I and H steel sections, possible because of the complexity.

The design methods suggested in Chapter 5 including the equivalent initial curvature method and the exact end moment method are ready for immediate use

for design of practical steel structures with angle sections. However, the research on the advanced plastic analysis method proposed in Chapter 6 is still ongoing and requires a great deal of experimental data to support its reliability since the computed result can be occasionally greater than the tested failure load for a single angle strut. The concept underlying the proposed theory can also be extended to other sections like channels and unequal angles. At present, the proposed method can be adopted conservatively with a linear interaction equation. The reserve in strength can be treated as the last resort due to the sudden increase in ultimate load or damage of a member for study of collapse load of the angle structures.

Finally, although not of a concern for most angle structures, angle members may fail by torsional mode and the design of short angle needs to consider this mode together with larger end moments due to eccentric connections. The design should include this consideration when it is widely used in industry to prevent failure of stocky angle struts.

References

[1] Gere JM and Timoshenko SP. Mechanics of Materials, Fourth Edition, PWS Publishing Company, London, 1997.

[2] Trahair NS. Flexural-Torsional Buckling of Structures, E and FN Spon, 1993.

[3] BSI. Structural Use of Steelwork in Building – Part 1: Code of Practice for Design – Rolled and Welded Sections, BS5950-1, BSI, London, 2000.

[4] Kitipornchai, S. Torsional-Flexural Buckling of Angles: A Parametric Study. Journal of Constructional Steel Research, 1983; 3(3): 27-31.

[5] Kitipornchai S and Lee HW. Inelastic Buckling of Single Angle Tee and Double Angle Struts. Journal of Constructional Steel Research, 1986; 6(1): 3-20.

[6] Goodier JN. The buckling of compressed bars by torsion and flexure. Cornell Univ Engineering Experimental Station Bulletin, 1941;27 Dec.

[7] Goodier JN. Flexural-torsional buckling of bars of open section, under bending, eccentric thrust or torsional loads. Cornell Univ Engineering Experimental Station Bulletin 1942; 28 Jan.

[8] Vlasov VZ. Thin Walled Elastic Beams, Second Edition, National Science Foundation, Washington DC, 1961.

[9] Timoshenko SP. Theory of Bending, Torsion and Buckling of Thin-Walled Members of Open Cross Sections Journal of the Franklin Institute, 1945; 239(3,4,5).

[10] Culver CG. Exact Solution of the Biaxial Bending Equations. Journal of Structural Engineering ASCE, 1966; 92(2): 63-83.

[11] Dabrowski R Thin-Walled Members under Biaxial Eccentric Compression. Stahlbau, Dec 1961; 30: 360-35. (In German)

[12] Trahair NS. Restrained Elastic Beam-Columns. Journal of the Structural Division ASCE, 1969; 95(12): 2641-63.

[13] Foehl FP. Direct method of designing single angle struts in welded trusses. Design Book of Welding. Lincoln Electric Co., Cleveland, OH, 1948.

[14] Trahair NS, Usami T, Galambos TV. Eccentrically loaded single angle columns. Research Report No. 11. Structural Division, Civil and Environmental Engineering Department, School of Engineering and Applied Science, Washington University, St Louis, Missouri, USA, 1969.

[15] Adluri SMR, Madugula MKS. Eccentrically loaded steel angle struts. Engineering Journal AISC, 1992; 31(3): 59-66.

[16] AISC. Load and resistance factor design specification for structural steel buildings. AISC Inc, Chicago, 1986.

[17] AISC. Specification of Allowable Stress Design. AISC Inc, Chicago, 1989.

[18] Wakabayashi M, Nonaka T. On the buckling strength of angles in transmission towers. Bulleting of the Disaster Prevention Research Institute, Kyoto University, Japan, Nov 1965; 15(2): 1-18.

[19] Mueller WH, Erzurumlu H. Behaviour and strength of angles in compression: an experimental investigation. Research Report of Civil-Structural Engineering. Division of Engineering and Applied Science. Portland State University, Oregon, USA, 1983.

[20] Ishida A. Experimental study on column carrying capacity of “SHY” steel angles. Yawata Technical Report. Yawata Iron and Steel Co Ltd, Tokyo, Japan, Dec 1968; 265: 8564-82, 8761-63.

[21] Adluri SMR and Madugula MKS. Development of Column Curve for Steel Angles. Journal of Structural Engineering ASCE, March 1996; 122(3): 318-25.

[22] Adluri SMR and Madugula MKS. Flexural Buckling of Steel Angles: Experimental Investigation, March 1996; 122(3): 309-17.

[23] Bathon L, Mueller WH and Kempner L. Ultimate Load Capacity of Single Steel Angles. Journal of Structural Engineering, 1993; 119(1): 279-300.

[24] ASCE. Manuals and reports on engineering practice no 52. Guide for Design of Steel Transmission Towers, ASCE, New York, 1988.

[25] Elgaaly M, Davids W and Dagher H. Non-slender Single Angle Struts. Engineering Journal AISC, 1992; 31(3): 49-59.

.

[26] Woolcock ST and Kitipornchai S. Design of Single Angle Web Struts in Trusses. Journal of Structural Engineering, 1986; 112(6), 1327-45.

[27] SAI. Steel Structures, AS 4100: 1998. Standards Australia International Ltd. North Sydney, New South Wales, Australia,1998.

[28] Sakla SSS. Neural Network Modeling of the Load-carrying Capacity of Eccentrically-loaded Single-angle Struts. Journal of Constructional Steel Research, 2004; 60(7): 965-87.

[29] Oran C. Tangent Stiffness in Plane Frames. Journal of the Structural Division ASCE, 1973; 99: 973-85.

[30] Oran C. Tangent Stiffness in Space Frames. Journal of the Structural Division ASCE, 1973; 99: 987-1001.

[31] Connor J Jr, Logcher RD and Chan SC. Nonlinear Analysis of Elastic Framed Structures. Journal of the Structural Division ASCE, 1968; 94(6): 1525-47.

[32] Meek JL and Tan HS. Geometrically Nonlinear analysis of space frames by an incremental iterative technique. Computer Methods in Applied Mechanics and Engineering Elservier Science Publishers BV (North-Holland), 1984; 47: 261-82.

[33] Chan SL and Chui PPT. Non-linear Static and Cyclic Analysis of Steel Frames with Semi-regid Connections, Elsevier, 2000.

[34] Hu XR, Shen ZY and Lu LW Inelastic Stability Analysis of Biaxially Loaded Beam Columns by the Finite Elements Methods Proceeding International Conference Finite Element Methods, Shanghai, China, 1982; 2: 52-7.

[35] Lu LW, Shen ZY and Hi XR Inelastic Instability Research at Lehigh University. Michael R Horne Int Conf Instability Plastic Collapse Steel Structures, University of `Manchester England, 1983.

[36] Kitipornchai S and Chan SL. Nonlinear Finite Element Analysis of Angle and Tee beam-columns. Journal of Structural Engineering ASCE, 1987;113(4):721-39.

[37] Sun J and Butterworth JW. Behaviour of Steel Single Angle Compression Members Axially Loaded through One Leg. Proceedings of Australasian Structural Engineering Conference, Aucklkand, 1998; 859-66.

[38] SNZ. Steel Structures Standard. NZS 3404: 1. Standard New Zealand, 1997.

[39] Kalaga S and Adluri SMR. Beam-columns with finite deflection. Journal of Structural Engineering, ASCE, February 2000; 126(2): 266-69.

[40] Albermani FGA and Kitipornchai S. Nonlinear Analysis of Thin-walled Structures using Least Element/Member. Journal of Structural Engineering ASCE, 1990; 116(1): 215-34.

[41] CEN. Eurocode 3, Part 1-1: General Rules and Rules for Building, EN 1993-1-1. British Standards Institute, London, 2005.

[42] Chan SL and Zhou ZH. Pointwise Equilibrating Polynomial Element for Nonlinear Analysis of Frames. Journal of Structural engineering ASCE, 1994; 120(6): 1703-17.

[43] Zhou ZH and Chan SL. A Self-equilibrium Element for Second-order Analysis of Semi-rigid Jointed Frames, Journal of Engineering Mechanics ASCE, 1995; 121(8): 896-902.

[44] Chan SL and Zhou ZH. Second-order Elastic Analysis of Frames Using Single Imperfect Element per Member. Journal of Structural Engineering ASCE, 1995; 121(6): 939-45.

[45] Chan SL and Zhou ZH. Second-order Analysis of Slender Steel Frames Under Distributed Axial and Member Loads. Journal of Structural Engineering ASCE, 1997; 123(9): 1187-93.

[46] Chan SL and Gu JX. Exact Tangent Stiffness for Imperfect Beam-column Members. Journal of Structural Engineering ASCE, 2000; 126(9): 1094-101.

[47] Chen WF and Chan SL. Second-order Inelastic Analysis of Steel Frames Using Element with Mid-span and End Springs. Journal of Structural Engineering ASCE, 1995; 121(3): 530-41.

[48] Zhou ZH and Chan SL. Elastoplastic and Large Deflection Analysis of Steel Frames by One Element per Member I: One Hinge along Member. Journal of Structural Engineering, 2004; 130(4): 538-44.

[49] Chan SL and Zhou ZH. Elastoplastic and Large Deflection Analysis of Steel Frames by One Element per Member I: Three Hinges along Member. Journal of Structural Engineering ASCE, 2004; 130(4) 545-53.

[50] Gu JX and Chan SL. A Refined Finite Element Formulation for Flexural and Torsional Buckling of Beam-Columns with Finite Rotations. Engineering Structures Elsevier, 2005; 27(5):749-759

[51] White DW and Hajjar JF. Stability of Steel Frames: the Cases for Simple Elastic and Rigorous Inelastic Analysis/Design Procedures. Engineering Structures Elsevier, 2000; 22: 155-67.

[52] AISC. Load and Resistance Factor Design Specification for Structural Steel Buildings. AISC Inc, Chicago, 1999.

[53] Task Committee on Effective Length. Effective Length and Notional Load approaches for Assessing Frame Stability: Implications for American Steel Design. ASCE, 1997.

[54] Roy S, Fang S and Rossow E. Secondary Stresses on Transmission Tower Structures. Journal of Energy Engineering ASCE, 1984; 110(2):157-72.

[55] Albermani FGA and Kitipornchai S. Numerical Simulation of Structural Behaviour of Transmission Towers. Thin-Walled Structures Elsevier 41(2003) 167-177.

[56] Kitipornchai S, Albermani FGA and Peyrot AH. Effect of bolt slippage on the Ultimate Strength of Latticed Structures. Journal of Structural Engineering ASCE, 1994; 120(8): 2281-7.

[57] Ungkurapinan N, Chandrakeerthy SRDeS, Rajapakse RKND and Yue SB. Joint Slip in Steel Electric Transmission Towers. Engineering Structures Elsevier, 2003; 25: 779-88.

[58] Shakourzdeh H, Guo YQ and Batoz JL. Modeling of Connections in the Analyses of Thin-walled Space Frames. Computers and Structures Elsevier, 1999; 71: 423-33.

[59] Kang WJ, Albermani F, Kitipornchai S and Lam HF. Modelling and Analyzing of Lattice Towers with More Accurate Models. (To be submitted)

[60] Teh LH, Hancock GJ and Clarke MJ. Analysis and Design of Double-Sided High-Rise Steel Pallet Rack Frames. Journal of Structural Engineering ASCE, 2004; 130(7): 1011-21.

[61] SAI. Steel Storage Racking, AS 4084. Standards Australia International Ltd. North Sydney, New South Wales, Australia, 1993.

[62] BD. Code of practice for structural design of steel structures – A limit state approach. Buildings Department, Hong Kong, 2005. (http://www.bd.gov.hk/english/documents/index_crlist.html)

[63] AISC. Load and Resistance Factor Design Specification for Single-angle Members. AISC Inc, Chicago, 2000.

[64] Chan SL. Geometrical and material non-linear analysis of beam-columns and frames using the Minimum Residual Displacment method. International Journal for Numerical Methods in Engineering, 1998; 26: 2657-69.

[65] Clarke MJ and Hancock GJ. A Study of Incremental-iterative Stragtegies for Nonlinear Analysis. Research Report R587. Scholl of Civil and Mining Engineering, University of Sydney, 1990.

[66] NIDA. Non-linear Integrated Design and Analysis Computer Program Manual Version 7 – ElePlast, NAF Series, User's Manual. The Hong Kong Polytechnic University, Hong Kong, 2005.

[67] BSI. Structural Steel Equal and Unequal Leg Angles - Part 1: Dimensions, BS EN 10056-1. The British Standards Institute, London, 1999.

[68] Chan SL and Cho SH. Design of Steel Frames Using Calibrated Design Curves for Buckling Strength of Hot-rolled Members. In: Chan SL, Teng JG, Chung KF, editors. Proceedings of Advances in Steel Structures Elsevier, 2002; 1193-9.

[69] BD. Code of Practice on Wind Effects in Hong Kong. Buildings Department, Hong Kong, 2004. (http://www.bd.gov.hk/english/documents/index_crlist.html)

[70] BD. Chimneys and Flues, PNAP 45. Practice Note for Authorized Persons and Registered Structural Engineers. Buildings Department, Hong Kong, July 1994. (http://www.bd.gov.hk/english/documents/index_pnap.html)

[71] BLIS. The Hong Kong Building Ordinance, Chapter 123. The Bilingual Laws Information System, Department of Justice, Hong Kong,1997. (http://www.legislation.gov.hk/eng/home.htm)

[72] Trahair NS. Moment Capacities of Steel Angle Sections. Journal of Structural Engineering ASCE, 2002;128(11):1387-93.

[73] BSI. Metallic Materials – Tensile Testing – Part 1: Method of Test at Ambient Temperature, BS EN 10002:1. The British Standards Institute, London; 2000.